Russian Original Vol. 34, No. 5, May, 1973

November, 1973

SATEAZ 34(5) 417-530 (1973)

File

SOVIET ATOMIC ENERGY

АТОМНАЯ ЭНЕРГИЯ
(ATOMNAYA ÉNERGIYA)

TRANSLATED FROM RUSSIAN

c/b CONSULTANTS BUREAU, NEW YORK

SOVIET ATOMIC ENERGY

Soviet Atomic Energy is a cover-to-cover translation of *Atomnaya Énergiya*, a publication of the Academy of Sciences of the USSR.

An arrangement with Mezhdunarodnaya Kniga, the Soviet book export agency, makes available both advance copies of the Russian journal and original glossy photographs and artwork. This serves to decrease the necessary time lag between publication of the original and publication of the translation and helps to improve the quality of the latter. The translation began with the first issue of the Russian journal.

Consultants Bureau journals appear about six months after the publication of the original Russian issue. For bibliographic accuracy, the English issue published by Consultants Bureau carries the same number and date as the original Russian from which it was translated. For example, a Russian issue published in December will appear in a Consultants Bureau English translation about the following June, but the translation issue will carry the December date. When ordering any volume or particular issue of a Consultants Bureau journal, please specify the date and, where applicable, the volume and issue numbers of the original Russian. The material you will receive will be a translation of that Russian volume or issue.

Subscription
$80 per volume (6 issues)
2 volumes per year
(Add $5 for orders outside the United States and Canada.)

Single Issue: $30
Single Article: $15

CONSULTANTS BUREAU, NEW YORK AND LONDON

227 West 17th Street
New York, New York 10011

Davis House
8 Scrubs Lane
Harlesden, NW10 6SE
England

Published monthly. Second-class postage paid at Jamaica, New York 11431.

SOVIET ATOMIC ENERGY

A translation of *Atomnaya Énergiya*
November, 1973

Volume 34, Number 5 May, 1973

CONTENTS

CONTENTS

(continued)

CONTENTS

(continued)

The Russian press date (podpisano k pechati) of this issue was 4/20/1973. Publication therefore did not occur prior to this date, but must be assumed to have taken place reasonably soon thereafter.

SYSTEM FOR MONITORING THE ENERGY DISTRIBUTION IN THE RBMK REACTOR

I. Ya. Emel'yanov, L. V. Konstantinov,
V. V. Postnikov, V. K. Denisov,
and V. Ya. Gurovich

UDC 621.039.564

A knowledge of the distribution of energy evolution in the nuclear reactor is a vital condition for the economically effective and danger-free exploitation of a nuclear power station. At the present time the problem is usually solved by means of a set of sensors placed discretely in the active zone [1]. The analysis of the signals arising from these sensors by data-processing equipment facilitates the operative monitoring of the reserve of each fuel channel relative to the critical thermal load, and hence allows the field of energy evolution to be optimized in such a way as to increase the power, the heat-technological reliability of the reactor, and the average integrated power development of the charge.

The purpose of the system used for monitoring the energy distribution in the RBMK reactor (which we shall subsequently call simply the "monitor") is that of measuring the flux of radioactive radiations characterizing the energy evolution in the reactor.

The monitor analyzes the signals arriving from the energy-distribution sensors, compares these with the specified limiting (optimum) values, and then advises the operator as to how to reshape the field of energy evolution. The optimum positioning of the sensors inside the reactor is calculated in an external electronic computer.

For the additional correction of the field of energy evolution, making due allowance for the particular work being carried out in the reactor, provision is made for a connection between the monitor and a data-processing unit, so as to facilitate the periodic calculation of the energy evolution from each fuel channel.

Description of the System

The monitor is a complex of instruments and devices which facilitate the operative monitoring of the distribution of energy evolution. The monitor incorporates the following main components: a sensor for monitoring the energy release with respect to the radius of the reactor; a sensor for monitoring the energy release with respect to the height of the reactor; a calibrated sensor for monitoring the total energy evolution; an auxiliary system for measuring the induced activity in the steel cables and the activity of fuel assemblies withdrawn from the reactor; the secondary part of the system; a signalling circuit.

In order to estimate the principal metrological characteristics of the monitor and obtain various relationships between the signals arising from the sensors, the burn-up of the fuel in the fuel assemblies, the positions of the control rods, etc., provision is made in the reactor for measuring the strength of 60 technological reference channels, furnished with steam-content sensors, flow meters, and temperature sensors.

In order to monitor the energy evolution, special provision is made for the establishment of 153 fuel assemblies with suspensions under a calibrated monitoring sensor, in which miniature fission chambers may be placed during physical experiments and calibrated sensors (γ chambers) during the shutdown period of the reactor. The neutron distribution is determined in the first of these, and the residual energy evolution in the second; the corresponding data are used in order to determine the principal metrological characteristics of the system and the coefficients required for calculating the power of the channels.

Translated from Atomnaya Énergiya, Vol. 34, No. 5, pp. 331-334, May, 1973. Original article submitted February 2, 1973.

Radial Energy-Evolution Sensor. The principle underlying the energy-evolution monitor of the reactor is based on the so-called physical monitoring technique (i.e., the measurement of the fluxes of radioactive radiations, which are related to the energy evolution in accordance with known relationships).

The neutron density constitutes the principal parameter for the monitor. For monitoring the radial neutron density distribution in the reactor, 117 β-emission neutron sensors are distributed uniformly over the active zone.

The energy-evolution sensor is placed in the central aperture of the fuel assembly – it consists of three main parts: a sensitive element made from a cable-type sensor, a protective sleeve with a head section, and a coupling line made from a high-temperature cable with magnesian insulation. The sensor cable is a high-temperature cable 3 mm in diameter with magnesian insulation, a central silver filament, and an outer casing of stainless steel. The length of the sensitive part of the sensor is equal to the height of the active zone of the reactor. The outer diameter of the protective stainless steel sleeve is 6 mm.

The operating principle of the energy-evolution sensor is as follows. When the silver (emitter) is irradiated with neutrons, radioactive silver isotopes are formed. When these decay, high-energy β-particles escape from the emitter, as a result of which the latter becomes positively charged. The short-circuit current from the emitter to the collector (the sleeve or sheath of the cable) is proportional to the neutron density.

The measured sensor current fluctuates according to the disposition of the sensor in the active zone (from 3 to 10 μA).

The sensor is changed by means of the lifting crane in the central reactor room. Laying of the cable run is effected when the reactor is being assembled. The actual cable of this run is analogous to the sensor cable, except that its central core is made of stainless steel. In laying the run, special measures are taken to ensure resistance to interference.

Height Energy-Evolution Sensor. For monitoring the neutron density distribution with respect to the height of the reactor, twelve seven-section β-emission neutron sensors are used. These are arranged uniformly in the central (with respect to radius) part of the reactor, close to special control rods intended for correcting the height distribution of energy evolution.

The height energy sensor is a hollow sleeve made of an aluminum alloy, 70 mm in diameter and 2 mm thick. Inside the sleeve at equal distances from one another are seven elementary β-emission neutron detectors (sections). The centers of the lower and upper sections are displaced relative to the boundaries of the active zone by 500 mm in the direction of the center. The sensitive element of each section is made in the form of a spiral 62 mm in diameter and 115 mm high; the total length of the cable with the silver core in each sensitive element is 7000 mm. The signal from the sensitive element is conveyed to the top of the sensor by means of a high-temperature magnesian cable with a steel central core. The whole construction is supported by a special central tube, which at the same time serves for passing the cable to be activated into the reactor.

The signal from individual sections of the sensor may vary from 3 to 10 μA, depending on their position in the active zone.

In laying the cable lines, special measures are taken to ensure resistance to interference.

The Secondary Part of the System. The secondary part of the system is made in the form of individual functional units. As regards purpose and execution it may be divided into two parts: the secondary part of the height energy-evolution monitor, and the secondary part of the radial energy-evolution monitor of the reactor.

The Secondary Part of the Radial Energy-Distribution Monitor. The instrumental part of the system provides for the analysis of signals arriving from the 117 sensors. Successive questioning of the sensors is employed; thus common units may be used repeatedly and the data corresponding to each monitoring point processed in a uniform manner, so increasing accuracy and simplifying the use of the system.

The signals from the sensors pass through a circulating system to a normalizing device, in which the signal from each questioned sensor is divided (normalized) by the total current from all the sensors, this being proportional to the average power of the reactor. Normalization ensures a constant sensitivity of the system at all levels of power, eliminates the necessity of changing the reference signals (settings) of the

specified distribution of energy release in accordance with the power level of the reactor, and greatly reduces the effect of the delay which occurs in β-emission sensors during transient processes on the operation of the system.

From the output of the normalizing converter the signal passes to the deviation–detection unit; in this it is compared with a standard signal, the magnitude of which is set by means of the reference-signal sensor and the individual setting sensors.

Provision is made in the reference-signal sensor for smoothly varying all the reference signals by $\pm 12\%$ at the same time; this enables the operator to judge the extent to which the energy distribution approximates the specified (optimum) distribution.

When there is a deviation from the specified distribution, a light signal appears on a special display, corresponding to deviations of +5%, +10%, and −10%. When there is a deviation of +10% a hooter also operates.

Provision is made for detecting that part of the active zone having the greatest deviation (in the sense of increasing power) and for automatically recording this deviation, as well as recording all the normalized and total signals at the will of the operator.

For continuous monitoring, five normalized samples from any sensors may be measured directly by means of measuring instruments; any sensor may be directly connected to a measuring instrument.

For carrying out periodic calculations on the data-processing system the latter is connected directly to the monitor.

Irregularities leading to the emission of a signal representing too high a power ("excess" signals) are automatically monitored.

The Secondary Part of the Height Energy-Distribution Monitor. This system is based on successively running through the various sections of the sensor; the results are normalized to the total signal of all the sections of the sensor being monitored. Any deviations of the sensor section signal so normalized from the specified (optimum) value are recorded on a light display. For deviations of more than +5% a red light shows, for deviations of more than −5% a green light. For a deviation of more than +10% the red light flickers. In continuous monitoring, provision is made for connecting the seven sections of any sensor to the measuring (indicating) instruments. At the will of the operator the readings of all the sensor sections may be recorded.

In order to use the resultant data in subsequent optimizing calculations, the system is connected to the data-processing machine.

Irregularities are monitored and indicated by signals.

Auxiliary Energy Monitoring System

The purpose of the auxiliary system lies in making periodic measurements of the field of energy evolution over both the radius and the height of the reactor. The data resulting from these measurements are used to find the principal metrological characteristics defining the system as a whole. The auxiliary system consists of a device intended to monitor the energy distribution along the radius of the reactor, based on measurements of the γ-activity inside the fuel assemblies of the shut-down reactor by means of γ-chambers, and a device intended to calibrate the energy-distribution sensors and measure the activity of the fuel assemblies.

Device for Monitoring the Distribution of Energy Evolution along the Radius of the Reactor. In view of the fact that the γ-activity in the fuel assemblies of the shut-down reactor is proportional to their power before the shut-down, the results of activity measurements in fuel assemblies distributed uniformly over the active zone of the reactor, adjusted for the time which has elapsed between the instant of shutting down and the instant of measurement, as well as certain other specific corrections, provide useful information as to the distribution of energy evolution with respect to the reactor radius.

The measurements are made with the aid of γ-chambers placed in 153 specially provided central apertures of the fuel assemblies and constituting ionization chambers with two cylindrical electrodes. The length of the sensitive part is equal to the height of the active zone of the reactor. The external diameter

of the γ-chamber is 6 mm. The γ-chambers are installed and removed with the aid of the crane in the central hall.

In order to simplify the computing algorithm it is recommended that measurements should be made 6-10 h after shutting the reactor down.

Device for Calibrating the Sensors Monitoring the Energy Evolution and Measuring the Activity of the Fuel Assemblies. This device is intended to measure the neutron density distribution with respect to the height of the fuel assembly while the reactor is working and the activity of the fission fragments in the fuel assemblies extracted from the reactor. In the first case, a special coaxial γ-chamber with a collector is used to determine the induced γ-activity of a stainless steel cable passing through the central aperture of the γ-chamber, this cable being let down into the central aperture of the sensor monitoring the energy distribution over the height of the reactor. Using the same chamber, the induced activity of the fuel assemblies passing through the central aperture of the chamber is also measured. The results are used for the mutual calibration of the sensor sections, and for obtaining additional data required to determine the principal metrological characteristics of the system.

Algorithms for Calculating the Settings and the Field of Energy Evolution from the Sensor Readings

In the monitoring system under consideration, provision is made for comparing the sensor readings with specified settings. It is considered that if the settings match the measured signal then the energy distribution is at its optimum. For calculating these settings, the criteria employed include the fact that the power in any fuel assembly must not exceed a certain limiting value, and that the integrated power of the reactor should be as great as possible. In calculating the settings the method of linear programming is employed.

The energy distribution over all the fuel assemblies is calculated by a computing + experimental technique, based on the simultaneous use of the results of a physical calculation and the data emerging from discrete monitoring points.

The computing + experimental method [2] is based on the determination of a quantity V(r) for each sensor, this being the ratio of the sensor signal to an analogous quantity derived from a physical calculation of the neutron fields or fields of energy evolution. The relative power distribution of the fuel assemblies W(r) is in this case defined as the product of the energy distribution derived from the physical calculation and the distribution V(r) interpolated over the whole active zone. The distribution of V(r) is determined by a statistical interpolation method based on the theory of random functions, and gives better results than any other methods [3].

The method here considered has been verified in relation to the reactor of the I. V. Kurchatov Beloyarsk Atomic Power Station.

LITERATURE CITED

1. I. Ya. Emel'yanov, At. Energ., 30, 275 (1971).
2. W. Legget, Trans. Amer. Nucl. Soc., 9, 484 (1966).
3. I. Ya. Emel'yanov et al., At. Energ., 30, 423 (1971).

RELIABILITY ACCOUNTING OF PROCESS CHANNELS IN NUCLEAR POWER STATION COSTS ACCOUNTING

S. V. Bryunin, Yu. I. Koryakin, and V. Ya. Novikov

UDC 338.4:621.039.516

A broad range of design solutions considered at the stage of engineering design of the reactor core prompts the need for engineering costs comparison of different design variants which feature contrasting degrees of reliability. Raising the reliability of the reactor core is generally a task involving changes in the physical design parameters and cost parameters, such as: percentage burnup of fuel, dimensions and number of fuel elements in a fuel assembly, specific cost of the fuel. The intimate relationship between the engineering cost figures and reliability figures results in neglect of the latter in engineering cost calculations leading to severe errors in some instances, and on occasion even to conclusions that are fundamentally unsound.

In the nuclear power industry [1, 2], reduced losses incurred at nuclear power stations are broken down into two components: the fuel component of the reduced costs and a constant component. The fuel component of the reduced costs [2] allows us to arrive at a correct solution to the problem of how effectively the nuclear fuel is utilized, particularly from the vantage point of reliability. This cost accounting criterion can be used independently, when application of different fuel loadings would not entail design changes in the nuclear power station or related changes in the volume of basic production capital.

Let us consider some expressions for the fuel component of the net cost of electric power and of capital investments in the circulating capital of nuclear power stations figured as component parts in the expressions for the fuel component of the reduced expenses.

The fuel component of the net cost of electric power characterizes instantaneous expenses in fuel consumed by the nuclear power station, and is arrived at by transferring the cost of the nuclear fuel, materials, and preparation of fuel assemblies over to the electric power released to the power grid.

Power station performance, fuel utilization and fuel expenses, can be represented most fully when we consider the entire design service life of the power station. In that case the fuel component of the net electric power cost is expressed in terms of the ratio of integrated expenses to the integrated volume of power generated over the service life of the power station.

Two methods for calculating the fuel component of the net cost of electric power are found in use in engineering cost calculation practice: one for the performance of the nuclear power station in a fuel cycle incorporating chemical reprocessing of spent fuel, and the other without consideration of fuel reprocessing ("discard").

Let us consider these two cases more closely, starting with the first.

Here we introduce the notation: l for the total number of channels loaded into the reactor over a time equal to the service life of the nuclear power station; n for the number of channels loaded into the reactor over the service life of the nuclear power station and experiencing no damage or accidents (surviving for the rated on-power lifetime); m(t)dt is the number of channels loaded into the reactor during the service life of the nuclear power station and experiencing no accidents over the time interval (t, t + dt) of its rated campaign; φ is the utilization factor of the installed power; T_K is the design campaign of the channel, in years; g_K is the uranium load on the channel, in kg; N_T^K is the thermal power output of the channel, in kW;

Translated from Atomnaya Énergiya, Vol. 34, No. 5, pp. 335-339, May, 1973. Original article submitted December 14, 1972.

η is the efficiency; C is the initial specific cost of the fuel, in rubles per kg U. The following formulas are applicable:

$$m+n=l; \quad \int_0^{T_к/\varphi} m(t)\,dt = m;$$

$$0 \leqslant t < T_к/\varphi.$$

Under stationary reactor operating conditions, the fuel component of the net cost of electric power, with emergency malfunctioning of fuel channels taken into account (actual fuel component of the net cost of electric power) is

$$C_т^* = \frac{100 g_к C_г}{8760 \eta N_т^к T_к} \cdot \frac{l}{n + \frac{\varphi}{T_к} \int_0^{T_к/\varphi} tm(t)\,dt} \text{ kopeks/kWh.}$$

If we recall that

$$C_т = \frac{100 g_к C_г}{8760 \eta N_т^к T_к} \text{ kopeks/kWh},$$

is the fuel component of the net cost of electric power generated when malfunctioning of channels in service is not figured into the sum, (rated fuel component of net cost of electric power), and introduce the notation: $\rho_н = n/l$ as the fraction of channels escaping malfunctioning in the total number of channels; $\rho(t)dt = m(t)dt/l$ as the fraction of channels experiencing malfunctioning over the time interval (t, t + dt), i.e., the campaign rating ($0 \leq t < T_К/\varphi$), out of the total number of fuel channels, then we have

$$C_т^* = \frac{C_т}{\rho_н + \frac{\varphi}{T_к} \int_0^{T_к/\varphi} t\rho(t)\,dt}.$$

Clearly, the condition

$$\rho_н + \int_0^{T_к/\varphi} \rho(t)\,dt = 1$$

must hold.

Consider the reliability factors of the process channels (technological channels) and expression derived when they are taken into account.

The fraction of channels escaping malfunctioning over the time $T_К/\varphi$ (living out their design on-power lifetime) out of the total number of channels loaded into the reactor during its service life is equal to the probability of failure-free operation of the channel over a span of time $T_К/\varphi$–$P(T_К/\varphi)$, or to the reliability function of the process channel.

The fraction of channels malfunctioning within an element of time interval (t, t + dt) in its design campaign ($0 \leq t < T_К/\varphi$) out of the total number of channels loaded into the reactor during the reactor's service life is equal to an element of the probability of failure-free performance: dF(t) = f(t)dt, i.e., equal to the probability that the time the channel is out of service will accept some value lying within the time interval element (t, t + dt). Here F(t) is the integrated distribution function of the time of failure-free performance, and f(t) is the failure probability density, or the differential distribution pattern of the time of failure-free performance.

Consequently, we can now state

$$C_т^* = \frac{C_т}{P(T_к/\varphi) + \frac{\varphi}{T_к} \int_0^{T_к/\varphi} tf(t)\,dt}.$$

The integral in the denominator is the mean value of the random variable t, the time of failure of the process channel over the time interval (0, $T_К/\varphi$). Let us break up this integral by parts:

$$\int_0^{T_к/\varphi} tf(t)\,dt = \frac{T_к}{\varphi} P(T_к/\varphi) + \int_0^{T_к/\varphi} P(t)\,dt.$$

Substitution of this integral expression into the preceding formula yields the final value of the actual fuel component of the net cost of electric power with reliability figured in:

$$C_T^* = \frac{C_T}{\frac{\varphi}{T_K} \int_0^{T_K/\varphi} P(t)\,dt}.$$

The following meaning is attached to this expression. The actual fuel component of the net cost of electric power is equal to the rated fuel component of the net cost of electric power divided by the mean value of the probability of failure-free performance on the part of the process channel during the time it is present in the reactor core.

In the case of a multizone reactor, the formula for the fuel component of the net cost of electric power can be arrived at by considering each of these zones separately, and then summing them up with the power contribution made by each reactor zone considered. Hence

$$C_T^* = \sum_{j=1}^{r} \frac{\rho_j C_{Tj}}{\frac{\varphi}{T_{Kj}} \int_0^{T_{Kj}/\varphi} P_j(t)\,dt},$$

where $\rho_j = N_{Tj}/N_T$ is the fraction of thermal power output from the j-th zone to the total thermal power output of the reactor; $\sum_{j=1}^{r} \rho_j = 1$; r is the number of reactor zones; N_{Tj} is the thermal power output of the j-th zone, in kW; N_T is the reactor thermal power output, in kW.

The subscript j attached to all of the factors indicates that the factors so marked are referable to the j-th zone.

The term reactor zone is applied to any group of process channels exhibiting their own physical, process, or cost indices distinct from those of the other process channels in the core.

In the case where the nuclear power station is operating in a closed fuel cycle within the nuclear power industry, fuel expenses must be figured with cost of fuel discharged from the reactor and expenditures associated with marketing realization. These expenditures, as well as the market realization of the residual cost, shift in time relative to fuel acquisition and purchase expense. This effect can be taken properly into account by reducing expenses in reprocessing spent fuel and in the residual cost to the instant of time corresponding to fuel acquisition discounting). In principle, this involves no difficulties, but the need for simplicity in our further calculations dictates the assumption that these expenses appear in the expression of the fuel component of the net cost of electric power in discounted form to begin with.

It is worth pointing out that the cost of spent fuel from channels that have been taken out of service for malfunctioning or that have not lived out their rated on-power lifetime differs from the cost of fuel in channels that have spent their rated campaign time on stream.

Dependences of the concentration of isotopes in the fuel on the residence time of the fuel in the reactor core are determined at the stage of physical calculations, for each specific reactor type and pattern of fuel loading. These dependences can be approximated with ease, say in the form of polynomials.

The cost of the uranium is in turn a function (practically a linear function) of the content of the isotope U^{235} in the uranium sample. This means that finding the dependence of the fuel cost on the fuel residence time in the reactor is a relatively simple matter for each specific reactor type and fuel loading pattern. In their most general form, these dependences can exhibit the following form:

$$C_{sp}(t) = \sum_{n=0}^{m_1} a_n (\varphi t)^n + C_{Pu}\left[\sum_{n=0}^{m_2} b_n (\varphi t)^n + \sum_{n=0}^{m_3} C_n (\varphi t)^n\right] \text{ rubles/kg U},$$

where C_{sp} is the specific cost of the spent fuel unloaded form the reactor over a time t elapsed after the loading, in rubles per kg U; C_{Pu} is the price of the fissionable plutonium (here we assume, for sake of simplicity, that the price of the fissionable plutonium is independent of the Pu^{240} content in the mixture of isotopes), in rubles/g; a_n, b_n, C_n are coefficients of the polynomials approximating the dependences of the cost of the uranium and of the concentrations of Pu^{239} and Pu^{241} in the uranium on the residence time of the fuel in the reactor.

Performing further operations similar to the preceding ones, we arrive with ease at the expression for the fuel component of the net cost of electric power generated by a nuclear power station operating in a closed fuel cycle incorporating chemical reprocessing of spent nuclear fuel:

$$C_T^* = \frac{C_T - I}{\frac{\varphi}{T_K}\int_0^{T_K/\varphi} P(t)\,dt} \text{ kopeks/kWh,}$$

where C_T is the rated fuel component of the net cost of the electric power generated, in kopeks/kWh units, and:

$$C_T = \frac{100}{8760\eta B}[C_g + C_x - (1-\varepsilon)\,C_{sp}\,(T_K/\varphi)]$$

(here B is the design percentage fuel burnup, in MW days per ton U; C_X is the specific cost of the storage, transportation, and chemical processing of the spent fuel, in rubles per kg U; ε are the uranium losses in chemical reprocessing steps, in fractions of unity; C_{sp} is the cost of the spent fuel withdrawn from the channel that has lived out its design on-power service life, in rubles per kg U).

$$I = \frac{100\,(1-\varepsilon)}{8760\eta B}\int_0^{T_K/\varphi} f(t)\,C'_{sp}\,(t)\,dt \text{ kopeks/kWh,}$$

where

$$C'_{sp} = C_{sp}\,(t) - C_{sp}\,(T_K/\varphi) \text{ rubles/kg U.}$$

J is the ratio of the mean value, taken over the interval $(0, T_K/\varphi)$, of the difference in the fuel cost at the time $t(0 \leq t > T_K/\varphi)$ and at the time the design campaign comes to an end to the electric power generated over the course of the design campaign.

In the case of a multizone reactor, the fuel component of the net cost of electric power

$$C_T^* = \sum_{j=1}^{r} \frac{C_{Tj} - I_j}{\frac{\varphi}{T_{Kj}}\int_0^{T_{Kj}/\varphi} P_j(t)\,dt}.$$

As the calculations show, values of the integral J are several orders of magnitude smaller, in the case of power reactors, than the values of the fuel component of the net cost of electric power per sec. It can be safely neglected in practical calculations, with no loss of practical accuracy. In this case the two expressions for the fuel component of the net cost of electric power coincide.

Emergency malfunctioning of process channels and replacement of failed channels by new channels mean increasing capital investments in the rotating capital of nuclear power stations; these increased costs reflect fuel loading costs.

With reliability taken into account, the circulating capital of a nuclear power station will mean that actual fuel loading needed in order to bring about the power production rating over the course of the design reactor compaign, as well as the supply of fuel on hand for the planned or scheduled reloading. The actual fuel load is made up of the rated fuel loading and the emergency fuel reserves intended to replace channels that have malfunctioned and have to be withdrawn. The dimensions of the emergency reserves are a function of the reactor reliability.

After the actual instantaneous fuel costs (fuel component of the net cost of electric power) have been determined, the actual capital investments in the circulating capital of the nuclear power station can be readily determined in volume.

In effect, by multiplying both parts of the formula for the fuel component of the net cost of electric power figured for a nuclear power station with no chemical reprocessing of spent nuclear fuel by the amount of electric power generated during the reactor design campaign, we obtain, in the left-hand member of the formula, the actual capital investments in the circulating capital of the nuclear power station, and in the right-hand member their expression in terms of the nominal capital investments in the circulating capital and the reliability factors (ignoring fuel reserves for scheduled reloading operations on hand at the nuclear power station).

In order to take the availability of fuel channel reserves for scheduled reloading at the station into account, that being, in the general case, the fraction α of the rated loading (about 10%), we add to the left-hand and right-hand members of the expression the cost of these reserves. After some straightforward transformations, we obtain

$$K_T^* = \frac{K_T}{\frac{\varphi}{T_K}\int_0^{T_K/\varphi} P(t)\,dt} \cdot \frac{1+\alpha\frac{\varphi}{T_K}\int_0^{T_K/\varphi} P(t)\,dt}{1+\alpha} \text{ rubles.}$$

Here the nominal capital investments in the circulating capital of the nuclear power station

$$K_T = (1+\alpha)\,G\,C_g \text{ rubles,}$$

where G is the rated loading of the reactor core, in kg U.

Since α is small, and the product $\varphi/T_K \int_0^{T_K/\varphi} P(t)dt$ is close to unity, the second cofactor can be neglected with no essential loss of accuracy in the formula. In that case the actual capital investments in the circulating capital of a nuclear power station with single-zone and multizone reactors will appear in the respective forms:

$$K_T^* = \frac{K_T}{\frac{\varphi}{T_K}\int_0^{T_K/\varphi} P(t)\,dt};$$

$$K_T^* = \sum_{j=1}^{r} \frac{K_{Tj}}{\frac{\varphi}{T_{Kj}}\int_0^{T_{Kj}/\varphi} P_j(t)\,dt}.$$

The specific reduced expenses in electric power, with the reliability of the reactor process channels taken into account, are

$$z_T^* = C_T^* + E_H K_T^* \text{ kopeks/kWh,}$$

where E_H is the assigned effectiveness factor of the capital investments, 1/year (assigned the value 0.12 at the present time).

Here capital investments in the circulating capital are presented in specific form, i.e., referred to the yearly output of electric power. This expression of capital investments in the circulating capital clearly does not change the relationships derived above.

Consequently, the actual fuel component of the reduced expenses is expressed by the formula

$$z_T^* = \frac{C_T + E_H K_T}{\frac{\varphi}{T_K}\int_0^{T_K/\varphi} P(t)\,dt}$$

or

$$z_T^* = \frac{z_T}{\frac{\varphi}{T_K}\int_0^{T_K/\varphi} P(t)\,dt} \text{ kopeks/kWh,}$$

In the case of a multizoned reactor, we have, respectively,

$$z_T^* = \sum_{j=1}^{r} \frac{\rho_j z_{Tj}}{\frac{\varphi}{T_{Kj}}\int_0^{T_{Kj}/\varphi} P_j(t)\,dt}.$$

In the expressions cited above, we see the utilization factor of the installed power φ. This factor is calculated at stages preceding the cost calculations, and with the reliability factor and the index of mean expected power output taken into account.

Clearly, different patterns of distribution of the random variables and correspondingly different reliability laws are considered in practice when calculating the reliability of technological systems. Here we consider the exponential reliability law, which corresponds to the simplest stream of failures of process channels satisfying the following requirements: stationarity [channel failure probability in any time interval $(t, t + \Delta t)$ determined solely by Δt within the limits T_K/φ, and independent of t] and absence of aftereffects [channel failure probability within the interval of time $(t, t + \Delta t)$ within the limits of the ratio T_K/φ independent of the number and time distribution of preceding channel features]. In some cases of practical interest, the exponential law does a fairly good job of describing the operational reliability of the reactor channels [3].

Consider the expressions derived above for the exponential reliability law.

The reliability function for that law is

$$P(t) = e^{-\lambda t},$$

where λ is the intensity of the stream of failures (the number of failures per unit time). This is constant for an exponential law.

The integrated distribution function of the failure-free performance time is

$$F(t) = 1 - e^{-\lambda t}.$$

The function of the stream of failures (restitution function) is

$$H(t) = \lambda t.$$

Substitution of the reliability function for the exponential law into the formulas so derived, followed by some straightforward transformations, yields:

$$C_T^* = \sum_{j=1}^{r} \rho_j \frac{H_j(T_{Kj}/\varphi)}{F_j(T_{Kj}/\varphi)} C_{Tj};$$

$$z_T^* = \sum_{j=1}^{r} \rho_j \frac{H_j(T_{Kj}/\varphi)}{F_j(T_{Kj}/\varphi)} z_{Tj}.$$

In actual practice, however, recourse to other expressions derived by expanding the exponent into a series and substituting it into the formulas cited is more convenient. Given the smallness of the values of $\lambda T_K/\varphi$, we can discard all but the first three terms of the expansion.

After some slight transformations, we obtain

$$C_T^* = \sum_{j=1}^{r} \frac{\rho_j C_{Tj}}{1 - \frac{1}{2}\lambda_j \frac{T_{Kj}}{\varphi}}$$

$$z_T^* = \sum_{j=1}^{r} \frac{\rho_j z_{Tj}}{1 - \frac{1}{2}\lambda_j \frac{T_{Kj}}{\varphi}}$$

We cite the computational example for an increase in the fuel components of the net cost of electric power and the reduced electric power expenses with due account given to the reliability of the reactor process channels (exponential reliability law). Consider a hypothetical single-zone channel reactor exhibiting the following parameters: effective campaign lasting three years; utilization factor of installed power with reliability of process channels and of power station equipment taken into account: 0.75; intensity of failures of process channels $5 \cdot 10^{-6}$ 1/hour. Substitution of these parameters into the formulas so obtained yields

$$\frac{C^* - C}{C} = \frac{z^* - z}{z} = 9.6\%.$$

In conclusion, the authors express their thanks to A. I. Klemin and M. M. Strigulin for the interest they showed in the work and for their invaluable comments.

LITERATURE CITED

1. "Standard procedure for determining cost savings in capital investments," Ekonomicheskaya Gazeta, September, No. 39 (1969).

2. V. V. Batov and Yu. I. Koryakin, Nuclear Power Economics [in Russian], Atomizdat (1969).
3. A. I. Klemin and M. M. Strigulin, Some Topics Pertaining to Nuclear Reactor Reliability [in Russian], Atomizdat, Moscow (1968).

EMERGENCY COOLDOWN OF THE BOR-60

O. D. Kazachkovskii, G. K. Antipin,
V. A. Afanas'ev, V. F. Bai,
V. A. Borisyuk, E. V. Borisyuk,
V. M. Gryazev, V. N. Efimov,
V. P. Kevrolev, V. I. Kondrat'ev,
N. V. Krasnoyarov, and A. M. Smirnov

UDC 621.039.526

One of the prerequesites for safe operation of fast reactors when the sodium coolant in them heats up vigorously is reduction of thermal stresses in the structural elements of the reactor pressure vessel and of the loop equipment, in scramming and cooldown. The magnitude of these thermal stresses is determined by the changes in the rate and in the absolute drop of the temperature, and becomes maximized in massive equipment assemblies. Ideal scramming conditions are arrived at in those cases when the temperature level of the preceding steady state is virtually maintained in practice in the most hazardous and most difficult-to-replace components of the reactor loops, with cooldown of the facility proceeding subsequently at an allowable rate (allowable in terms of thermal stressing). Under actual service conditions, the rate and time of the change in power output and in the rate of coolant flow through the loops must be made and kept commensurate. A complex program of theoretical and experimental research geared to optimizing scramming and cooldown conditions for the startup and runup of the BOR-60 fast facility has been completed.

The BOR-60 fast facility is a three-loop two-subloop fast reactor facility [1]. Two centrifugal circulation pumps keep the sodium flowrate through the reactor at levels as high as 1200 m^3/h (Fig. 1). The throughput of the pumps is regulated smoothly by varying pump shaft rpm anywhere from 15% to 100% of rated rpm.

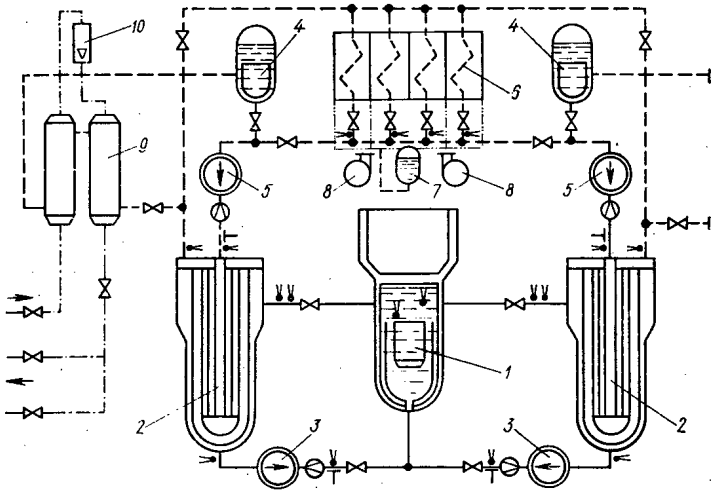

Fig. 1. Layout of BOR-60 fast facility: 1) core; 2) intercoolers; 3) circulation pumps in primary loop; 4) steam generator buffer tanks; 5) secondary-loop circulation pumps; 6) air cooler; 7) air cooler buffer tank; 8) fans; 9) steam generators; 10) steam separator.

Translated from Atomnaya Énergiya, Vol. 34, No. 5, pp. 341-344, May, 1972. Original article submitted September 18, 1972.

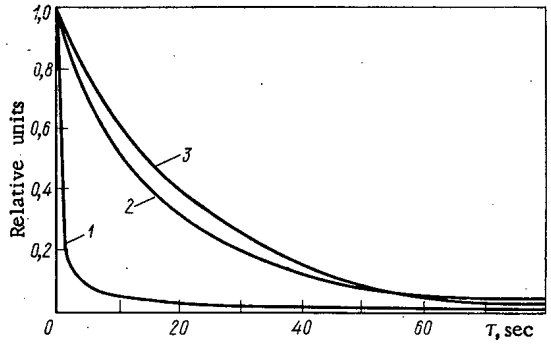

Fig. 2

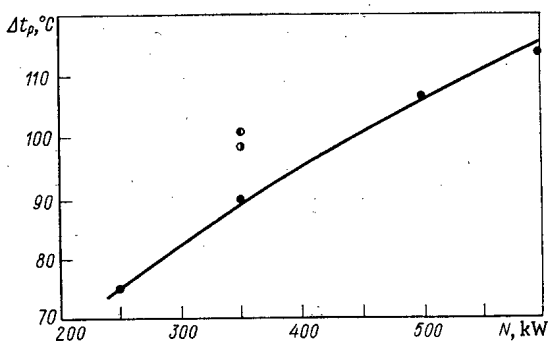

Fig. 3

Fig. 2. Change in power output level and in coolant flowrate through BOR-60 reactor core in scramming response: 1) power output in fast scramming; 2) power output in slow scramming; 3) rate of coolant flow with pumps shut off.

Fig. 3. Dependence of coolant warmup, Δt_p, on reactor power output N in natural circulation flow: ●) both subloops operated in parallel; ◑) one subloop operating; ◐) only the second subloop operating.

Within the reactor plant, the sodium flows in parallel through the core and side shield packages, through clearances between the steel shielding enclosures of the pressure vessel, and arrives at the top-side mixing chamber. The heated sodium then emerges from the mixing chamber through two pipe outlets to arrive at intermediate heat exchangers where it passes on the shell side from above to below and gives up heat to the secondary-loop sodium stream. The sodium passes out of these intermediate heat exchangers (intercoolers) and on into a tee-branch which joins the pressure piping of the parallel subloops, and from there it passes through a piping run to enter the reactor pressure header.

Each of the two secondary-loop subloops comprises a unit with a thermal output rating of 30 MW and incorporating an intercooler, a circulation pump, and a steam generator. There is also an air cooler designed to give off 30 MW thermal power, which can be connected up to either subloop instead of the corresponding steam generator, or which can be connected simultaneously to both subloops. The air heated in the air cooler is ejected by the fans into a special venting dust which also provides natural air suction in the case of an emergency cooldown.

The reactor is scrammed by introducing control rods into the core, both in fast scrams and in slow scrams. When a fast scram command is given, the scram rods and the peripheral compensating rod are introduced into the core within ~1 sec, the control rods are thrust in within 40 sec, and the central compensating rod remains in place. When the slow scram is activated, the central compensating rod remains in its previous position and all of the other control rods are introduced into the core within 40 sec.

Changes in relative reactor power output when fast scram and slow scram responses are activated are shown in Fig. 2.

Automatic switching of the circulation pumps to low rpm levels with the flowrate through the reactor at 300 m^3/h is provided for in the design of the facility [2], as part of the fast and slow scram responses. "Cold" shocks in the "hot" parts of the subloops were observed in fast and slow scramming experiments at 10 MW and 20 MW power output levels with the circulation pumps switched to low rpm levels. The rates of sodium temperature change at the reactor exit reached levels of 1 deg/sec. Strain gages recorded short-term stresses of 36 kg/mm^2 in the top of the intercooler. Clearly, temperature jumps and thermal stresses in the structures will be even more impressive when that type of scramming is initiated from a high power output level.

The option of shutting off the pumps and utilizing the inertia of the stream and the inertia of the rotating parts to diminish residual power release during the power drop, with subsequent switching to natural circulation flow, was investigated as a possible means of minimizing thermal stresses in response to scramming.

Investigations of changes in flowrate with the two primary-loop pumps shut off showed that the fall-off in the flowrate is close to the fall-off in reactor power output during the first 90 sec from the time the slow scram command is given (Fig. 2).

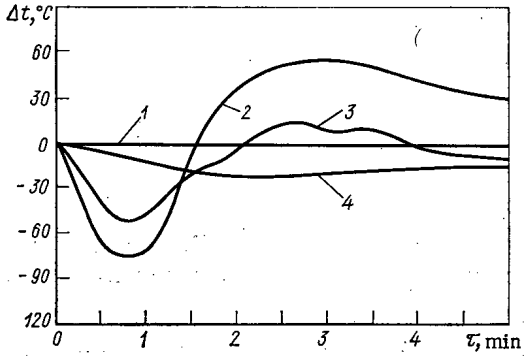

Fig. 4

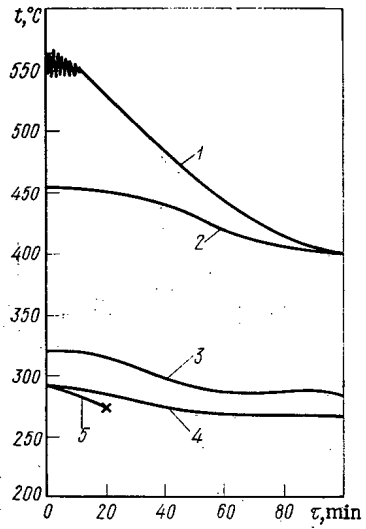

Fig. 5

Fig. 4. Departure of temperature (Δt) from steady-state value when slow scram is activated at 20 MW: 1) reactor entrance temperature; 2) core exit temperature (in thermal package); 3) temperature above core packages; 4) temperature at reactor exit.

Fig. 5. Time variation of temperatures after slow scram at power level 40 MW: 1) temperature above core packages; 2) temperature at reactor exit; 3) temperature at reactor entrance; 4) sodium temperature at air cooler exit; 5) sodium temperature at steam generator exit; ×) instant steam generator is shut off.

When natural circulation flow was studied over a range of power output levels from 250 to 600 kW, it was shown that the extent to which the coolant in the reactor heated up under those sets of conditions was close to the amount of warmup under scramming conditions at power levels of 20 to 40 MW with 1000 m^3/h flowrate through the reactor (Fig. 3).

The rate of coolant flow through the secondary-loop subloops connected to the air cooler is almost three times higher than in the primary loop. The reason is that the geometrical center of the air cooler is six meters higher than the geometrical center of the intercooler.

Natural circulation regimes in each subloop of the primary loop were tested separately and together at the level of 350 kW. The characteristics of the two subloops in the natural circulation flow regime (Fig. 3) proved to be identical in practice (Δt_p = 100°C), and differ only slightly from the characteristics when the parallel connection was made (Δt_p = 90°C). Hence, we can infer that the principal contribution to resistance to flow in natural circulation through the primary loop is made by the reactor. The fraction of resistance in the subloop is insignificant, so that it is possible to execute reactor cooldown with a single subloop.

Experimental data on natural flow, and variations in the power output level and in the rate of flow through the reactor when the protection system is activated, were used in calculations of several scramming and cooldown variants in the slow-scram and fast-scram modes with the primary-loop and secondary-loop pumps shut off and the air cooler fans shut off. Results of calculations showed that no temperature discontinuities occur in the exit pipes and in the loops in response to fast scramming or slow scramming. At the core exit, there is a 100-200°C temperature rise over the steady-state level when the pumps are shut off completely. When fast scram is executed, the temperature peaks ends up higher and steeper in slope than when slow scram is executed. The effect of the coolant flowrate ratios on the size of the temperature peak in the secondary loop in relation to the flowrates in the first, stationary state was studied. The temperature peak flattens out as the flowrate ratio increases. The reason is that the center of heat removal shifts upward as the flowrate ratio in the intercooler increases, and then better conditions are brought about for forming a moving pressure head in natural circulation flow after the pumps have been shut off.

With the reactor operating at 20 MW output level with the subloops of the secondary loop connected up to the air cooler, an experiment was staged on activating the slow scram with simultaneous disengagement

of the pumps of both loops and the fans. Along with measurements of coolant flowrates and power levels, measurements were taken of the coolant temperatures at the reactor entrance, at the reactor core exit (with the aid of thermocouples installed above the fuel packages, and thermocouples in a thermometric package), at exit pipe outlets, at the entrance and exit of the intercoolers on both the primary-loop and secondary-loop ends, and also of the temperatures in the air cooler. The most typical changes in temperatures in the reactor and in the primary loop with time are plotted graphically in Fig. 4. The temperatures in the intermediate coolers and in the secondary-loop coolant in response to activation of the reactor protection system remained the same as at the 20 MW power level, and then dropped down uniformly with the temperatures in the primary loop and in the reactor at rate of 6 deg/h.

The maximum coolant temperature increment at the exit from the core packages, over the steady-state value, is ~60°C, and the maximum rate of temperature change on the cladding of the fuel elements is about 2 deg/sec, which is considerably less than the variant in which protection is activated without shutting off the pumps.

An extended series was staged for the purpose of further checking out the safety of scram shutdown and cooldown. The reactor power level, the coolant flowrates through the loops, and the rate of decline of power level and flowrate were all varied in these tests.

In order to eliminate temperature discontinuities over the tubesheets of the steam generators (when the facility was operated in an electric power generating mode), a set of conditions geared to reduce the feedwater flowrate was selected. Feedwater flowrate kept at a constant level means rapid cooling of the steam generator. Shutting off the supply of feedwater at the same time the scram system is activated means an abrupt rise in the temperature of the sodium at the exit from the evaporator. The set of conditions under which the feedwater flowrate declines within 50 sec as the level in the separator is maintained is the quietest one for steam generator performance. The set of conditions under which the shutoff of the feedwater pump is delayed for 30 sec while the total rate of feedwater flow through the steam generator is maintained at the previous level is also satisfactory.

Figure 5 shows the variation with time of temperatures taken over the loops after slow scram was instituted with the circulation pumps and fans shut off, at 40 MW power level with heat removal by means of the air cooler and steam generator (principal operating mode of the entire facility). The feed water pump was shut off with a 30 sec delay. It is clear from the graph that no abrupt changes occurred in any of the structural members.

When the facility is operated with the air cooler and steam generator active after the subloops and the steam generator are shut off and the protection response is activated, further cooldown of the facility takes place via the air cooler (for greater simplicity and in order to eliminate temperature nonuniformities).

The following schemata, deemed safe and sample in execution, were arrived at on the basis of scram and cooldown investigations:

1. Fast scram is activated with the circulation pumps shut off in response to the signals: 20% power excursion, doubling time (period) shortened to 20 sec; complete electrical supply outage.

2. Slow scram is activated with the circulation pumps shut off in response to the signals: temperature rise at reactor exit; sodium flowrate in one of the subloops dropping off; feedwater flowrate dropping off; one of the circulation pumps shut off; feedwater pump shut off; one of the air cooler fans shut off; pressure rise in the steam generator surge tank.

LITERATURE CITED

1. A. I. Leipunskii et al., At. Energ., 21, 450 (1966).
2. Yu. S. Bagdasarov et al., Fast Neutron Reactor Engineering Problems [in Russian], Atomizdat, Moscow (1969).

THE EFFECT OF ADDED ZIRCONIUM ON THE SURFACE TENSION OF COPPER – ALUMINUM ALLOY AND THE INTERPHASE TENSION WITH URANIUM DIOXIDE

V. G. Pastushkov, G. P. Novoselov, and G. B. Borisov

UDC 669.017:669.3:541.451:542.942.3

In view of the wide use of uranium dioxide in nuclear power production [1-3], a certain interest also attaches to such problems as wetting, surface tension, and contact interaction between solid uranium dioxide and fused metals and alloys.

It has been shown [4] that copper, aluminum, and copper–alluminum alloys used to make cermets [5] do not wet uranium dioxide and do not interact with it up to 1300°C.

It is known [6] that when a surface-active alloying additive (e.g., titanium) is used to the fused metal, the surface properties of the alloy may undergo marked changes. This is explained [5] by the facts that titanium interacts with most oxides and that oxygen is very soluble in titanium. Therefore we can expect that zirconium, which has high affinity for oxygen and differs from copper and aluminum in its thermodynamic and chemical characteristics, will cause changes in the surface properties when it is used to alloy melts based on copper and aluminum. In this connection, in our present work we have investigated how the alloy Cu + 30 wt. % Al is affected by alloying as regards wetting and interaction with briqueted uranium dioxide.

To study the interaction of uranium dioxide with metallic melts and surface phenomena in this system, we used the method of standing drops. We used tablets of uranium dioxide sintered at 1700°C in hydrogen, and containing (wt. %) 87.73 uranium, 0.026 iron, 0.04 carbon, 0.03 silicon, remainder, oxygen. The oxygen coefficient of the UO_2 was 2.003. The ends of the tablets were polished, The density of the specimens of substrate was 10.25-10.35 g/cm^3, and the open porosity varied in the range 1-5%. The test alloys, containing (according to the chemical analysis data) 5, 10, 15, and 20 wt. % of zirconium, were prepared by remelting aluminum mark AV-00, copper M-1, and zirconium iodide, in a vacuum of $1 \cdot 10^{-3}$ mm, at 1500°C, for 30 min.

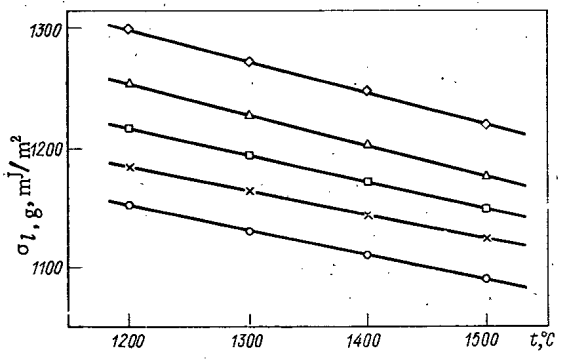

Fig. 1. Polytherms of surface tension of liquid alloys of system (Cu + 30% Al)–Zr: ○) (Cu + 30% Al); ×) (Cu + 30% Al)–5% Zr; □) (Cu + 30% Al)–10% Zr; △) (Cu + 30% Al) –15% Zr; ◇) (Cu + 30% Al)–20% Zr.

The experiments were carried out in the range 1200-1500°C in purified argon. After fusion, the metallic

TABLE 1. Properties of Liquid Alloys of the System (Cu + 30% Al)–Zr at Interface with Uranium Dioxide

Zr content, wt%	σ_l, g, mJ/m^2		θ, deg		$\sigma_{s.l}$, mJ/m^2		W_a, mJ/m^2	
	t_1	t_2	t_1	t_2	t_1	t_2	t_1	t_2
0	1090	1150	107	117	780	1040	780	620
5	1125	1185	112	122	890	1140	700	550
10	1150	1220	117	127	990	1250	630	470
15	1180	1250	122	133	1100	1310	550	440
20	1225	1290	130	137	1225	1440	440	350

Translated from Atomnaya Énergiya, Vol. 34, No. 5, pp. 345-348, May, 1973. Original article submitted June 20, 1972.

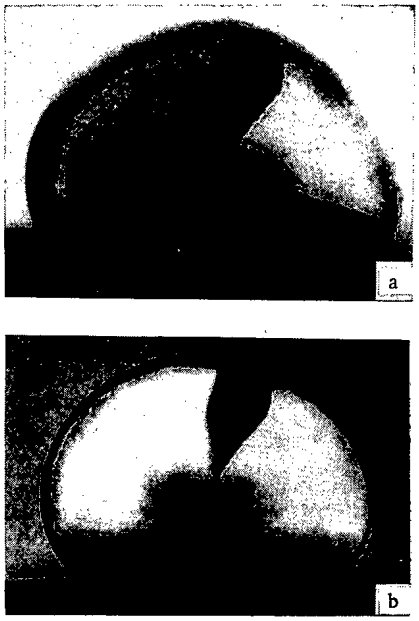

Fig. 2. Wetting of uranium dioxide by metallic melts at 1500°C: a) (Cu + 30% Al); b) (Cu + 30% Al) −20% Zr.

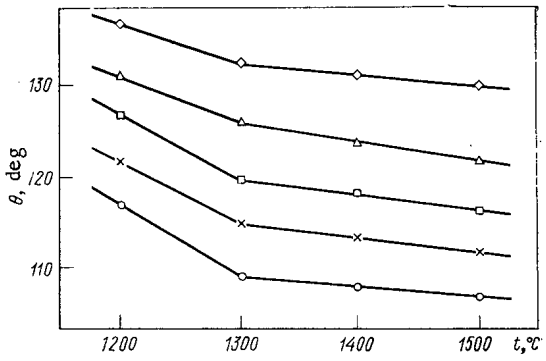

Fig. 3. Polytherms of wetting of uranium dioxide by melts of the system (Cu + 30% Al) −Zr (for notation of curves see Fig. 1).

specimen was kept at the given temperature for 20 min. The drop of alloy and the substrate were photographed immediately after formation of the drop and again after every 5 min.

The surface tension of the doped copper–aluminum alloys was calculated by the Dorsey method [7] with the aid of tables [8] by means of the formula

$$\frac{\sigma_{l,g}}{\Delta\rho g} = a^2 = f\left(\frac{H}{R}\right) r^2,$$

where H is a dimensionless parameter depending on the ratio of the diameter of the drop to its height, $\sigma_{l,g}$ is the surface tension of the alloy, $\Delta\rho = \rho_l - \rho_g$ is the difference between the densities of the liquid metal and gas at a given temperature, g is the acceleration due to gravity, a is the capillary constant, and r is the radius of the drop across its meridional section. The ratio a^2/r^2 was determined from tables [8] for the experimental values of r and H.

The densities of the liquid alloys were calculated from the data in [9] and were compared with the experimental data for copper–aluminum alloy obtained in [10].

The angles of contact were determined experimentally from photographs of the drops of fused metals. The angles were measured to within 1-2°. Each point was the mean of three determinations.

The solidified alloy was removed from the oxide substrate and after solution of the whole drop was analyzed for uranium content. The work of adhesion at the given temperature was calculated from the equation

$$W_a = \sigma_{l,g}(1 - \cos\Theta),$$

and the interfacial tension of the alloys of the system (Cu + 30% Al)−Zr at the interface with the uranium dioxide was calculated from the formula

$$\sigma_{l,g} = \sigma_{s,g} - \sigma_{l,g}\cos\Theta.$$

The surface tension of the solid uranium dioxide at temperature T was determined from the data in [4] with allowance for the temperature coefficient, equal to -0.1 mJ/m^2.

The results of the experiments are plotted in Figs. 1-5 and listed in Table 1. As we see from Fig. 1, the temperature dependence of the surface tension of alloys of the system (Cu + 30% Al)−Zr is linear with a negative temperature coefficient. The values obtained for $\sigma_{l,g}$ of the alloys indicate that addition of zinc to the alloy (Cu + 30% Al) has little effect on its surface tension. The temperature dependence of $\sigma_{l,g}$ for the copper–aluminum alloy agrees with the extrapolated data of Eremenko et al. [5].

To explain the interphase activity of zirconium at the interface between (Cu + 30% Al) and UO_2, we determined the temperature and concentration dependences of the angle of contact. For all the melts a constant angle was attained in 15-17 min. Photographs of drops of alloys at 1500°C are shown in Fig. 2.

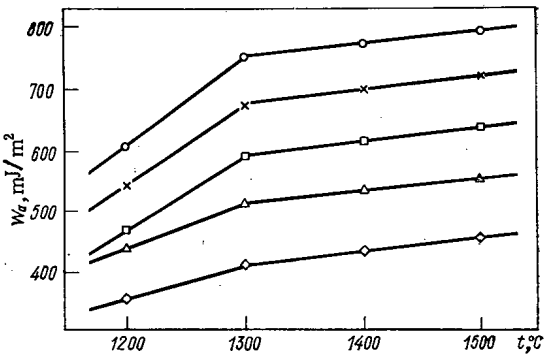

Fig. 4

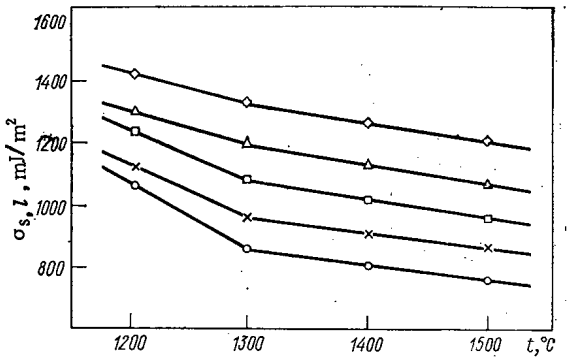

Fig. 5

Fig. 4. Polytherms of work of adhesion at interface of melts (Cu + 30% Al)–Zr with UO_2 (for notation of curves see Fig. 1).

Fig. 5. Polytherms of interphase tension between melts of the system (Cu + 30% Al)–Zr and UO_2 (for notation of curves see Fig. 1).

For most of the alloys we observe a small change in contact angle with rise of temperature. The fall in the values over the interval 1200-1500°C is 8-12°.

From Fig. 3 we see that alloying of copper–aluminum alloy with zirconium markedly increases the angle of contact on uranium dioxide. After addition of 20% of zirconium, the value of Θ for the alloy (Cu + 30% Al) in the range of temperatures under test increases by 20-24°.

Table 1 lists data characterizing the influence of zirconium on the surface properties of the system melt (Cu + 30% Al) – solid uranium dioxide at 1200 and 1500°C (t_2 and t_1 respectively).

Figure 4 plots the work of adhesion of the melts vs temperature. Owing to the low wettability of uranium dioxide by fused copper–aluminum alloys alloyed with zirconium, the work of adhesion is nearly halved, which shows that zirconium is inactive in the melt of (Cu + 30% Al) and that there is no interaction between zirconium and uranium dioxide, in contrast with chemisorption of zirconium on a substrate of aluminum oxide [11].

Note the weak cohesion between a substrate of uranium dioxide and the alloys under test. Solidified drops of the alloys freely separated from the tablets, leaving a slight trace on them. Chemical analysis of the drops of alloys after the experiments showed that their uranium constants did not exceed 0.03 wt. %. This shows that uranium dioxide is only slightly reduced by the metallic melts of the system (Cu + 30% Al)–Zr, which is confirmed by x-ray diffraction analysis of the UO_2 (lattice parameter 5.4702 Å).

Figure 5 shows the values of the interphase tension at the fused metal–uranium dioxide boundary, calculated on the basis of the experimental data. From Fig. 5 and Table 1, it follows that addition of zirconium to the melt of (Cu + 30% Al) increases the interphase tension at the boundary with the uranium dioxide by 400-450 mJ/m².

According to the data in [4], in copper–aluminum alloys which in solid form are close to the composition of the compound Cu_2Al, aluminum has the least surface activity with minimum work of adhesion. In [12] this phenomenon is explained by the formation of the chemical compound Cu–Al, which is stable in the liquid and solid states over a certain temperature range.

As a result of our present investigations, we have established that zirconium in the melt (Cu + 30% Al) is an interphase additive. Clearly this can be explained by the formation of double and triple complexes of zirconium with copper and aluminum [13], which are stable in the melt. As a result, the surface activity of the individual components is reduced and the system becomes more stable.

LITERATURE CITED

1. A. S. Zaimovskii et al., Heat-Emitting Elements for Nuclear Reactors [in Russian], Atomizdat, Moscow (1965).

2. M. Gumenik and T. J. Whelan, in: cermets, (J. R. Tinklepo and U. B. Crendall, editors) [Russian translation], Izd-vo Inostr. Lit., Moscow (1962).
3. High Temperature Techniques, (I. E. Campbell, editor) [Russian translation], Izd-vo Inostr. Lit., Moscow (1959).
4. D. T. Levey and P. Murray, in: Refractory and Corrosion-Resistant Metal–Ceramic Materials [Russian translation], Oborongiz, Moscow (1959).
5. V. N. Eremenko, V. I. Nizhenko, and Yu. V. Naidich, Izv. Akad. Nauk SSSR, Metallurgiya i Toplivo, No. 3, 150 (1961).
6. V. N. Eremenko and V. I. Nizhenko, Zh. Fiz.-Khim., 35, 1301 (1961).
7. N. Dorsey, J. Wash. Acad. Sci., 18, 505 (1928).
8. Yu. N. Ivashchenko, B. B. Bogatyrenko, and V. N. Eremenko, in: Surface Phenomena in Melts and Processes of Powder Metallurgy [in Russian], Izd-vo AN UkrSSR, Kiev (1963).
9. M. P. Slavinskii, Physicochemical Properties of Elements [in Russian], Metallurgizdat, Moscow (1952).
10. V. I. Nizhenko and V. N. Eremenko, Poroshkovaya Metallurgiya, No. 2, 17 (1964).
11. V. N. Eremenko, V. I. Nizhenko, and L. I. Sklyarenko, in: Surface Phenomena in Melts and Solid Phases Arising from Them [in Russian], Nal'chik, Kabard.-Balkar. Kn. Iz-vo (1965).
12. A. M. Korol'kov, Izv. Akad. Nauk SSSR, Metallurgiya i Toplivo, No. 3, 146 (1961).
13. O. S. Zarechnyuk et al., Izv. Akad. Nauk SSSR, Metally, No. 6, 201 (1967).

NEUTRON SPECTRA FROM ISOTOPIC (α, n) SOURCES

N. D. Tyufyakov, L. A. Trykov, and A. S. Shtan'

UDC 539.12.03

One of the fundamental characteristics of an isotopic neutron source which determines the possibility and conditions of its use for solution of specific problems in many cases is the energy spectrum of the neutrons. Although the investigation of this characteristic for such sources as Po^{210}–Be, Pu^{239}–Be, and Ra^{226}–Be have been carried on for many years, results obtained up to the present time by various authors often differ considerably even for sources of the same kind. Such disparities are observed in the spectral shape and in the average energy of the neutrons; they are particularly large in the low-energy portion of the spectrum at neutron energies below 2-3 MeV. As an example of this, neutron spectra from Po^{210}–Be and Am^{241}–Be sources are shown in Figs. 1 and 2 based on data from [1-5].

The indicated discrepancies in the spectra are usually explained by a strong dependence of spectral shape of neutron spectra from isotopic (α, n) sources on source parameters and method of preparation. However, existing information on this question is fragmentary and insufficiently confirmed by experimental data.

This paper presents results of experimental studies of the effect of certain parameters of isotopic (α, n) sources on the shape of the neutron spectrum and discusses possible reasons for the disparities mentioned above. Spectra were measured with a neutron spectrometer having a stilbene crystal 20 × 30 mm in size, and the low-energy portion of the spectrum was measured with a 10 × 10 mm crystal. An FEU-93 photomultiplier with high photocathode conversion efficiency was used in the spectrometer. The time constant of the input circuit of the electronics was $1.2 \cdot 10^{-6}$ sec and the total nonlinearity of the electronics (including the pulse-height analyzer) was less than 2%. All measurements of one particular kind were carried out under identical conditions.

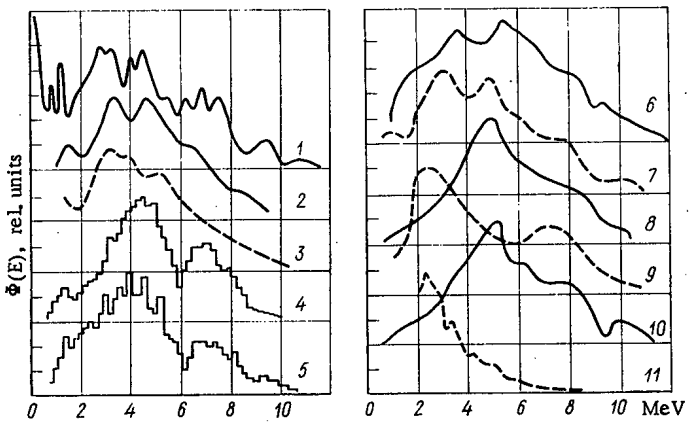

Fig. 1. Energy spectra of neutrons from Po^{210}–Be sources measured: 1) by spectrometer with stilbene crystal, from data in [3]; 2) by spectrometer with $Li^6I(Eu)$ and $Li^7I(Eu)$ crystals, from data in [2]; 3-11) with photographic plates, from data in [1].

Translated from Atomnaya Énergiya, Vol. 34, No. 5, pp. 349-353, May, 1973. Original article submitted August 14, 1972.

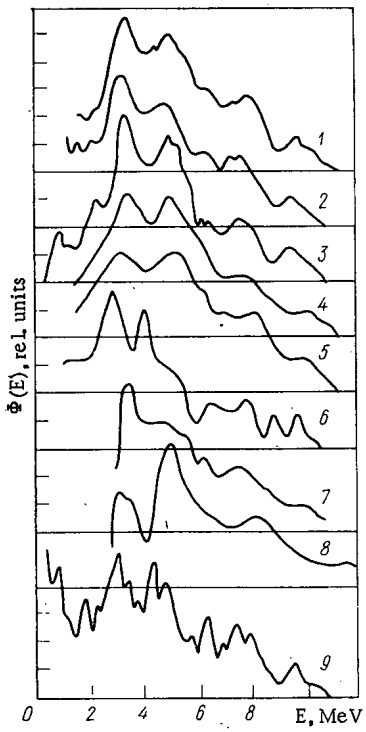

Fig. 2. Energy spectra of neutrons from Am^{241}–Be sources: 1-8) data from [4]; 9) results of present work.

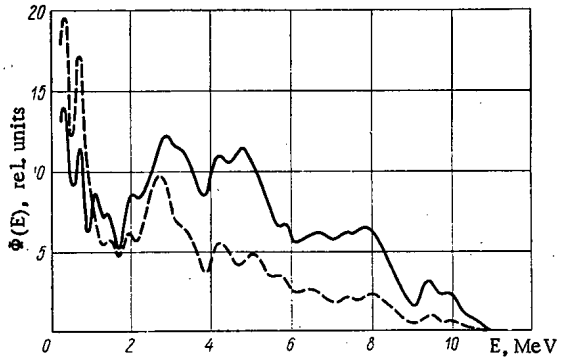

Fig. 3. Energy spectra of neutrons from Po^{210}–Be sources: ——) single source (20 mm in diameter, 40 mm high); - - - -) assembly consisting of 10 sources.

Unfolding of the neutron energy spectrum Φ(E) from the instrumental pulse-height distribution was performed by differentiation. Correction for the dependence of pulse height P(E) on neutron energy E including nonlinearity and anisotropy of the light yield from the crystal and nonlinearity in the transformation of a light pulse into an electrical impulse was introduced by means of the empirical relation

$$P(E) = B(\omega) E^{1.5} \exp(0.016E^{-1.5} - 0.021E^{0.9}),$$

where $B(\omega)$ is a coefficient which depends on the direction of neutron incidence on the crystal. For neutron incidence on the crystal which corresponds to minimum light yield, the coefficient $B(\omega = 0°) = 0.176$ and for maximum light yield $B(\omega = 90°) = 0.212$. This relation was established on the basis of experiments with monoenergetic neutrons in the energy range 0.1-20 MeV and for stilbene crystals in the size range 10 × 10 to 70 × 70 mm.

In the study of neutron spectra from isotopic (α, n) sources, the effect of source dimensions on the shape of the neutron spectrum was determined in the first series of experiments. Measurements were made of the neutron spectrum from a single Po^{210}–Be source (20 mm in diameter and 40 mm high) and from ten similar sources enclosed in an aluminum capsule with a wall thickness of 6 mm. The results are shown in Fig. 3.

Figure 4 shows the neutron spectrum for a Pu^{239}–Be source containing 8 g of plutonium and also data from [6] for sources of the same kind containing 2 and 160 g of plutonium. Figure 5 shows neutron spectra from a Pu^{238}–Be source having a strength of $1.67 \cdot 10^8$ n/sec measured from the side and from the end (diameter of the active portion, 16 mm, height, 36 mm, stainless steel capsule with wall thickness of 2 mm) and the spectrum from a similar source having a strength of $1.5 \cdot 10^5$ n/sec (diameter, 8 mm, height, 15 mm).

It is clear from Figs. 3-5 that the effect of mass and dimensions of the active portion of an (α, n) source primarily appears in the low-energy portion of the spectrum. For example, with an increase in the mass of the active portion of a Pu^{239}–Be source by approximately a factor of 10, the fraction of neutrons with energies below 1-2 MeV increased two to three times and the average energy of neutrons from the source decreased by 20-30%. In the case of (α, n) sources with targets of such isotopes as boron, fluorine, and lithium, these factors have a smaller effect on the shape of the neutron spectrum. This follows from Fig. 6 which shows neutron spectra from the isotopic sources Pu^{238}–Li–F, Am^{241}–Li–F, Pu^{238}–B, and Am^{241}–B. For sources employing Am^{241}, the ratio of target mass to mass of the α-radioactive isotope is two to three times greater than for the same type of sources employing Pu^{238}. Figure 6 also indicates that variation over relatively broad limits of the composition of the active portion of (α, n) sources displays no noticeable effect on the shape of the neutron spectrum. A similar result was obtained for Pu^{238}–Be sources.

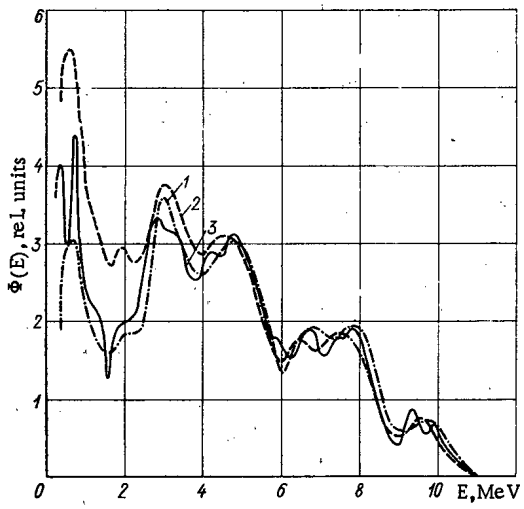

Fig. 4

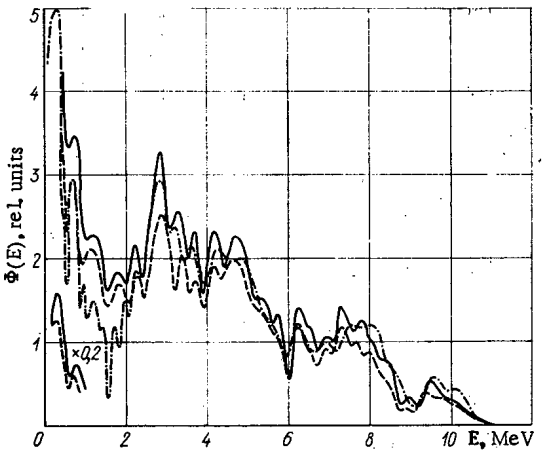

Fig. 5

Fig. 4. Energy spectra of neutrons from Pu^{238}–Be sources: 1-3) sources containing respectively 2, 160 [7], and 8 g of plutonium.

Fig. 5. Energy spectra of neutrons from Pu^{238}–Be sources: ——) spectrum from source with strength of $1.67 \cdot 10^8$ n/sec measured from the side; - - - -) the same, measured from the end; - · - · -) spectrum from source with strength of $1.5 \cdot 10^5$ n/sec.

The effect of the energy of the α-particles from a radioactive isotope on the shape of the neutron spectrum from (α, n) sources is shown in Figs. 7 and 8. Each pair of these sources was prepared by the same technique and had identical dimensions and composition of the active portion. It is clear from the figures that a comparatively small change in the energy of the α-particles from a radioactive isotope has a considerable effect on the shape of the neutron spectrum with the general tendency being that the average energy of the neutrons is reduced as the α-particle energy increases and the fraction of neutrons in the low-energy portion of the spectrum rises.

The effect of the method of preparing (α, n) sources on the shape of the neutron spectrum was studied with Pu^{238}–Be sources. For this purpose, the neutron spectra from a mixture of Pu^{238} dioxide and beryllium were measured at various times over a period of 1-6 h of continuous mixing. Similar measurements were made after pressing the mixture into pellets, after thermal treatment, and after sealing in a capsule. In all cases, the shapes of the neutron spectra were identical within the limits of experimental error of ±5%. The experiment showed that the method of preparation of isotopic (α, n) sources does not have the significant effect on neutron spectra which is sometimes ascribed to it. A similar conclusion can also be reached from a comparison of the neutron spectra from Po^{210}–Be and Am^{241}–Be sources for which the methods of preparation are different.

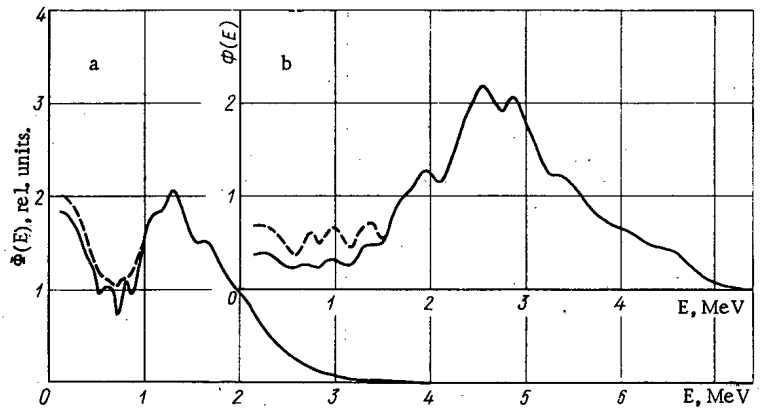

Fig. 6. Neutron energy spectra. a: ——) Pu^{238}–Li–F; - - - -) Am^{241}–Li–F; b: ——) Pu^{238}–B; - - - -) Am^{241}–B.

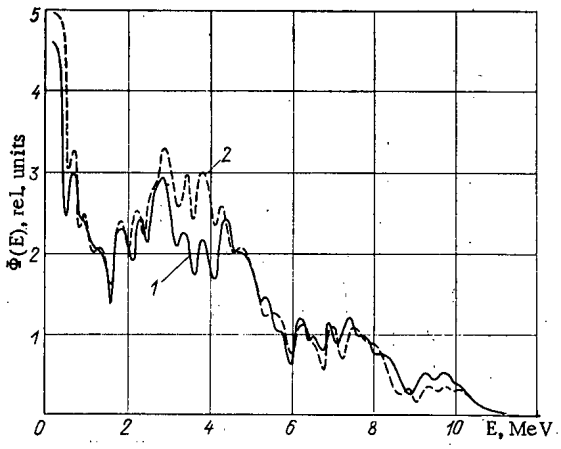

Fig. 7

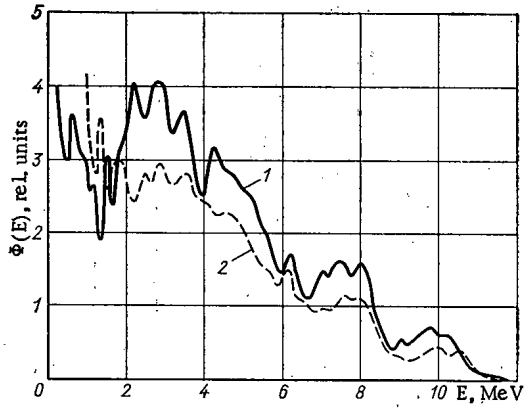

Fig. 8

Fig. 7. Energy spectra of neutrons from Pu^{239}–Be and Pu^{238}–Be sources (curves 1 and 2 respectively).

Fig. 8. Energy spectra of neutrons from Cm^{244}–Be and Cm^{242}–Be sources (curves 1 and 2 respectively).

If a predominant direction of α-particle motion with respect to the target is created in a source, the neutron spectrum from such a source may be significantly different from the neutron spectrum from a source of the same kind in which all directions of α-particle motion are equally probable. As an example, Fig. 9 shows the neutron spectrum from a Pu^{238}–Be source, the active portion of which consists of layers of plutonium and beryllium deposited on separate backings and then placed in contact. Figure 10 shows the neutron spectrum from such a source but with an α-particle collimator. A brass wire mesh of mesh size 0.3 × 0.3 mm was used as a collimator.

The data presented above indicates that the effect of the parameters of an isotopic (α, n) source on the shape of the neutron spectrum appears primarily in the low-energy portion of the spectrum; this effect is relatively minor at neutron energies above 2-3 MeV. It is therefore impossible to explain existing discrepancies in spectral shape (particularly for sources of the same kind) by a difference in parameters. Apparently, the basis for these discrepancies is to be found in systematic error and inexact information about the actual characteristics of the detectors used to measure the neutron spectra. For example, in the spectra from all Be (α, n) sources (see Figs. 1 and 2) measured with nuclear emulsions, the fraction of neutrons below 1-2 MeV is no more than a few percent while the data presented above, together with that derived indirectly from experiment and calculation, indicate that this fraction may amount to 10-30% of the total neutron yield from a source depending on source parameters. As a result of the underestimate of the low-energy portion of the spectrum, the average neutron energy calculated from a spectrum measured by means of nuclear emulsion is greatly overestimated in comparison with the energy determined by indirect measurements (for example, from slowing-down length).

In some cases, the methods for analyzing the results of measurement introduce considerable distortion of the spectral shape. Thus it was shown [7] that the use of the counting efficiency method for unfolding the neutron energy spectrum from the intrumental pulse-height distribution measured with a stilbene-crystal neutron spectrometer leads to significantly different spectral shapes being obtained from the same set of measurements.

In order to eliminate existing discrepancies in neutron spectra measured and analyzed by different methods, one ought to make a comparison of average energy and neutron output from a source calculated from the resultant spectrum with the same quantities determined from other, independent measurements.

In our experiments, such a comparison was made for a large number of isotopic sources of different kinds. In all cases, for example, the neutron yield, measured by an indirect method with an error of 3-5%, agreed with the yield calculated from the corresponding neutron spectrum within the limits of error indicated. Measurement of the neutron spectra and analysis of the results were made by the method described above.

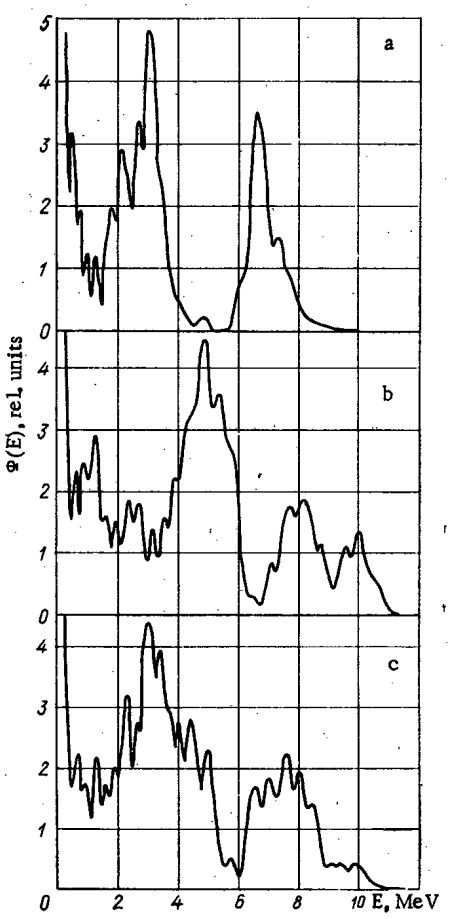

Fig. 9

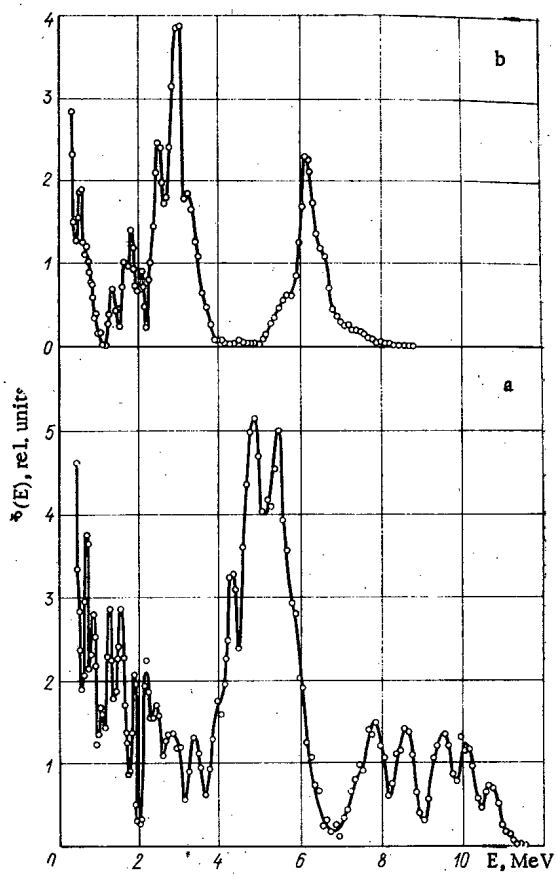

Fig. 10

Fig. 9. Neutron energy spectrum for a Pu^{238}–Be source with a layered active portion at an angle with respect to the predominant direction of α-particle motion: a) 180°; b) 0°; c) 90°.

Fig. 10. Neutron energy spectrum from Pu^{238}–Be source with layered active portion and mesh collimator between layers at angles of 0° (a) and 180° (b) to the predominant direction of α-particle motion.

It should be noted that agreement of the quantities mentioned, which were determined by different methods, is one of the fundamental, but still unsatisfactory, criteria for the reliability of the resultant neutron spectra. A more reliable estimate of the correctness of the results is obtained by an analysis of the fine structure in the spectrum.

LITERATURE CITED

1. S. Notarrigo, Nucl. Phys., 29, No. 3, 507 (1962).
2. P. L. Gruzin et al., At. Energ., 13, 583 (1962).
3. I. V. Goryachev et al., Neutron Monitoring, IAEA, Vienna (1967), p. 187.
4. K. Geiger and L. Van der Zwan, Appl. Radiation and Isotopes, 21, No. 4, 193 (1970).
5. V. I. Fominykh, At. Energ., 28, 159 (1970).
6. M. Anderson and R. Neff, Trans. ANS, 11, 481 (1968).
7. G. G. Doroshenko, in: Problems in Dosimetry and Radiation Protection [in Russian], No. 11, Atomizdat, Moscow (1970), p. 144.

THERMAL AND EPITHERMAL NEUTRON CROSS SECTIONS FOR VANADIUM ISOTOPES

V. P. Vertebnyi, M. F. Vlasov,
N. L. Gnidak, R. A. Zatserkovskii,
A. I. Ignatenko, A. L. Kirilyuk,
E. A. Pavlenko, N. A. Trofimova,
and A. F. Fedorova

UDC 539.172.4.162.2

There are a number of reasons for interest in the determination of neutron cross sections for vanadium isotopes. Determination of neutron absorption and scattering cross sections in the thermal region makes it possible to estimate radiation widths, which are little known in the region of medium mass numbers.

In addition, natural vanadium is often used as a standard in studies of neutron elastic and inelastic scattering in matter since it is an unique metal in which scattering is practically completely incoherent. Despite this, the energy dependence of neutron cross sections in the thermal and epithermal regions for vanadium isotopes and natural vanadium has been measured with insufficient accuracy. Values of the scattering cross section for natural vanadium, according to various authors [1-4], fall in the range 4.7-5.13 b with this spread often exceeding the announced accuracy. These discrepancies stimulated us not only to measure the energy dependence of the total cross section for natural vanadium but also to compare the vanadium scattering cross section in the epithermal region with the scattering cross sections of those nuclei for which cross sections are known with great accuracy (C, Bi).

For V^{50}, an odd–odd isotope rare in nature, there is no reliable data on neutron cross sections whatever. The tabulation [4] gives n, γ cross section values of (220 ± 180) and (55 ± 75) b for v = 2200 m/sec.

Measurements of Total Neutron Cross Section Energy Dependence for Natural Vanadium and V^{50}

All measurements were made by time of flight at the VVR-M reactor of the Institute for Nuclear Research, Academy of Sciences, Ukrainian SSR. A neutron spectrometer with a mechanical chopper was used for the measurements [5]. Energy ranges, energy resolutions and some parameters of the samples used are given in Table 1.

TABLE 1. Neutron Cross Section Values for Vanadium Isotopes at v = 2200 m/sec

Sample	Energy range, eV	Resolution, μsec/m	Cross section, b		
			σ_{tot}	$\sigma_{tot}(E \to \infty) = \sigma_s$	σ_a
$V_{(I)}$	110—0,1	0,5	—	4,7±0,1	5,5±0,6
$V_{(II)}$	4—0,03	1,8	—	4,70±0,03	5,31±0,05
$V_{(I)}$	1,7—0,007	3,5	10,06±0,05	4,6±0,1	5,4±0,1
$V_{(II)}$	1,7—0,007	3,5	10,11±0,06	4,79±0,06	5,37±0,09
$V_{(III)}$	1,7—0,007	3,5	10,00±0,05	4,8±0,1	5,28±0,15
$V_{(IV)}$	1,7—0,007	3,5	10,12±0,08	4,75±0,03	5,17±0,05
$V_2^{50}O_5$	1,7—0,007	3,5	48,3±0,5	4,1±1	44±2

Translated from Atomnaya Énergiya, Vol. 34, No. 5, pp. 355-358, May, 1973. Original article submitted July 21, 1972.

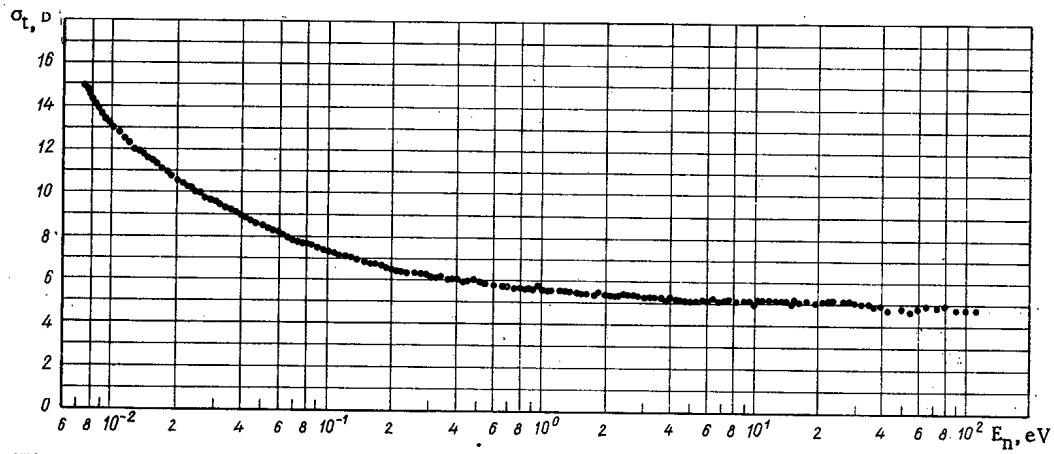

Fig. 1. Energy dependence of total neutron cross section for natural vanadium.

Pure vanadium metal of two kinds with a purity not less than 99.7% was used in measurements of the total cross section of natural vanadium. The samples were prepared in the form of tetragonal prisms in order that measurements might be made for various thicknesses. The vanadium metal samples V(I)–V(III) were produced by repeated electronic remelting of an ingot with a purity of 99.7%. As a result, a purity better than 99.8% was achieved. Certified data for the samples is given in Table 2. Corrections for impurities amounted to no more than 0.01 b. The isotope V^{50} was available only in the form of the pentoxide $V_2^{50}O_5$ with an enrichment of 22.7% in the desired isotope. To eliminate possible errors associated with atomic structure of the material, measurements were also made on the pentoxide of natural vanadium.

The dependence of total cross sections for natural vanadium on neutron time of flight was linear over the entire energy range.

Figure 1 shows total neutron cross sections for natural vanadium in the energy range 0.007–110 eV. All the measurements were analyzed by the least-squares method using the total cross section energy dependence

$$\sigma_{tot} = \text{const} + \sigma_a \sqrt{\frac{0.0253}{E}},$$

where the constant coincides with the scattering cross section and is designated in Table 1 by σ_{tot} ($E \to \infty$); σ_a is the neutron absorption cross section at v = 2200 m /sec.

TABLE 2. Characteristics of Vanadium Samples Used in Total Cross Section Measurements

Sample	Amount, nuclei /cm² · 10^{-20}	Impurity
$V_{(I)}$	115	Al, Fe, Si, Ni $< 10^{-2}$; S $< 5 \cdot 10^{-3}$; C $< 2 \cdot 10^{-2}$; $N_2 < 8 \cdot 10^{-2}$; $O_2 < 10^{-1}$
$V_{(II)}$	65	The same
$V_{(III)}$	194	" "
$V_{(IV)}$	110	C—0,02; N_2—0,01; O_2—0,03; H_2—0,001; Al $< 0,02$; Fe $< 0,01$; S $< 0,18$
V_2O_5	230	V_2O_4<2%; ammonium salts, $1.5 \cdot 10^{-2}$; heavy metals, $1 \cdot 10^{-2}$; alkali earths, $1 \cdot 10^{-1}$ sulfates, $4 \cdot 10^{-2}$; chlorides, $2 \cdot 10^{-2}$; material insoluble in hydrochloric acid, $3 \cdot 10^{-1}$
$V_2^{50}O_5$	221	Fe $< 0,025$; Na $< 0,12$; Ca $< 0,007$; K $< 0,004$; Cu $< 0,005$; Cr—0,06

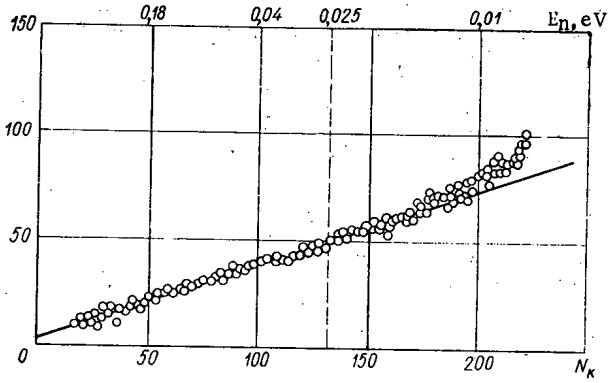

Fig. 2. Total neutron cross section of V^{50} as a function of neutron energy (upper scale) or of neutron time of flight (lower scale), where N_k is the time analyzer channel number. The dashed line denotes the neutron velocity v = 2200 m /sec.

TABLE 3. Characteristics of Samples Used in Scattering Cross Section Measurements

No.	Sample	Amount, nuclei/cm² · 10⁻²⁰	$n\sigma_{tot}$ at v = 2200 m/sec	Element content, %
1	$V_{(I)}$ (metal)	72,6	~0,07	> 99,7
2	$V_{(II)}$ (metal)	371	0,378	99,7
3	$V_{(III)}$ (metal)	711	0,725	99,7
4	Reactor graphite $C_{(I)}$	170	~0,1	—
5	Reactor graphite $C_{(II)}$	351	0,15	—
6	Bi (metal)	52,1	0,05	99,9
7	$V_2^{50}O_5$	9,9	0,056	—

TABLE 5. Neutron Cross Section Values for Vanadium Isotopes Recommended by the Authors

Isotope	σ_{tot}, b	σ_a, b	σ_s, b
V^{50}	48,3±0,5	41±4	7,5±1
Natural vanadium	10,06±0,03	5,28±0,03	4,75±0,03

TABLE 4. Vanadium Scattering Cross Sections Relative to Bismuth and Graphite

No.	Sample	Standard	σ_s of standard, b	σ_s of sample, b
1	$V_{(I)}$	Bi	9,29 [9]	4,73±0,08
2	$V_{(II)}$	Bi	9,29 [9]	4,80±0,08
3	$V_{(III)}$	Bi	9,29 [9]	4,79±0,08
4	$V_{(I)}$	$C_{(I)}$	4,74 [10]	4,75±0,02
5	$V_{(I)}$	$C_{(II)}$	4,74 [10]	4,71±0,05
6	$V_2^{50}O_5$	$V_{(I)}$	4,74	7,5±0,6

Measurements on natural vanadium pentoxide in that energy region where one can correctly allow for Bragg scattering agree, within the limits of statistical error, with calculated values for the cross sections if one uses the value 4.2 b for the scattering cross section in oxygen and 4.75 b for the scattering cross section in vanadium. Values for the total cross sections of vanadium pentoxide obtained in our measurements agree within the limits of statistical error with values obtained in [2]. However, these data were not used for the determination of σ_s and σ_a since it is difficult to account correctly for the effect of the dynamics of atomic motion on the value of the observed cross section for the V_2O_5 lattice over the entire neutron energy range. However, these difficulties may lead to an error of no more than 8% in determining the neutron absorption cross section for V^{50}.

Measurements of the total neutron cross section for V^{50} are shown in Fig. 2. These values were obtained by solution of a system of equations for the V_2O_5 and $V_2^{50}O_5$ samples and subsequent subtraction of the oxygen cross section equal to 4.2 b. The linear dependence of $\sigma_{tot}(E)$ for V^{50} is described by the equation $\sigma_{tot} = 7.1 + 41\sqrt{0.0253/E}$ with the scattering cross section being determined by direct measurement in 4π geometry. This dependence agrees with better than 5% accuracy with experimental data in the energy range 0.12-0.025 eV.

Neutron Scattering Cross Sections for V^{50} and Natural Vanadium

The total scattering cross section for natural vanadium was compared with the total neutron scattering cross section for reactor graphite and high-purity bismuth. The measurements were made in 4π geometry by time of flight using an He^3-filled neutron counter. The detector efficiency at a neutron energy of 0.0253 eV was 100% and 50% at 1 eV. The technique for taking into account multiple scattering and neutron flux attenuation in the sample is given in [7, 8] along with other details. The energy range 0.5-5 eV was used in obtaining the results. Table 3 shows the characteristics of the samples used and Table 4, values of the scattering cross section obtained as the result of measurements of the vanadium cross section relative to the cross section of bismuth and graphite (standard). The statistical accuracy of the measurements was 0.6% over a broad range of energies.

Measurements 2, 3, and 5 were made not so much to determine the vanadium scattering cross section as to check the correctness of the technique for introducing corrections which take into account multiple scattering and neutron flux attenuation in the sample. The corrections to measurements 1 and 4 are about 2%; they are large in measurements 2, 3, and 5. Nevertheless, consistent results were obtained. Scattering cross sections for the standards were taken from [9, 10]. It should be noted that in the literature there is a set of cross sections for bismuth which differ by amounts that go beyond the limits of statistical error. The only value given in Table 4 agrees with the most probable value for the vanadium scattering cross section according to our results, which is 4.75 ± 0.03 b.

The scattering cross section for V^{50} was determined by subtracting from the total scattering cross section of the $V_2^{50}O_5$ sample enriched in V^{50} the scattering cross section of V^{51} and the oxygen cross section, which was assumed to be 3.8 b. In the energy range 0.5-5 eV, the scattering cross section is independent of energy within the limit of 0.6 b and the average value over the range is 7.5 ± 1 b. The comparatively large error in the scattering cross section is associated with the fact that the effect of oxygen binding in the crystal lattice on the magnitude of the cross section is not precisely known.

DISCUSSION OF RESULTS

The most reliable values of the total and partial cross sections for vanadium isotopes on the basis of our measurements are shown in Table 5. They were obtained by statistical averaging over all series of measurements on different samples with inclusion of all known errors. Furthermore, the values of σ_{tot} and σ_a refer to the point v = 2200 m /sec; σ_s has the meaning of a scattering cross section for the free nucleus; σ_a is the neutron absorption cross section, and σ_{tot} is the total cross section. Note that the uncertainty in the scattering cross section, which was obtained by extrapolation of the total cross section to $E \to \infty$, associated with inaccuracy in determining the time of flight may amount to 0.2 b. The upper limit of the error associated with uncertainty in the concentration of chemical impurities can be no more than 0.02 b. The errors shown in Table 5 actually take into account both statistical spread and possible time drift of the equipment. The data for V^{50} were obtained by direct measurement for the first time and comparison with previous results is therefore inadvisable.

The total neutron scattering cross section for natural vanadium obtained by the authors is markedly below values obtained by others: 5.07 ± 0.1 [3] and 5.13 ± 0.02 b [6]. There is agreement within limits of error with the value 4.8 ± 0.2 b from data in [2] and with the scattering cross section value of 4.74 b at E_n = 1.44 eV given in [11]. It should be noted that there is good agreement between values for the scattering cross section determined by the authors by direct measurements (4.74 ± 0.03 b) and for the scattering cross section determined from the energy dependence of the total cross section (4.75 ± 0.02 b).

Using the known resonance parameters of the "positive" levels of V^{50}, and the total cross section and scattering cross section at v = 2200 m/sec, we showed that the total reaction width $\Gamma_a \leq 2.2$ eV and the relatively large absorption cross section is mainly produced by "negative" levels. If it is assumed there is only radiation capture in V^{50}, using Γ_γ = (0.6 ± 0.08) eV from [12], we obtain the following parameters for a level with negative energy: $|E_0| = \left(125^{+10}_{-40}\right)$ eV, $2g\Gamma_n^0 = \left(0.4^{+0.1}_{-0.2}\right)$ eV. For V^{51}, it was found that $\Gamma_\gamma \leq 2$ eV. In [13], it was indicated that Γ_γ = 2.05 eV for V^{51}. However, published sources do not confirm this value. With such a width, the cross section at the thermal point is completely explained by the contribution of "positive" levels with the optical scattering length having to be 6.4 F.

In conclusion, the authors are grateful to M. V. Pasechnik for consideration of the work, to V. S. Zolotarev and L. D. Gruzdeva for kindly supplying the isotope V^{50}, and to G. S. Padun and V. L. Nechitailo for assistance.

LITERATURE CITED

1. R. Schmunk et al., Nucl. Sci. and Engng., 7, 193 (1960).
2. P. Egelstaff, M/R 1147, AERE (1953).
3. V. Brockhouse, Canad. J. Phys., 31, 432 (1953).
4. Neutron Cross Sections, BNL-325, Second Edition, Suppl. No. 2, Vol. II, AZ-21 to 40.
5. M. F. Vlasov and A. L. Kirilyuk, Ukr. Fiz. Zh., 8, 947 (1963).
6. I. V. Gordeev et al., Nuclear Physics Constants [in Russian], Gosatomizdat, Moscow (1963).
7. V. P. Vertebnyi et al., Neutron Physics [in Russian], Proceedings of Conference, Naukova Dumka, Kiev (1971).
8. V. P. Vertebnyi et al., Ukr. Fiz. Zh., 13, 605 (1968).
9. W. Trifshäuser, Z. Physik, 186, 23 (1965).
10. L. Koester and W. Nistler, Phys. Rev. Lett., 27, 956 (1971).
11. L. Rayburn and E. Wollan, Nucl. Phys., 61, 381 (1965).
12. S. P. Kapchigashev, At. Energ., 19, 294 (1965).
13. S. M. Zakharov et al., Yadernye Konstanty, No. 7(2), 49 (1971).

NEUTRON-RADIATION ANALYSIS OF ROCKS AND ORES USING Ge(Li) SPECTROMETER

A. M. Demidov, V. A. Ivanov, and N. K. Tarykchieva

UDC 539.1.074.55:539.1.06

It has been noted [1-6] that Ge(Li) detectors broaden the possibility of neutron-radiation analysis methods of the composition of materials using thermal neutrons. The present paper analyzes in more detail the application of this method to elementary analysis of rocks and ores.

The experiments utilized a reactor thermal-neutron beam and isotope neutron beams (Po–Be and Cf^{252}). The γ-ray spectra were measured by 5 and 10 cm^3 Ge(Li) detectors; the pulses were recorded on an AI-4096 analyzer. During long-term measurements (more than 6 h), the spectrometer resolution was 12-18 keV when $E_\gamma > 3.5$ MeV. The measurements using thermal-neutron beams (intensity $4 \cdot 10^7$ neutrons $/cm^2 \cdot$ sec) were conducted with samples weighing 1-30 g. Here, despite the small solid angle through which the detector scans the sample ($\Omega \approx 5 \cdot 10^{-4}$ of 4π), good statistical accuracy is achieved in 1-2 h.

Figure 1 shows the experimental setup for using isotope neutron detectors. The samples weighed 10-25 kg. The samples were placed in polyethylene packets; fine samples were mixed with water. When the source activity was 10^7 neutrons/sec, the spectrum measurement time was about 6 h. The γ-ray spectra obtained under various conditions for a single sample were identical above 4 MeV (except for the 6129 keV oxygen line, which is most intense for the Po–Be source type).

We will survey the results of analyzing copper–nickel, mercury, and rare-earth ores.

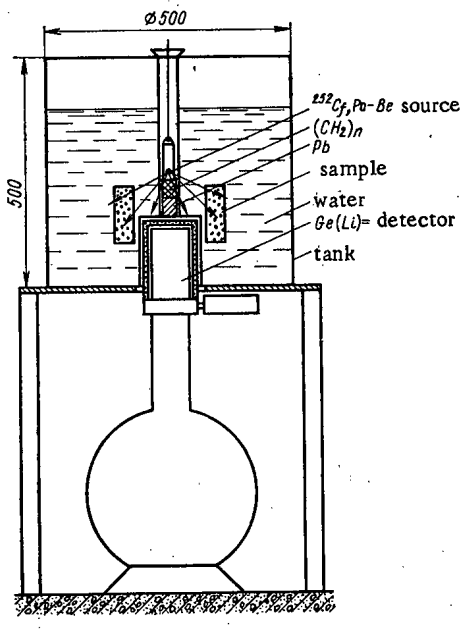

Fig. 1. Experimental setup using isotope source.

The elementary composition of Cu–Ni ores was studied using Po–Be and Cf^{252} neutron sources, and also using the IRT-M reactor neutron beam. The spectrum obtained with the Po–Be source is shown in Fig. 2. In the energy range above 4 MeV, the peaks with emission of two annihilation γ-rays are most intense; above these peaks we show the corresponding γ-transition energies. The total-absorption peaks and the peaks corresponding to emission of a single annihilation γ-ray are indicated by f and s, respectively. On all three peaks, we indicate the element to which they belong.

The element content was determined from analysis of characteristic line intensities (8996 keV for Ni; 7914 keV for Cu). Table 1 shows the relative content for several Cu–Ni ore samples (the Si content was taken to be 100).

Based on chemical-composition data (mainly for oxides), we can estimate the Cu and Ni content (in wt. %) and also find the analysis sensitivity threshold. Thus, for sample number 2, the Cu and Ni contents are both approximately 4% and the sensitivity threshold for Ni is 0.1% and for Cu is 0.2%. The sensitivity threshold was determined on the assumption that we can record a peak with amplitude equal to twice the rms error on the continuous-distribution background.

Translated from Atomnaya Énergiya, Vol. 34, No. 5, pp. 359-363, May, 1973. Original article submitted June 28, 1972.

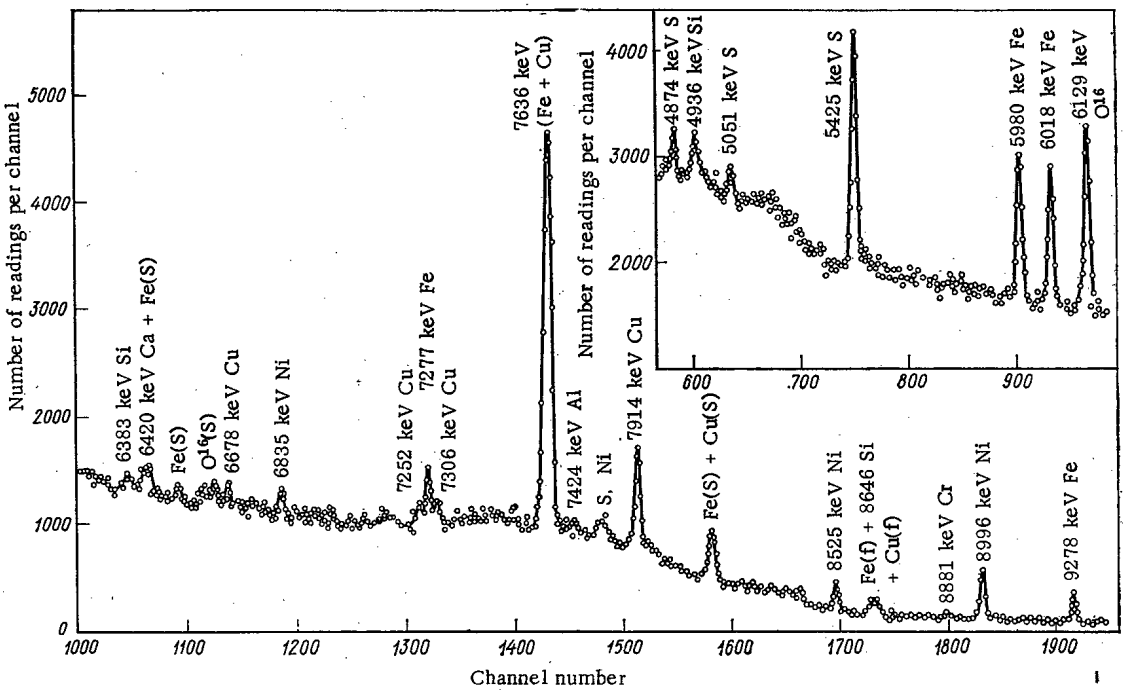

Fig. 2. γ-Ray spectrum for Cu–Ni ore (sample number 2).

The mercury-ore samples were analyzed only in an isolated beam of thermal neutrons in the IRT-M reactor. Five samples with various mercury content were studied. Since the base of the sample was SiO_2 (98% by chemical analysis), it was convenient to determine the content relative to the very intense silicon radiative-capture γ-line E_γ = 4936 keV (I_γ = 61%). There are many intense mercury γ-lines in the spectrum; most of them appeared in the investigated samples: 4676, 4740, 4759, 4843, 5050, 5388, 5658, 5907, and 6458 keV. For quantitative determination of the Hg content in these samples, it is convenient to choose those γ-lines close to the silicon 4936 keV line, i.e., 4740 keV + 4759 keV (I_γ = 6.81% + 2.46%), 4843 keV (I_γ = 5.24%), and 5050 keV (I_γ = 5.35%). Unfortunately, the most intense Hg line – 5967 keV (I_γ = 15.5%) – is of little use for determining Hg content, because the total-absorption peak for the Si line 4936 keV is energetically close to the peak for double emission of the Hg line 5967 keV.

For the sample whose spectrum is shown in Fig. 3, the Hg content is 0.28 ± 0.05%. Here the accuracy is determined mainly by the size of the errors in nuclear data (thermal-neutron capture cross sections and absolute values of γ-line intensities). Under the given conditions, we can reliably determine Hg content higher than 0.03%. By improving the experimental conditions, we can lower this figure by about a factor of 3.

When ores containing rare-earth elements are studied, main attention is given to gadolinium, whose content can be determined with high sensitivity by the neutron-radiation method because of its very large thermal-neutron capture cross section. Measurements were made using a Cf^{252} source and the reactor neutron beam. The gadolinium content was determined from the 5584 keV γ-line. The more intense lines with energies 6750 and 5903 keV were not used, since the former is close in energy to the very intense titanium line 6762 keV, and the latter coincides with a calcium line. Besides this, the analysis is complicated

TABLE 1. Relative Content of Elements in the Samplies Studied

Sample No.	S	Na	Ca	Ti	Al	Cl	Cu	Cr	Ni	Fe
1	13	—	4,5	1,8	30	0,5	$\ll 1$	4,6	2,8	44
2	210	16	5,7	—	34	—	67	39	71	296
3	—	—	29	3,4	71	0,3	1,0	4,5	1,3	41

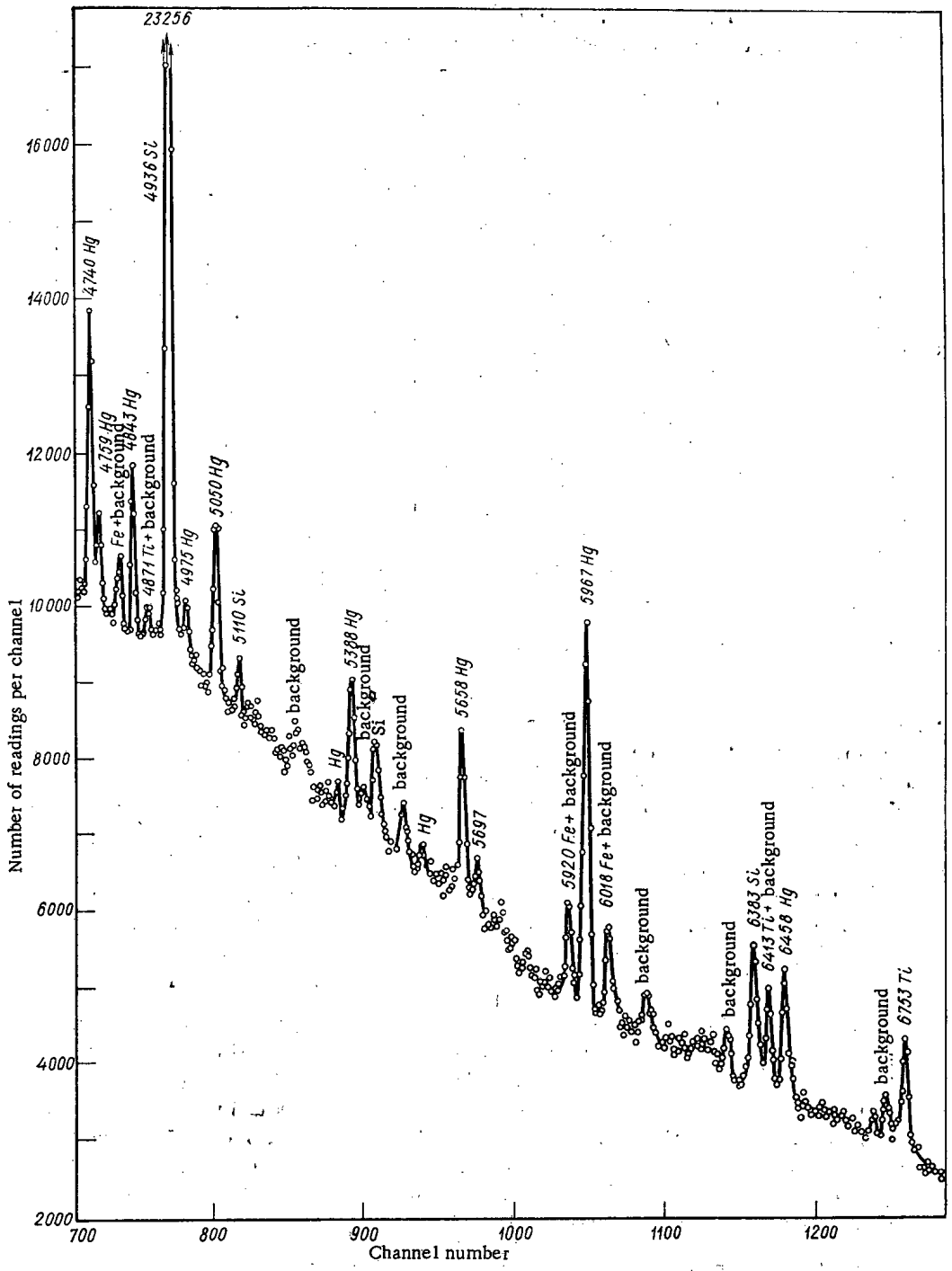

Fig. 3. γ-Ray spectrum for mercury ore.

by the fact that the intense titanium line at 6420 keV coincides with the most intense calcium line. Therefore, calcium in the presence of titanium must be analyzed using the 4419 keV line.

The method's sensitivity threshold for gadolinium when using the 5584 keV line is $2 \cdot 10^{-3}\%$. This was $5 \cdot 10^{-4}\%$ during analysis using the 6750 keV line in the absence of titanium (the gadolinium content in the sample was $1.2 \cdot 10^{-2}\%$). Detailed analysis of the line intensities showed that in the investigated sample there was less than 1% calcium and about 1.5% titanium.

We should note that when analysis is made in a neutron beam one can use the low-energy portion of the spectrum, where, moreover, the sensitivity for determining Gd is higher than during spectral measurements with $E_\gamma > 4$ MeV [6].

TABLE 2. Abundance P, Minimum Industrially Useful Content M, and Sensitivity K of the Neutron-Radiation Method when Studying Rocks and Ores

Element	P, %	M, %	K, %	Element	P, %	M, %	K, %	Element	P, %	M, %	K, %
H	0,88	—	0,02	Cu	0,01	0,7	0,2	La	$7\cdot10^{-5}$	0,06	1,0
He	$8\cdot10^{-7}$	—	—	Zn	$2\cdot10^{-2}$	3	1,7	Ce	$3{,}1\cdot10^{-4}$	0,2	6
Li	$5\cdot10^{-3}$	0,3	2	Ga	$5\cdot10^{-4}$	0,001	0,7	Pr	$5\cdot10^{-5}$	0,05	2
Be	$5\cdot10^{-4}$	0,007—0,7	7	Ge	$1\cdot10^{-4}$	—	5	Nd	$1{,}8\cdot10^{-4}$	0,03	0,2
B	$1{,}4\cdot10^{-3}$	0,06	14	As	$5{,}5^{-4}$	5	2	Sm	$7\cdot10^{-5}$	0,02	0,01
C	$8{,}7\cdot10^{-2}$	—	24	Se	$8\cdot10^{-5}$	0,002	0,5	Eu	$0{,}2\cdot10^{-5}$	0,002	0,1
N	$3\cdot10^{-2}$	10	3	Br	$6\cdot10^{-4}$	0,02	3,8	Gd	$7\cdot10^{-5}$	0,01	0,0005
O	49,5	—	—	Kr	$1{,}9\cdot10^{-8}$	—	0,4	Tb	$1\cdot10^{-5}$	0,002	2
F	$2{,}7\cdot10^{-2}$	15	64	Rb	$3{,}4\cdot10^{-3}$	0,1	20	Dy	$7\cdot10^{-5}$	0,003	0,03
Ne	$5\cdot10^{-7}$	—	6,4	Sr	$1{,}7\cdot10^{-2}$	1,4	6	Ho	$1{,}2\cdot10^{-5}$	0,004	1,1
Na	2,64	10	0,6	Y	$5\cdot10^{-3}$	0,002	16	Er	$6\cdot10^{-5}$	0,02	0,5
Mg	1,94	3	26	Zr	$2{,}3\cdot10^{-2}$	0,4	11	Tu	$1\cdot10^{-5}$	0,002	0,8
Al	7,5	10	2	Nb	$6\cdot10^{-5}$	0,02	26	Yb	$7\cdot10^{-5}$	0,005	0,04
Si	25,7	40	1,1	Mo	$1{,}7\cdot10^{-4}$	0,005—1	3,3	Lu	$1{,}5\cdot10^{-5}$	0,002	1,5
P	0,12	3,5	4	Tc	$1\cdot10^{-8}$	—	—	Hf	$2\cdot10^{-3}$	0,1	0,3
S	0,048	5	0,6	Ru	$5\cdot10^{-6}$	—	16	Ta	$2\cdot10^{-5}$	0,03	5
Cl	0,19	20	0,02	Rh	$1\cdot10^{-6}$	—	0,2	W	$7\cdot10^{-3}$	0,2	0,8
Ar	$3{,}5\cdot10^{-4}$	—	0,5	Pd	$5\cdot10^{-6}$	—	5,5	Re	$1\cdot10^{-7}$	0,01	1,1
K	2,4	8	1,0	Ag	$4\cdot10^{-6}$	0,003	0,5	Os	$5\cdot10^{-6}$	—	2,3
Ca	3,4	20	1,1	Cd	$1{,}1\cdot10^{-5}$	0,1	0.005	Ir	$1\cdot10^{-6}$	—	0,1
Sc	$6\cdot10^{-4}$	0,04	0,06	In	$1\cdot10^{-5}$	0,01	0,4	Pt	$2\cdot10^{-5}$	0,0003	1,7
Ti	0,58	2	0,05	Sn	$6\cdot10^{-4}$	0,1	100	Au	$5\cdot10^{-7}$	0,0001	0,1
V	$1{,}6\cdot10^{-2}$	0,3	0,2	Sb	$2{,}3\cdot10^{-5}$	1	6	Hg	$2{,}7\cdot10^{-6}$	0,1—1	0,01
Cr	$3{,}3\cdot10^{-2}$	20	0,1	Te	$1\cdot10^{-6}$	0,002	3	Tl	$1\cdot10^{-6}$	0,01	13
Mn	$8\cdot10^{-2}$	25	0,1	J	$6\cdot10^{-6}$	0,001	4,5	Pb	$8\cdot10^{-4}$	1,2	4,2
Fe	4,7	25	0,3	Xe	$2{,}9\cdot10^{-9}$	—	0,3	Bi	$3{,}4\cdot10^{-6}$	0,01—2	80
Co	$4\cdot10^{-3}$	0,15	0,06	Cs	$7\cdot10^{-5}$	0,05	1,5	U	$5\cdot10^{-4}$	0,02—0,1	4,6
Ni	$1{,}8\cdot10^{-2}$	0,25	0,1	Ba	$4{,}7\cdot10^{-2}$	10	7				

When the sensitivity threshold for determining various elements in ores and rocks is evaluated, one should take into account the fact that when the element's content is low and the capture cross sections are large, the overall character of the spectrum will be determined by elements such as Fe, Cl, Si, K, Ti, Al, Na, and Ca. When the spectrum remains relatively constant, the sensitivity will be determined mainly by the quantity $\sigma I_\gamma / A$ for the element being studied (here, σ is the thermal-neutron capture cross section; I_γ is the intensity of the strongest nuclear γ-transition; A is the atomic weight). Taking this into account, we determined the sensitivity threshold of the neutron-radiation method for other elements. Here, we utilized values found by the present authors for Cu, Ni, Hg, and Gd. The results obtained are shown in the last column of Table 2. The other columns of the table give the abundance P of the elements in the earth's crust and the minimum industrially useful concentrations M of these elements in ores [7].

We must note that the figures given in Table 2 were obtained from experiments with a neutron source producing $1\cdot10^7$ neutrons/sec and a detector with volume 10 cm^3 and resolution ≤ 18 keV when $E_\gamma \approx 7$ MeV. Increasing the neutron flux and improving the detector characteristics will allow us to shorten the measurement time or increase the method's sensitivity by a factor of 3-5. The data in Table 2 cannot be used when the Fe content is very high; they are also not applicable to highly enriched ores. The sensitivity decreases when the most characteristic line of the given element changes to overlap the γ-line of the main rock components. Despite the indicated limitations, Table 2 allows one to evaluate qualitatively the capabilities of the neutron-radiation method in analyzing rocks and ores.

The authors express their thanks to G. V. Sukhov for his help in the work.

LITERATURE CITED

1. R. Greenwood, Trans. Amer. Nucl. Soc., 10, 28 (1967).
2. A. M. Demidov, L. I. Govor, and V. A. Ivanov, At. Energ., 28, 115 (1970).
3. D. Duffey et al., Nucl. Instr. and Meth., 80, 149 (1970).
4. J. Trombka et al., Nucl. Instr. and Meth., 87, 37 (1970).
5. L. I. Govor, A. M. Demidov, and V. A. Ivanov, At. Energ., 30, 66 (1971).
6. L. I. Govor, A. M. Demidov, and N. K. Tarykchieva, Program and Theses of Reports at the XXI Annual Conference on Nuclear Spectroscopy and the Structure of the Atomic Nucleus (Moscow, 1971) [in Russian], Part 2, Nauka, Leningrad (1971), p. 135.
7. Industrial Requirements for Grades of Raw Minerals. Handbook for Geologists [in Russian], Vol. 1-69 (First and Second Editions), Gosgeotekhizdat, Moscow (1959-1971).

YIELDS OF FRAGMENTS OF THE SPONTANEOUS FISSION OF Cf^{252}

N. V. Skovorodkin, G. E. Lozhkomoev,
K. A. Petrzhak, A. V. Sorokina,
B. M. Aleksandrov, and A. S. Krivokhatskii

UDC 539.173.7:546.799.8

The yields of fragments of the spontaneous fission of Cf^{252} have been determined in a number of studies [1-3], but in only one of them [3] were the yields of a sufficiently large number of fragments, and a curve of the dependence of the yields of the fragments on their mass constructed. In the latter study, the yields were determined according to the method of R-values, relative to the yields of the fragments of fission of U^{235} by slow neutrons. The comparison fragment selected was Mo^{99}, the absolute yield of which was determined by a radiochemical method. In earlier studies [1, 2], the yields of only a few fragments were obtained, with a rather large error, since a very small amount of californium was used. Therefore, we were interested in repeating the determination of the yields with a larger amount of californium, and using a different method of rendering absolute.

At the time this work ended, the article [4] was published, in which the yields of fragments of the spontaneous fission of Cf^{252} in the region of masses 95-147 were determined relative to the yields of the fragments of fission of U^{235} with thermal neutrons. The comparison fragment selected was Ba^{140}, the yield of which for the spontaneous fission of Cf^{252} was taken equal to the yield of mass 140 (5.8%), obtained by measuring the kinetic energies of the fragments [5].

In this work several methods were used in the determination of the yields. For one group of fragments the absolute yields were determined with a measurement of the number of fissions in a sample of californium and a measurement of the absolute β-activity of the isolated fragments. For another group of fragments the yields were determined either relative to the yield of some fragment with known absolute yield or according to the method of R-values, using γ-spectroscopy, with respect to the yields of fragments of the fission of Pu^{239} by slow neutrons.

TABLE 1. Absolute Yields of Fragments of the Spontaneous Fission of Cf^{252}

Isotope	$T_{1/2}$	Absolute yield, %	Number of experiments	Literature	
				[3]	[4]
Zr^{95}	65,5 days	1,29±0,04	3	1,37	1,2±0,1
Mo^{99}	66,96 h	2,76±0,08	5	2,57±0,03	2,7±0,1
Pd^{109} *	13,47 h	7,65±0,35	4	5,69±0,59	—
Pd^{112}	21,0 h	3,77±0,11	3	3,65±0,18	—
Ag^{113g} *	5,3 h	2,99±0,10	4	4,23±0,28 †	—
Te^{132}	77,7 h	1,78±0,08	5	1,75±0,03	2,5±0,1
Ba^{139}*	82,9 min	6,24±0,20	4	5,73±0,16	5,7±0,2
Ba^{140}	12,8 days	6,49±0,17	6	6,32±0,54	5,8
Pr^{143}	13,59 days	7,13±0,18	3	5,94±0,35	6,4±0,2
Nd^{147}	11,06 days	4,48±0,14	3	4,69±0,08	4,5±0,2

* The yields of Ba^{139}, Ag^{113g}, and Pd^{109} were calculated on the basis of the relative yields of Ba^{139} in comparison with Ba^{140}, Ag^{113g} in comparison with Ag^{111}, and Pd^{109} in comparison with Pd^{112}, determined in this work: 0.960 ± 0.013; 0.585 ± 0.007, 2.030 ± 0.061, respectively.
† Total yield of Ag^{113}.

Translated from Atomnaya Énergiya, Vol. 34, No. 5, pp. 365-371, May, 1973. Original article submitted July 27, 1972.

TABLE 2. Relative and Absolute Yields of Isotopes of the Rare Earth Elements and Yttrium

Isotope	$T_{1/2}$	Relative yield	Absolute yield, %	Number of experiments	Literature	
					[3]	[4]
Y^{91}	58,8 days	0,153±0,002	0,69±0,03	3	0,59±0,06	—
Y^{92}	3,53 h	0,157±0,002	0,70±0,03	3	—	—
Y^{93}	10,18 h	0,222±0,004	1,00±0,04	3	0,83±0,03	—
Ba^{140}	12,8 days	1,452±0,021	6,50±0,24	4	6,32±0,54	5,8
La^{141}	3,85 h	1,372±0,024	6,15±0,23	3	—	—
Ce^{141}	32,51days	1,427±0,023	6,39±0,24	8	5,9±0,3	5,8±0,4
La^{142}	85 min	1,397±0,099	6,26±0,49	3	—	—
Ce^{143}	33,4 h	1,478±0,032	6,62±0,26	3	5,94±0,35	—
Pr^{143}	13,59 days	1,501±0,021	6,73±0,25	5	—	6,4±0,2
Ce^{144}	284,3 days	1,396±0,020	6,25±0,23	5	—	5,7±0,2
Pr^{145}	5,98 h	1,250±0,019	5,60±0,20	3	—	—
Nd^{147}	11,06 days	1,000	4,48*	8	4,69±0,08	4,5±0,2
Nd^{149}	1,8 h	0,630±0,027	2,82±0,15	3	—	—
Pm^{149}	53,09h	0,697±0,003	3,12±0,11	3	2,65	—
Pm^{151}	28,40 h	0,447±0,007	2,00±0,07	3	2,18	—
Sm^{153}	47,1 h	0,289±0,004	1,29±0,05	3	1,41±0,03	—
Sm^{156}	9,4 h	0,118±0,002	0,53±0,02	3	—	—
Eu^{156}	15,21 days	0,151±0,002	0,68±0,02	5	0,703±0,008	—
Eu^{157}	15,15 h	0,126±0,002	0,56±0,02	3	—	—
Gd^{159}	18,0 h	0,0794±0,0010	0,36±0,01	3	—	—
Tb^{161}	7,2 days	0,0454±0,0007	0,20±0,01	4	0,15	—

* The absolute yield of Nd^{147} was taken from Table 1.

In the experiment we used a source of californium containing 2.911 μg Cf^{252}. Collectors in which fission fragments were retarded were subjected to analysis. The collectors, representing disks 24 mm in diameter from aluminum foil 0.1 mm thick, were situated at a distance of 0.1 mm from the source. The solid angle of collection was equal to 0.494 of 4π. A thin (50 $\mu g/cm^2$ thick) nickel film was placed between the source to the collector, and only in the case of determination of the absolute yields was the film removed. The time of exposure was varied from several hours to several days, depending on the fragments studied.

The working source was prepared by electrolytic deposition of californium on disks of polished platinum 0.1 mm thick. The diameter of the active spot was ~8 mm; the thickness of the layer on account of deposition of extraneous impurities did not exceed 50 $\mu g/cm^2$.

The efficiency of collection, i.e., the influence of absorption of fragments in the layer of the substance of the source, was determined by a comparison of the specific (per event of fission) β-activity of the fragments collected on collectors from the working and standard targets. The foil for the collection of fragments was placed at a distance of 0.1 mm from the targets, covered with thin collodion films (10-15 $\mu g/cm^2$) to prevent transfer of californium from the source to the collector, exposed for 20 min, and the summary β-activity of the collectors measured after a definite time in a 4π-counter. The efficiency of collection for the conditions selected proved equal to 0.94 ± 0.005. Thus, (46.8 ± 0.3)% of the total number of fission fragments in the working source fell on the collectors.

The standard target was prepared by collection of recoil aggregates in an electric field on platinum foil polished to the twelfth class [6]. The number of fissions in this sample was measured by an argon–methane 2π-ionization chamber with a grid.

The number of fissions in the working source was determined by comparison with a standard source according to number of neutrons. The neutrons were recorded with a crystal of stilbene. The pulses from the neutrons and γ-quanta were separated according to time of deexcitation in the crystal [7]. The degree of discrimination of the γ-quanta was brought to 10^{-3}. A comparison of the samples was performed repeatedly in various geometries, to exclude the influence of scattering of neutrons from the surrounding objects.

The number of fissions in the working volume proved equal to $(1.081 \pm 0.14) \cdot 10^8$ fissions/min, which corresponds to (2.911 ± 0.038) μg Cf^{252} at $T_{1/2}$ = (84.9 ± 0.4) years [8].

TABLE 3. Absolute Yields of Fragments of the Spontaneous Fission of Cf^{252}, Determined According to the Method of R-Values

Isotope	$T_{1/2}$	Absolute yields, %		Number of experiments	Pu^{239} [13]	Literature	
		scintillation spectrometer	crystalline spectrometer			[3]	[4]
Zr^{95}	65,5 days	1,35±0,07	—	3	4,99	1,37	1,2±0,1
Zr^{97}	17,0 h	—	1,64±0,07	2	5,55	1,54±0,15	1,8±0,1
Ru^{103}	39,6 days	—	5,67±0,23	2	5,63	—	4,8±0,4
Rh^{105}	35,9 h	—	5,98±0,37	2	5,50	5,99±0,21	—
Ag^{111}	7,5 days	5,11±0,18	—	3	0,27	5,19±0,29	—
Pd^{112}	21,0 h	3,85±0,21	—	2	0,12	3,65±0,18	—
Ag^{113g}	5,3 h	2,99±0,10	—	4	—	4,23±0,38*	—
Cb^{115g}	53,5 h	1,89±0,08	—	3	0,038	2,28±0,13*	—
Sb^{127}	91,2 h	0,110±0,005	—	2	0,378	0,130±0,008	—
I^{131}	8,05 days	—	1,21±0,07	2	3,75	1,27±0,18	1,8±0,1
Te^{132}	77,7 h	1,79±0,06	1,92±0,08	3+2	5,13	1,75±0,03	2,5±0,1
I^{133}	20,8 h	—	3,28±0,15	2	6,90	2,77±0,20	3,9±0,3
Xe^{135}	9,2 h	—	3,87±0,14	2	7,25	4,33±0,08	4,9±0,4
Cs^{136} †	13,5 days	0,038±0,002	—	3	0,0835	0,0351	—
Cs^{141}	30 yrs	4,84±0,20	—	3	6,48	4,40	5,2±0,2
Ce^{143} ‡	32,51 days	—	6,39 ••	2	5,13 ••	5,9±0,3	5,8±0,4
Ce^{143}	33,4 h	—	6,29±0,47	2	3,99	5,94±0,35	6,4±0,2
Ba^{140} †	12,8 days	6,49 ••	6,41±0,23	2	5,58	6,32±0,54	5,8
Mo^{99} ‡	66,96 h	—	2,76 ••	2	6,17••	2,57±0,03	2,7±0,1

* Total yields of masses 113 and 115.

† Value of the independence of the yield of Cs^{136} in the fission of Pu^{239} by thermal neutrons, taken from [19].

‡ Reference isotopes, relative to which the comparison was performed.

•• Values of the yields taken from Tables 1 and 2 (this work) and from [10].

The absolute cumulative yields of Zr^{95}, Mo^{99}, Pd^{112}, Te^{132}, Ba^{140}, Pr^{143}, and Nd^{147} were obtained directly. Immediately after exposure, the collector of fragments was dissolved in hydrochloric acid in the presence of isotopic carriers, individual elements were isolated, and then aliquot portions of solutions of the purified elements were applied on ashed collodion films to measure the absolute acitivity in a flow-type 4π-β-counter. The time from the end of irradiation to the moment of separation from californium was the same in all cases (1.5-3 h), which made it possible to neglect the correction for the decay of Cf^{252}, transferred from the source to the collector. The amount of californium transferred to the collectors was determined according to the α-activity of the latter. For each successive collector, a correction was introduced for loss of californium. The correction was negligible; even for the 10th collector it was only $\sim 0.5\%$.

Molybdenum, tellurium, and palladium were isolated successively by an anion exchange method from the same sample. Molybdenum was separated from tellurium by its extraction with ether from 6 M HCl and then analyzed, analogously to [9]. Tellurium was purified by precipitation of metallic tellurium with SO_2, repeated anion exchange purification, and repeated precipitation of metallic tellurium. For the purification of palladium, the dimethylglyoximate of palladium was precipitated, still another anion exchange cycle was conducted, AgCl precipitated twice, and, finally, metallic palladium was precipitated with formic acid.

The activity of Pd^{112} was determined according to the activity of the daughter Ag^{112}.

Barium, zirconium, and the rare earth elements were isolated from individual samples. The purification of zirconium was accomplished by the phenylarsonate method [10]. Barium was purified by precipitation of $BaCl_2$, $BaSO_4$, and a cation exchange cycle [11]. Two precipitations of cerium and lanthanum fluorides, followed by separation with ammonium α-hydroxyisobutyrate, was used for the purification of the rare earth elements [12]. Cerium was used as a carrier for neodymium and praseodymium, since it is eluted from the column after praseodymium and does not interfere with the determination of neodymium and praseodymium. The chemical yield of cerium was determined by a colorimetric method [9].

The yields of Ba^{139}, Ag^{113}, and Pd^{109} were measured relative to the yields of Ba^{140}, Ag^{111}, and Pd^{112}, respectively. In this case barium was purified by three precipitations of $BaCl_2$ (the first precipitation was conducted in the presence of a strontium carrier), precipitation of $La(OH)_3$, and rapid purification with NH_4CH_3COO on a small column with a cation exchange resin [9]. Silver was purified by the usual method [10]. The absolute yields of the indicated elements, obtained in this work, are cited in Table 1.

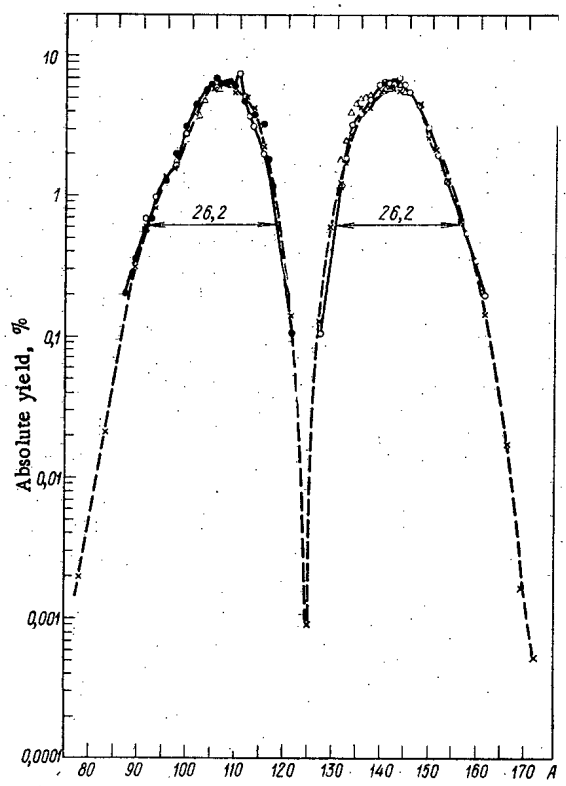

Fig. 1

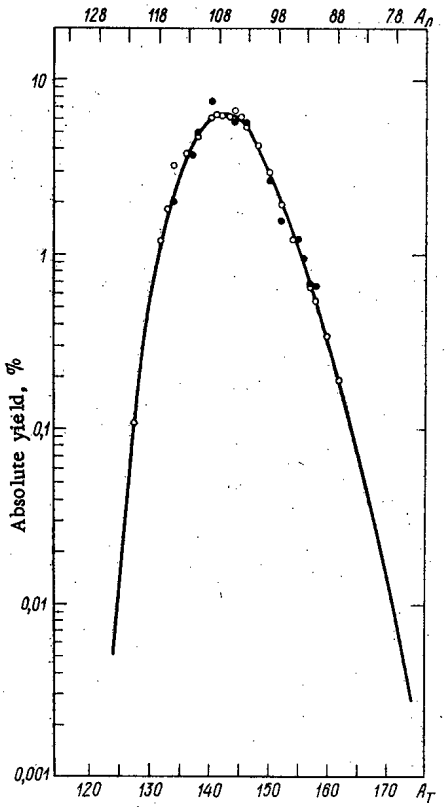

Fig. 2

Fig. 1. Curve of the yields of fragments of spontaneous fission of Cf^{252}: –○–, –●–) this work [○) experimental values, ●) reflected points]; ———×———) data of [3]; Δ) data of [4].

Fig. 2. Curve of the yields of fragments of spontaneous fission of Cf^{252}: ●, ○) light and heavy fragments, respectively; reflection was performed symmetrically relative to mass 124.

The yields of isotopes of the rare earth elements and yttrium were determined analogously to [12], by a radiochemical method relative to the yield of Nd^{147}. Not Ce^{144}, but Nd^{147} was selected as the comparison isotope, since cerium, as was indicated above, served as a carrier in the determination of the absolute yields of Pr^{143} and Nd^{147}. The results of this series of measurements are cited in Table 2.

The yields of Zr^{95}, Zr^{97}, Ru^{103}, Rh^{105}, Ag^{111}, Pd^{112}, Cd^{115g}, Sb^{127}, Te^{132}, I^{131}, I^{133}, Xe^{135}, Cs^{136}, Cs^{137}, Ba^{140}, and Ce^{143} were determined by γ-spectrometry relative to the yields of the corresponding fragments in the fission of Pu^{239} with thermal neutrons according to the R-values [13, 14]:

$$R=\frac{(Y_X/Y_R)_{Cf^{252}}}{(Y_X/Y_R)_{Pu^{239}}}=\frac{(A_X/A_R)_{Cf^{252}}}{(A_X/A_R)_{Pu^{239}}}, \quad (1)$$

where Y_X and Y_R are the absolute yields of the investigated and comparison isotopes for the spontaneous fission of Cf^{252} and for the fission of Pu^{239} by slow neutrons; A_X and A_R are the intensities of the selected γ-lines of the investigated and comparison isotopes, corrected for accumulation during exposure and for decay by the moment of measurement.

The yields of stable members of the mass chains were taken from [13]. The corrections for the independent yields of these isotopes were calculated on the assumption of a Gaussian distribution of charge with C = 0.80 ± 0.14 and with Z_p for the fission of U^{235} with thermal neutrons taken from [15]. The values of Z_p for the fission of Pu^{239} with thermal neutrons was calculated according to a semiempirical formula [16]:

$$Z_p(Pu^{239})=Z_p(U^{235})+\Delta Z, \quad (2)$$

where

$$\Delta Z=\frac{1}{2}(Z_{Pu^{239}}-Z_{U^{235}})-0.19(A_{Pu^{239}}-A_{U^{235}})+0.19(\bar{\nu}_{Pu^{239}}-\bar{\nu}_{U^{235}}).$$

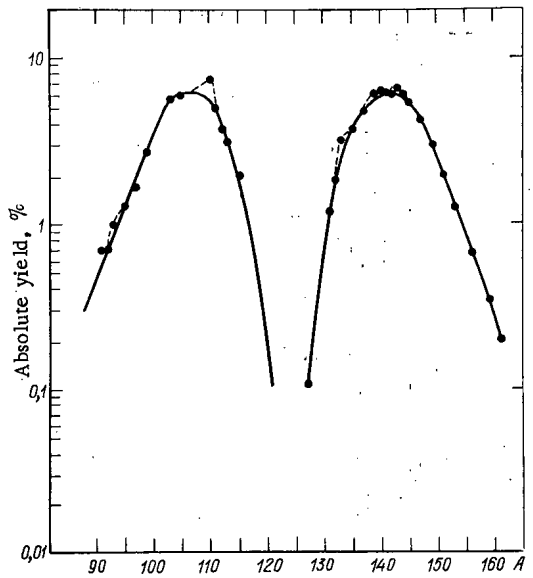

Fig. 3. Fine structure in the distribution of yields of fragments of the spontaneous fission of Cf^{252} (the solid line shows the smooth curve, while the dotted line shows the position of the fine structure).

TABLE 4. Cumulative Yields of the Final Members of the Mass Chains

Isotope	Absolute yield, %	
	of radioactive fragment	of stable member of chain
Zr^{97}	1,64±0,06	1,65±0,06
Pd^{112}	3,77±0,11	3,78±0,11
Ag^{113g}	2,99±0,10	3,21±0,11
Cd^{115g}	1,89±0,08	2,01±0,08
Te^{132}	1,82±0,06	1,87±0,06
Cs^{137}	4,84±0,18	4,85±0,18
Xe^{135}	3,87±0,14	3,88±0,14
Ba^{140}	6,50±0,18	6,51±0,18
La^{142}	6,26±0,49	6,27±0,49

Note. The total yields of masses 113 and 115 were calculated on the basis of the experimental data on the yields of the isomers of Cd^{115} in the fission of heavy elements with thermal neutrons [20], and also on the basis of the decay scheme of Pd^{113} [21].

A comparison of the γ-activity of isotopes with large yields, such as Zr^{97}, Ru^{104}, Rh^{105}, Te^{132}, I^{131}, I^{133}, Xe^{135}, Ba^{140}, and Ce^{143}, was performed on a semiconductor Ge(Li)-γ-spectrometer without preliminary chemical separation. The volume of the Ge(Li) crystal was equal to 13 cm^3; its resolution was 4 keV for the γ-line of Cs^{137}. We used Mo^{99} and Ce^{141} as the comparison isotopes.

A comparison of the γ-activity of Zr^{95}, Ag^{111}, Pd^{112}, Cd^{115g}, Sb^{127}, Cs^{136}, Cs^{137}, and I^{131} was conducted on a scintillation γ-spectrometer with NaI(Tl) crystal with dimensions 3 × 2 cm, after preliminary chemical isolation of the individual elements. The resolution was ~10% for the γ-line of Cs^{137}. Ba^{140} was used as the comparison isotope. The elements zirconium, antimony, and silver were isolated from individual samples and purified by the usual method [10]. The remaining elements were isolated successively from one sample. Tellurium and palladium were purified just as indicated above; the precipitation of CdS and $La(OH)_3$ from ammonia medium, followed by repetition of the anion exchange cycle, was used for the purification of cadmium. For the purification of cesium it was collected from alkaline medium on the resin KU-1, then cation exchange purification conducted on the resin Dowex 50 × 8 [17]; cesium and rubidium were separated with 0.5 M HCl on the resin KU-1 [18] and precipitated with Cs_2PtCl_6.

The results of these measurements are presented in Table 3.

The errors of the direct determination of the yields consist of the arithmetic mean errors of the measurement of the number of fissions in the sample, determination of the effectiveness of the collection of fragments, determination of the chemical yield of the carrier, and measurement of the absolute β-activity. The errors of the absolute yields, obtained by a relative method, include not only the indicated errors, but also the errors of the measurement of the β- or γ-activity, while in the method of R-values, also the errors of the determination of the absolute yields of the fragments of fission of Pu^{239} by slow neutrons.

The curve of the mass yields (Fig. 1) was constructed according to the yields of the stable members of the mass chain, corrections for the independent yields of which were introduced just as for Pu^{239} (see above). In most cases these corrections were very small. Table 4 presents the calculated values of the yields of the final members of the mass chains, differing from the measured yields of the precursors.

The results obtained in this work are presented in Tables 1-4 and in Figs. 1-3. The sum of the yields of heavy fragments (measured values and extrapolated according to the smooth curve) is equal to 102.7%. The complete width of the peak of the heavy fragments at 1/10 of the maximum height of the smooth curve is equal to 26.2 mass units, which is 4.4 mass units greater than in the fission of U^{235} by slow neutrons. This is due to the increase in the yields of fragments of highly asymmetrical fission.

The peak of the light fragments was constructed on the basis of the experimental values of the yields of the light fragments and reflected points (at $\bar{\nu} = 4$) in the region of the maximum. The total width of the

TABLE 5. Fine Structure of Mass Distributions of Primary and Secondary Fragments

Primary pair of fragments	Proposed position of fine structure	Experimental data on the presence of a fine structure	
		this work	other work
118	114	113 absent 114 not determined	113 [3] 113-114 absent [5]
134	133—134	133 134 not determined	135 [3] 134 [4] 137 [5]
112	109—110	109	110—111 [5]
140	139—140	139—140	140—141 [5]
106	104	104 not determined	104—105 [5]
146	144	143—144	143 [1, 2, 4, 5]
103	102	102 not determined	102 absent [5]
149	147	147 absent	147 absent [3-5]
100	99	99 absent	99 absent [3] 99—100 [5]
152	149—150 The peaks will probably be smoothed out	149—150 absent	149-150 absent [3, 5] [3, 5]
—	—	93—94	90 [5] 94 [3]
—	—	—	154 [3]

peak proved the same as for the heavy fragment, while the area under the curve of the yields was 98.2%. The average mass of the light and heavy fragments proved equal to 106.0 ± 0.8 and 141.9 ± 1.0, respectively, which is in good agreement with the data of [3, 5], while the value $\bar{\nu} = 4.1 \pm 1.0$.

From Fig. 2 it follows that the peaks of the heavy and light fragments coincide rather well when they are reflected relative to mass 124. The area under this curve is equal to 100.9%.

In the region of the peak of the heavy fragments, the fine structure for masses 133, 139-140, and 143-144 is distinctly visible, while in the region of the peak of the light fragments the fine structure for the mass 109 and a broadening of the curve for the masses 93-94 appear. From experiments on the transit time in spontaneous fission of Cf^{252}, an increased yield of mass pairs 123-129, 118-134, 112-140, 103-149 was detected in the distribution of the primary masses [22], while in [23] it was detected for the mass pairs 112-140, 106-146, 100-152.

The position of the fine structure in the distribution of the secondary masses is determined by the dependence of the number of emitted electrons on the mass of the primary fragments. Variations in the probability of the emission of neutrons with the mass of the fragments may leave this structure unchanged, increase it or smooth it out, and may also lead to the appearance of peaks not associated with the process of separation of fragments. On the basis of the dependence of the number of neutrons on the mass of the primary fragments, taken from [24, 25], we can roughly estimate for what masses in the final distribution the appearance of a fine structure of the primary distribution should be expected (Table 5).

Thus, the detected fine structure in the distribution of the final masses of the peak of heavy fragments is well correlated with the fine structure of the yields of the primary masses. The fine structure of the supplementary fragments of the peak of the light fragments is noted chiefly in [5], conducted by the method of correlated energies and rates with good resolution with respect to energies with the aid of semiconductor detectors. This fine structure was not detected by the radiochemical method, since it corresponds to very short-lived fragments, the measurement of the yield of which involves great difficulties.

The deviation of the yields from a smooth curve, which we detected in the region of masses 93-94, evidently was explained on account of the variation of $\nu(M)$. In this region of masses, $d\nu/dM$ differs sharply (0.3-0.2) from its average value (0.08) [24].

As was shown by Thomas and Vandenbosh [26, 27], the fine structure of the primary distribution of mass is correlated with the variation of the maximum energy of excitation of fragments, calculated from the semiempirical formula of masses of Cameron or Ziger. Considering that the energy of excitation in

the case of separation into even–even fission fragments is higher than the energy of excitation in the case of separation into fragments with odd masses and has a periodicity of ~5 mass units, Vandenbosh concludes that fission occurs primarily into even–even fragments.

The authors would like to express their deep gratitude to E. I. Biryukov for performing the measurements on the crystalline γ-spectrometer, and would also like to thank V. A. Yakovlev and E. I. Vystorobskii for providing the scintillation γ-spectrometer and for their aid in the measurements.

LITERATURE CITED

1. L. Glendenin and E. Steinberg, J. Inorg. Nucl. Chem., 1, 45 (1955).
2. J. Cuninghame, J. Inorg. Nucl. Chem., 6, 181 (1958).
3. W. Nerwik, Phys. Rev., 119, 1685 (1960).
4. R. Harbour et al., Radiochim. Acta, 15, 146 (1971).
5. H. Schmitt et al., Phys. Rev., 137B, 837 (1965).
6. B. M. Aleksandrov et al., At. Energ., 33, 821 (1972).
7. V. I. Kukhtevich, A. A. Trykov, and O. A. Trykov, Pribory i Tekhnika Eksperimenta, No. 2, 45 (1967).
8. B. M. Aleksandrov et al., At. Energ., 28, 361 (1970).
9. A. V. Sorokina et al., At. Energ., 31, 99 (1971).
10. Yu. M. Tolmachev (editor), Radiochemical Analysis of Fission Products. Collection of Articles [in Russian], Izd-vo AN SSSR, Moscow–Leningrad (1960).
11. O. M. Lilova and B. K. Preobrazhenskii, Radiokhimiya, 2, 731 (1960).
12. N. V. Skovorodkii et al., Radiokhimiya, 12, 487 (1970).
13. H. Fickel and R. Tomlinson, Canad. J. Phys., 37, 916 (1959).
14. D. Gordon et al., Nucleonics, 24, No. 12, 62 (1966).
15. A. Whal et al., Proc. of the Second Sympos. on the Phys. and Chem. of Fission, SM 122/116, Vienna (1969), p. 813.
16. C. Coryell et al., Canad. J. Chem., 39, 646 (1961).
17. V. M. Vdovenko, A. S. Krivokhatskii, and N. V. Skovorodkii, Radiokhimiya, 13, 416 (1971).
18. O. M. Lilova and B. K. Preobrazhenskii, Radiokhimiya, 2, 728 (1960).
19. W. Grummit and G. Milton, J. Inorg. Nucl. Chem., 20, 6 (1971).
20. Yu. A. Zysin, A. A. Lbov, and L. I. Sel'chenko, Yields of Fission Products and Their Mass Distribution [in Russian], Gosatomizdat, Moscow (1963).
21. H. Nakahara et al., J. Inorg. Nucl. Chem., 33, 3239 (1971).
22. S. Wheststoune, Jr., Phys. Rev., 131, 1232 (1963).
23. J. Fraser et al., Bull. Amer. Phys. Soc., 8, 370 (1963).
24. J. Terrell, Phys. Rev., 127, 880 (1962).
25. H. Bouman et al., Phys. Rev., 126, 2120 (1962).
26. T. Thomas and A. Vandenbosh, Phys. Rev., 133B, 976 (1964).
27. T. Thomas and A. Vandenbosh, Bull. Amer. Phys. Soc., 7, 37 (1962).

DEVELOPMENT OF NUCLEAR ENERGY AND PROBLEMS OF ENVIRONMENTAL PROTECTION IN CZECHOSLOVAKIA*

J. Neumann†

We can state unambiguously that a stage of rapid industrial growth has arrived in the field of nuclear energy. This is conditioned mainly by the following causes:

a) the electric energy produced by large atomic power stations in most areas of the world can compete economically with the electrical energy obtained by burning the classical fuels;

b) from the viewpoint of their effect on the environment, atomic power stations are more advantageous than electric power stations using coal and petroleum residues;

c) the production of nuclear energy is necessary from the viewpoint of the future fuel-energy balance of all industrially developed countries and is an important factor in the development of the "third world."

Broadening of the energy base is a presupposition of economic development. This can be confirmed by the following data:

	Industrially developed countries	Developing countries
Gross national product (dollars per capita per year)	2000-5000	100-200
Demand for primary energy (tons of conventional fuel per capita per year)	4-10	0.1-0.2
Demand for electrical energy (kWh per capita per year)	3000-10,000	100-200

In 1970, the 3.5 billion people in the world used approximately 6 billion tons of coventional fuel; however, 80% of this was used by the one third of humanity in the industrially developed countries. We expect that the world population by the year 2000 will be 6.5 billion and the demand for primary energy will grow to 36 billion tons of conventional fuel. Such growth is impossible to achieve using only the classical forms of fuel, both relative to supplies and relative to the environment. Therefore, it is necessary to give extraordinary attention to developing nuclear energy; in science and technology we must pay special attention to decreasing the negative environmental effects of producing electrical energy.

In connection with this, the main tasks are the development of fast reactors, magnetohydrodynamics installations, nuclear fusion, and cryogenic technology and superconductor technology for electric transmission.

Czechoslovakia is already one of the countries with high energy demand; the growth of energy demand in our country is shown by the following data:

* The articles on pp. 456-475 were given as reports at the International Conference on Radioecology, which took place in Czechoslovakia in 1972 (see the September, 1972, issue of Atomnaya Énergiya, p. 795). The report by J. Neumann is printed without change. The other reports were reworked by the authors for our journal.

† Chairman of the Commission on Atomic Energy, Czechoslovakia.

Translated from Atomnaya Énergiya, Vol. 34, No. 5, pp. 373-376, May, 1973.

	1970	1980	1990	2000
Demand for primary energy (tons of conventional fuel per capita)	5.7	7.2	9.0	12.0
Demand for electrical energy (kWh per capita)	3430	6400	11,000	19,000

Although further use of our own resources (mainly brown coal and hydroelectric potential) and significant increase in imports (mainly petroleum and natural gas) is planned, it is necessary to prepare the development of nuclear energy in Czechoslovakia approximately according to the following schedule: 1980, 1700 MW; 1985, 3700 MW; 1990, from 10,000 to 12,000 MW (integral).

Czechoslovakia participates in the integrated development of atomic energy of the member nations of COMECON which is directed towards:

a) constructing pressurized-water thermal reactors producing 4400 and 1000 MW (electrical);

b) developing fast sodium-cooled reactors, which would preduce 600 and 1000 MW (electrical);

c) jointly solving the problems of transporting and processing used fuel and safely storing radioactive wastes.

We can expect, according to the prognoses, that by the year 2000 this program will include the problems of jointly developing magnetohydrodynamics installations and thermonuclear reactors.

While integrated development of the classical and nuclear energy resources in the COMECON countries are being solved jointly, environmental protection must be taken into account; the socialist system has all the prerequisites for doing this.

With planned development of nuclear energy, we do not expect any significant increase in radioactivity over the natural background, while the probability of accidents producing radioactive fallout is very small. Moreover, we assume that, as the classical fuels are replaced by nuclear fuels, the living conditions and quality of the environment will improve. Despite this, I think it is necessary to give the required attention to problems of public health and the effect of nuclear installations on man and on the biosphere. This necessity is conditioned mainly by the fact that these installations will, nevertheless, have an influence on a significant part of the population. The psychological problem is not to be underestimated. Before nuclear energy is introduced, it will be necessary to prove that it will not adversely affect the environment. Therefore, nuclear energy is in worse condition than other branches of industry were when they first arose. The goal of the scientific-research programs financed by the Czechoslovak Commission on Atomic Energy is not only to prove the safety of nuclear installations, but also to find ways to improve living conditions while using atomic energy.

The problems being solved can be formulated as follows:

a) research, development, and introduction of measurement methods for controlling environmental radioactivity;

b) study of the effect of radioisotopes and ionizing radiation on the biosphere;

c) development of systems for preventing radiation accidents and effective measures to apply in case they occur;

d) the use of radioisotope methods for improving conditions in spheres of activity not directly related to radioactivity.

We expect that the results of scientific research will give us additional and sufficient information on estimating the dangers to workers at nuclear installations and the large population groups near them. Although any damage compared to the natural background is unlikely during the planned increase in radioactivity, it is necessary to give this problem the attention due to it. I should like to define in a few words the tasks included in the State scientific and technological plan, or which are directly related to this problem.

For example, in biology, medicine, and agriculture at present, the problem of population contamination is being studied using natural radioactive isotopes in several parts of Slovakia and sanitary evaluations are being made. A long-term evaluation of biosphere contamination is being conducted and information for

determining the effect of atomic power stations on the environment is being collected. Radioactive fallout is being systematically measured, and the Sr^{90} content in adults' and children's teeth is being determined as a measure of body irradiation. The relationship between Sr^{90} content in food and its retention in organisms is being analyzed in order to estimate the possible danger. Using experiments on models, the kinetics of hygienically important radioisotopes are being studied; this accumulates data for determining internal contamination of humans. Experiments conducted on various forms of animals should produce the necessary relationships which will allow a more realistic extrapolation of experimental data to man.

The second group of problems being solved concerns the effect of low radiation doses on biological systems. The goal in this study is to explain the mechanism of pathological changes caused by ionizing radiation and to estimate the probabilities of damage at low dose levels. Important in these studies are the search for appropriate methods for timely determination of radiation damage and working out biological methods for measuring low doses.

A system of sanitary measures is being worked out in case of radiation accidents, and methods for quickly determining their scale and danger with respect to external irradiation and internal contamination are being studied. Means are being examined for limiting the incidence of Cs^{137} on animal products, for separating out the most important uranium decay products in the biosphere, and for working out methods for choosing appropriate agricultural products for cultivation near energy-producing reactors.

The next part of the research program is still in embryo. We include here studies using radioisotope methods of the possibility of minimizing some harmful results of technological growth on living conditions. We will mention here, for example, the possibility of replacing chemical preservation means by radiation methods if the latter should prove harmless or nearly harmless. We also have studies of the genetic effect of chemicals and ionizing radiation. Using tracer compounds, we can study the activity of pesticides and the means by which they are carried to humans. Other chemical substances used in agriculture are also being studied. We expect that it will be possible to find rational methods for using these substances, while decreasing their negative effects on living conditions.

In nuclear technology there are several instruments for monitoring and measuring radioactive substances and ionizing radiation directly at the work site or outside of it. These include instruments for monitoring radioactivity in water, soil, the atmosphere, etc. Czechoslovak instrument manufacture produces detectors for radioactive air contamination, apparatus for measuring low activities, which is used for monitoring fluids, instruments for monitoring and measuring the radioactive aerosols used in atomic centers and radioisotope laboratories, individual and portable monitoring radiometers and special instruments for monitoring the radioactivity level at uranium mines, and also monitoring instruments for unusual emergency situations.

In the field of radioanalytic methods, there are being developed, first of all, methods for activation analysis of very small elemental impurities in materials, and also in sediments near industrial centers. The results of these studies were used successfully in determining traces of several elements in agricultural products.

In the field of measuring very low activities, there are being developed and applied, in part, methods for measuring H^3 and C^{14} acitivity using liquid scintillators and proportional counters; these are used especially for radioisotope dating of samples in hydrogeological and archeological studies. Besides this, methods are being developed for nondestructive determination of very low radioactivity levels by using $\beta-\gamma$- and $\gamma-\gamma$-coincidences. To apply the results of these studies, special laboratories are being planned which must answer current needs.

Under studies of radioactive indicators, methods are being developed for studying the flow of ground waters, especially when using a single bore hole, which can be used when studying hydrogeological conditions of a certain region, including various contamination sources. Besides this, new methods are being developed for studying the effect of SO_4^{-2} ions during atmospheric corrosion of construction materials and their coverings.

In the field of hydrogeology, methods are being developed for using radioactive indicators in the study of water flow in low reservoirs. These methods will serve to determine the feasibility of using reservoirs for the needs of projected central heating plants and for observing alluvial motion, especially on the Danube. Methods and efficiency studies are also being worked out for discharge-water purifying units, especially

methods for measuring characteristic delay time in standard round and square settling tanks and for checking the relationship between the delay time and the purification efficiency.

The State plan is to include also other research items, for instance, the determination of radioactivity in water both from natural sources and in water contaminated by atomic power stations.

We must mention the system of burying radioactive wastes. We should remember that transportation of low-activity wastes and their burial in the State "Richard" vault are provided for, and there are no organizational, technical, or economic problems at present. Experiments are being conducted jointly with public-health organizations on the incineration of biological radioactive wastes, and it should soon be decided whether Czechoslovakia will build a State center for incinerating them.

The problem of removing and storing radioactive wastes is being worked out taking into account the needs of nuclear energy and processing irradiated fuel. The following problems are being studied: selective methods for separating and fixing radioisotopes from highly active wastes; the technology for incorporating radioactive wastes in asphalt and concrete; radioactive wastes of the fuel cycle in fast reactors; gaseous radioactive separation; incorporation of highly active wastes in silicate melts; deactivation; storage of radioactive wastes in geological formations; separation of long-lived and technologically valuable isotopes; technical and economic questions of radioactive-waste decontamination and surface deactivation; purification of discharge water by electric coagulation; biological purification of radioactive discharge water.

The Institute for Study, Production, and Use of Isotopes provides the State's individual dosimetry service. At present, monitoring is provided for approximately 9000 radiologists and workers dealing with radioactive materials. There is a need for monitoring an additional 4000-5000 workers. β-, γ-, x-ray, and thermal-neutron doses are monitored. Dosimetry of fast neutrons using solid-state dosimeters and dosimetry of the background radiation using thermoluminescent glasses are being studied. Research is also being conducted in the field of photoluminescence.

The broad range of research being conducted will allow us to solve many important problems of environmental protection in Czechoslovakia.

PROBLEMS OF RADIOECOLOGY IN CONNECTION WITH THE DEVELOPMENT OF NUCLEAR POWER

M. Zaduban

The main purpose of this article is to draw attention to factors which accompany the development of nuclear power and produce an effect on the environment. Using the desirable and undesirable features of the development of nuclear power as a basis, mankind can and must set up the proper conditions for its peaceful "coexistence" with the biosphere. At the same time, it is essential to formulate criteria for an assessment of such coexistence, taking account of economics and of natural laws.

In ecological investigations there is a progression from an individual to a population, then to a biocenosis, to an ecosystem, to the environment, and finally to the biosphere [1]; in contrast to this, in radioecological investigations the sequence is reversed and the system of ecological investigation is enlarged by the addition of a source of unstable nuclides.

The purpose of radioecology is a comprehensive investigation of biospheric processes in which natural and artificial nuclides take part, their relationship to the environment and to the food chains of mankind, animals, and plants, and also the possibility of modifying these processes. Radioecological investigations must, in our opinion, be based on the following fundamental principles:

mankind's productive activity, intensively being increased through the effects of the scientific and technological revolution, is not an undesirable factor, as long as it takes place in accordance with the fundamental laws of development of nature and human society;

on the basis of the fundamental principles of socialist society, we must apply to the fullest extent all technological and restorative measures aimed at preventing or reducing the contamination of our external environment, and in particular, we must solve the problems involved in allocating sites for the construction of nuclear power complexes, bearing in mind the fact that this process must conform to fundamental natural laws and the requirements of economic expediency.

Sources of Radioactivity in the Biosphere

Unstable Natural Nuclides. Unstable natural nuclides may be classified as follows.

1. Nuclides with $Z < 80$ (K^{40}, V^{50}; Rb^{87}, etc.) and with $80 < Z < 93$ (members of the thorium series, the uranium series, the actinouranium series, and the neptunium series). These are important from the point of view of the formation of the natural background and the wastes produced in the processing of thorium and uranium. The amounts of nuclides in the biosphere may be arranged in decreasing order as follows: $Rb^{87} \gg Th^{232} > U^{235} + U^{238}$, $K^{40} > Sm^{147}$, $Nd^{144} > V^{50}$, $Bi^{209} > In^{115}$, Sb^{123} . . .

Natural unstable nuclides are present in different quantities in different media. Their total activity is assumed to be 10^{11} Ci [2]. The amounts of natural unstable nuclides present in the soil are shown in Table 1. The amounts of natural unstable nuclides in the waters of rivers are different; for example, the Danube near Gundremingen carries approximately 8 Ci of K^{40}, 1.4 Ci of Ra^{226}, and 0.4 Ci of U^{238} per year.

2. Unstable nuclides produced in nuclear reactions, such as (α, n), (α, p), (α, γ), $(n, 2n)$, (n, p), etc., for example, K^{38}, A^{38}, Li^{7}, C^{14}, U^{237}, etc.; their activity is very low.

Faculty of Natural Sciences, P. J. Šafarík University, Košice, Czechoslovak Socialist Republic.
Translated from Atomnaya Énergiya, Vol. 34, No. 5, pp. 376-380, May, 1973.

Declassified and Approved For Release 2013/09/15 :
CIA-RDP10-02196R000400010005-5

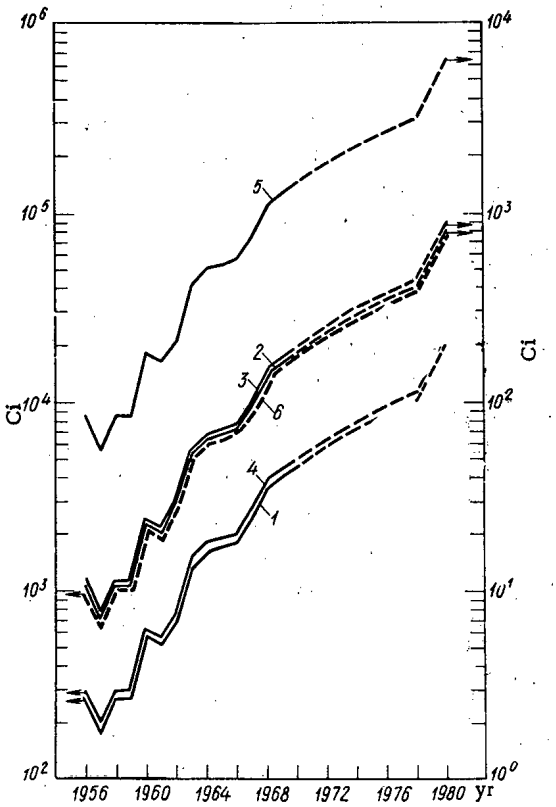

Fig. 1

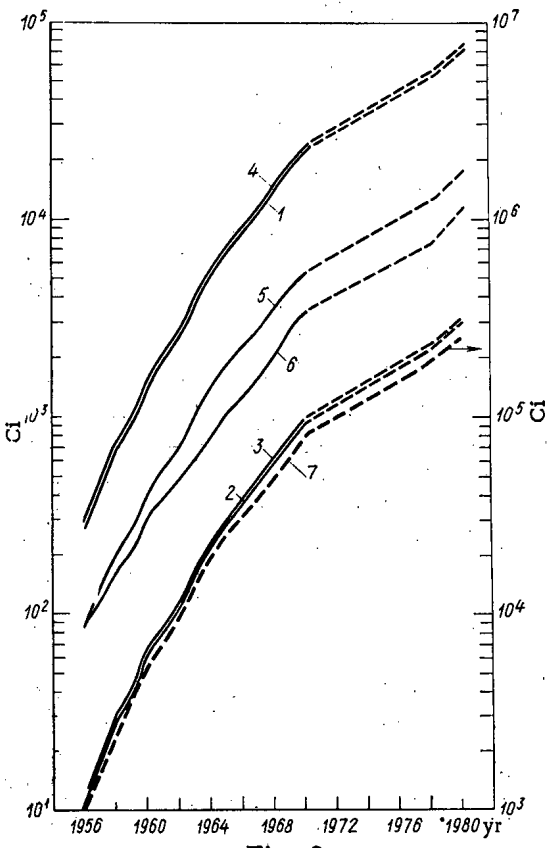

Fig. 2

Fig. 1. Amounts of the most important decay products formed in the processing of thorium and uranium in different years, including amounts predicted for the years up to 1980: 1) ionium, radium; 2) protactinium; 3) actinium; 4) RaD; 5) MsTh, RdTh; 6) total amount.

Fig. 2. Cumulative amounts of decay products formed in the processing of thorium and uranium, including amounts predicted for the years up to 1980: 1) ionium, radium; 2) protactinium; 3) actinium; 4) RaD; 5) MsTh; 6) RdTh; 7) total amount.

3. Unstable nuclides produced by nuclear reactions of cosmic-ray products – for example, H^3, Be^7, C^{14}, Na^{22}, P^{32}, P^{33}, S^{35}, and Cl^{39}; the nuclides formed in the largest quantities are H^3 and C^{14} (the amount of C^{14} so formed is 7.5 ± 2.7 pCi/g of carbon).

4. Nuclides heavier than uranium; the only such nuclides known in nature thus far are neptunium and Pu^{224}.

Artificial Unstable Nuclides. The sources of these nuclides are: indicator methods used in the investigation of biospheric processes; waste products of nuclear, radiochemical, and other laboratories; nuclear explosions, which have introduced large amounts (of the order of gigacuries) of fission products into the biosphere, mainly Sr^{90} and Cs^{137}, with the formation of so-called global fallout; and waste products from the nuclear-power industry, as well as waste products formed after the burial of radioactive substances.

Waste Products from the Nuclear-Power Industry. Waste products are formed at each step of the following sequence: extraction of thorium and uranium; processing of thorium and uranium; production of fuel elements; nuclear reactor; processing of irradiated fuel elements; burial of radioactive waste products.

Quantitative data concerning the waste products formed in the first two steps of this sequence are shown in Table 2. According to the data of [4], the activity of decay products formed during the extraction and production of thorium and uranium and present in the biosphere today is in excess of 10^5 Ci; in 1971 alone, the activity of decay products entering the biosphere was more than $2 \cdot 10^4$ Ci. The amount of thorium and uranium decay products will increase in the future (see Figs. 1 and 2). The activity of the waste products

TABLE 1. Amounts of Natural Unstable Nuclides Present in Soil [3]

Nuclide	dis/sec per kg of soil	Ci/km²
K^{40}	120—920	0,73—5,6
Rb^{87}	20—550	0,12—3,3
Ra^{226}	10—75	0,06—0,46
Th^{232}	0,4—50	0,0024—0,3
U^{235}	10—110	0,06—0,67
U^{238}	10—110	0,06—0,67

TABLE 2. Quantity and Activity of Fundamental Radioactive Nuclides Formed in the Extraction and Production of 1,000 kg of Uranium (Equilibrium state)

Nuclides	Amount, g	Activity, Ci
Io	18,5	0,349
Pa	0,31	0,014
Ac	$2{,}06 \cdot 10^{-4}$	0,015
Ra	0,35	0,35
RaD	$4{,}89 \cdot 10^{-3}$	0,382
MsTh	$4{,}80 \cdot 10^{-4}$	0,113
RdTh	$1{,}37 \cdot 10^{-4}$	0,114
Po	$8{,}52 \cdot 10^{-5}$	0,387
ThX	$7{,}17 \cdot 10^{-7}$	0,116

of a modern uranium plant amounts to several curies of long-lived unstable isotopes; in particular, according to the data of [5], this activity amounts to 2-3 Ci/day (Th^{230}, Ra^{226}, Pb^{210}, Po^{210}, etc.).

The radioactive wastes produced by a nuclear reactor consist of many nuclides (from zinc to dysprosium), transuranium elements, and neutron-activation products formed in the technological part of the reactor. Among the fission products most dangerous from the viewpoint of radiation hygiene are the unstable nuclides (mainly long-lived nuclides) of strontium, yttrium, zirconium, niobium, ruthenium, rhodium, iodine, cesium, barium, lanthanum, cerium, praseodymium, and promethium. The activation products include tritium, C^{14}, F^{18}, Na^{24}, Al^{28}, Cl^{38}, Ar^{51}, Cr^{51} Mn^{54}, Mn^{56}, Fe^{55}, Co^{58}, Co^{60}, Cu^{64}, Zn^{65}, etc. The gaseous waste products consist predominantly of inert gases, the most important of which is Kr^{85}.

Gaseous waste products formed by nuclear-power reactors, depending on the type of reactor, consist chiefly of radioactive nuclides of tritium, A^{41}, krypton, xenon, I^{131}, and I^{129}. The activity of the gaseous waste products also depends on the type of reactor: for example, for a pressurized-water reactor the activity is less than for a boiling-water reactor (the order is reversed only in the case of tritium). On the basis of the investigations of Martin et al. [6] and Beck et al. [7], it was found that the activity values of the gaseous waste products of nuclear power stations were between 10^{-4} and 0.6 times the maximum permissible amount; tritium wastes amounted to 14,000-15,000 Ci/year, inert-gas and activated-gas wastes to $2.1\text{-}2.6 \cdot 10^6$ Ci/year, halogen wastes to about 6 Ci/year, and A^{41} wastes to 650 Ci/day. The activity of the liquid waste products of the nuclear power stations investigated in 1970 amounted to 91 Ci [7], and for individual nuclear power stations the amount ranged from 20 to 100 pCi/liter [8].

The variation of waste-product activity with operating time is not uniform; the activity may increase or decrease.

If we consider a nuclear power station from the viewpoint of the quantity and quality of classical power-generation waste products, the advantages of nuclear power are obvious. Electric power stations operating on mineral fuel are also sources of radioactivity, depending on the amount of thorium and uranium in the fuel. The average activity of the gaseous waste products of thermal electric power stations is $10^2\text{-}10^3$ mCi /year (chiefly Ra^{226}).

A wide spectrum of artificial unstable nuclides enters the waters of the seas and oceans, where, under the influence of a number of factors, there is considerable accumulation of nuclides (up to $10^2\text{-}10^3$ pCi/g for such nuclides as Zr^{95}, Nb^{95}, Ru^{106}, and Ce^{144}).

Prognosis for the Possibilities of Contamination of the Biosphere

A reactor producing 1,000 MW (elec.) produces, on the average, 10^8 Ci of activity. The amount of fission products will increase continuously, in accordance with the increase in the number of nuclear reactors. According to Eisenbud's data [9], the radioactivity of fission products amounted to 18 GCi in 1970, and in 1980, 1990, and 2000 the value will reach 56 GCi, 150 GCi, and 380 GCi, respectively (Fig. 3). However, there are other hypotheses as well. For example, Sousselier and Pradel [2] predict that in the year 2000, nuclear power stations will produce 400-600 GCi of waste products, of which 20-25 GCi will be Sr^{90} activity and 30-40 GCi will be Cs^{137} activity; in addition, they assert, 300-400 MCi of tritium and C^{14} will enter the biosphere, and the waste products will include 6-8 tons of plutonium per year. If there will be 5,000 nuclear-power reactors operating in the year 2000, then approximately 5 kCi of I^{131}, 30-140 Ci of

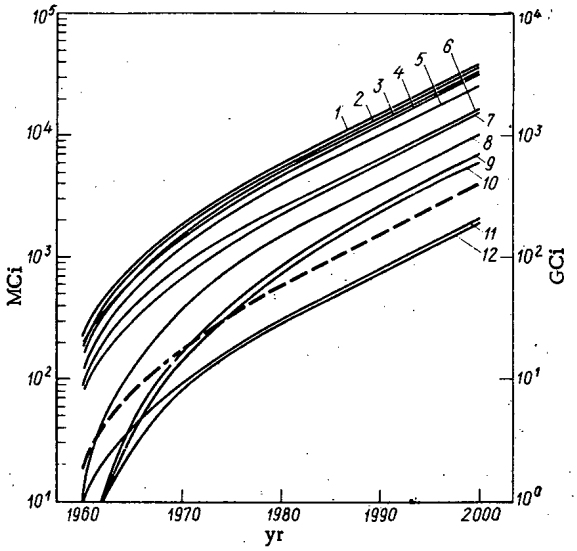

Fig. 3. Assumed amounts of the most important fission products (MCi) of nuclear-power reactors [1) Xe^{139}; 2) Zr^{95}, Nb^{95}, Ba^{140}, Ce^{141}, Pr^{143}; 3) V^{91}; 4) Ce^{144}; 5) Sr^{89}; 6) Ru^{103}, I^{131}; 7) Nd^{147}; 8) P^{147}; 9) Sr^{90}; 10) Cs^{137}; 11) Te^{130}; 12) Ru^{106}] and their total activity (- - -) in GCi.

Cs^{137}, 4-7 Ci of Sr^{89}, and about 1 Ci of Sr^{90} will enter the atmosphere annually. The plants processing irradiated fuel elements may discharge 3 GCi of Kr^{85} as waste products [10]. Today the activity of the global fallout is 0.2-6 GCi; according to hypotheses, in the year 2000 the waters of the seas and oceans will receive about 30 MCi of industrial wastes, which amounts to 10^{-3} times the total activity of the sea and ocean waters [11].

Particular attention should be paid to Kr^{85}, which is found in the gaseous waste products of reactors and of irradiated-fuel-element processing plants. The amount of Kr^{85} in the atmosphere is increasing year by year: in 1959 the amount was 64.5 dis/min/mmole, in 1969 it was 99.5 dis/min/mmole [12], and today the value ranges from $2 \cdot 10^{-2}$ to $3 \cdot 10^{-1}$ mCi/m^3 [13]. Tritium, formed in quantities of 10-30 Ci/MW, is also dangerous because of its capacity to be metabolized. When nuclear power stations have an installed capacity of 100 GW (elec.), we shall have to take account of the formation of I^{129} and xenon isotopes. After 1970, we may expect the rate of I^{131} formation to increase to 100 GCi /day, while the amount of tritium in sea water will reach 1 MCi/year [14].

Experience gained in the operation of nuclear-power reactors indicates that there is a satisfactory safety level, achieved by the application of technological measures based on present standards. We may expect these standards to become more rigorous and the maximum permissible concentration values to decrease. Even today, the value of the risk factor in normal reactor operation is between 10^{-3} and 10^{-4} of the possibility of an industrial accident, and for breakdown situations the factor is between 10^{-6} and 10^{-7}. According to the data of Beck et al. [7], the irradiation of persons working at nuclear power stations in the United States amounted to 1.25 rem or less for 5,352 persons, 1.25-2 rem for 160 persons, 2-3 rem for 144 persons, 3-4 rem for 70 persons, and 4-5 rem for 26 persons; only 7 persons were subjected to more than 5 rem of radiation, and nobody to more than 7 rem.

Nevertheless, it is essential that we begin at once to investigate the behavior of unstable nuclides in the biosphere, since by the year 2000 the influence of nuclear power stations will have extended to an area of about 10^7 km^2, which amounts to 6.7% of the earth's land area. The situation will be more complicated if the scientific and technological revolution is accompanied by an increase in population density (it is assumed that in 2030-2050 there will be approximately 12 billion people living on an area of 3000 million ha, constituting 2% of the earth's land area). In that case mankind will be faced with problems of energy production, the dispersion and discharge of heat, the dispersion of radioactivity, etc. Radioecological problems will arise in different forms in different countries; these problems must now be solved by taking account of the specific situation of each state from the geographical, geological, hydrological, dendrological, industrial, and agricultural viewpoints, and also in accordance with each country's population density. The purposes of these investigations will be: to prevent breakdowns; to work out rapid methods for indicating the presence of unstable nuclides in soil, water, plants, and animals; to determine critical objects and critical organs in biological objects; to determine the factors influencing the accumulation of nuclides in objects; to select agricultural crops suitable for cultivation in the vicinity of a nuclear reactor; to study the movement of unstable nuclides along the food chains and the possibility of stopping them; to develop monitoring methods; to determine the effect of small doses of chronic irradiation on plants and animals; to determine the minimal value of a genetically significant dose; to develop methods of rapid analysis for monitoring purposes, etc.

Radioecological investigations are of an interdisciplinary nature and very complicated, but they are absolutely essential for a knowledge of the processes in which unstable nuclides participate in individual biospheric systems; they are important for the preservation of the environment in which mankind lives.

LITERATURE CITED

1. J. Pelikán, O výuce ekologie na vysokých školah. Seminár, Košice (1971).
2. Y. Sousselier and J. Pradel, Fourth Geneva Conference (1971), Report No. 49/P/766 (France).
3. M. J. H. Bowen, Trace Elements in Biochemistry, Perg. Press, London (1966).
4. B. I. Spinrad, Symp. IAEA "Environmental aspects of nuclear power stations," Vienna (1971); Jaderná energie, 17, 205 (1971).
5. P. R. Kamath et al., Fourth Geneva Conference (1971), Report No. 49/P/536 (India).
6. J. E. Martin et al., Symp. IAEA "Environmental aspects of nuclear power stations," Vienna (1971).
7. C. F. Beck et al., Fourth Geneva Conference (1971), Report No. 49/P/038.
8. C. E. Kent et al., Symp. IAEA "Environmental aspects of nuclear power stations," Vienna (1971).
9. M. Eisenbud, Environmental Radioactivity, McGraw–Hill, New York (1963).
10. Yu. A. Izraél' and E. N. Teverovskii, At. Energ., 31, 423 (1971).
11. M. Saiki et al., Fourth Geneva Conference (1971), Report No. 49/P/850 (Japan).
12. J. Schroder et al., Nature, 233, 614 (1971).
13. M. M. Hendrickson, Symp. IAEA "Environmental aspects of nuclear power stations," Vienna (1971).
14. A. Preston et al., Fourth Geneva Conference (1971), Report No. 49/P/512.

CURRENT PROBLEMS IN THE RADIOECOLOGY OF SOILS AND PLANTS

G. Plitaková, T. Sabová,
and M. Zaduban

A biocenosis is characterized by complex processes taking place in the earth's biosphere. The investigation of the effects of various factors on organisms under natural conditions is known as ecology.

One of the new factors affecting the biosphere is the rise in the quantity of unstable nuclides in nature, resulting from the current development of nuclear industry and also from the testing of nuclear weapons. This factor may upset the equilibrium of the biosphere and pose a threat to mankind.

The main task of the relatively new scientific discipline known as radioecology is to investigate the laws governing the migration of radioactive substances in the biosphere and the effects of ionizing radiation on living organisms and on the earth's biosphere as a whole. From the fairly abundant experimental material already available today, we can conclude that mankind cannot afford to disregard the presence of radionuclides in nature.

The problem of the contamination of food products by radionuclides is one of the most important problems in the field of public health. This is so because we do not yet clearly understand the role of the biological effects of small doses of radiation; we have not yet established the magnitude of the doses caused by the presence of radioactive substances in our daily diet, we do not know how much is contributed to the dose by various ionization sources, we have not reached agreement on the assessment of food comtamination, etc.

The introduction of radioactive substances into the links of the biospheric chain depends on the location and nature of the sources of unstable nuclides.

The fission of heavy nuclei, chiefly those of U^{235}, Pu^{239}, and Th^{232}, gives rise to unstable nuclides (fission products), beginning with $_{30}Zn^{72}$ and ending with $_{66}Dy^{161}$, making a total of about 340 nuclides, of which 92 are stable.

In nuclear explosions and in "total" breakdowns of nuclear reactors, the important parameters of the radioactive fission products are their half-lives and the chemical properties characterizing their participation in the physiological processes of the living organisms of the biosphere. The fission products on which the greatest amount of research has been done are: Sr^{89}, $Sr^{90}-Y^{90}$, $Zr^{95}-Nb^{95}$, $Ru^{106}-Rh^{106}$, I^{131}, $Cs^{137}-Ba^{137m}$, $Ba^{140}-La^{140}$, $Ce^{144}-Pr^{144}$, and Pm^{147}.

Depending on the conditions of the nuclear explosion or breakdown, other unstable nuclides, arising chiefly from the neutron activation of elements of the external environment, may also be of interest from the viewpoint of radioecology.

In the normal operation of a nuclear reactor and in breakdowns of a local (technological) nature, the group of unstable nuclides entering the atmosphere in the form of gaseous or liquid wastes differs from the spectrum of unstable nuclides produced in a nuclear explosion. The gaseous wastes, depending on the types of nuclear reactors involved, consist of radioactive inert gases and also of iodine and cesium, with traces of strontium, barium, and other elements. Gaseous wastes may also contain corrosive products formed during the neutron activation of structural and technological components of a nuclear reactor. The most important of these are H^3, C^{14}, and others (Ar^{41}, unstable isotopes of chromium, manganese, iron, tantalum,

Faculty of Natural Sciences, P. J. Šafarik University, Košice, Czechoslovak Socialist Republic.
Translated from Atomnaya Énergiya, Vol. 34, No. 5, pp. 380-390, May, 1973.

tungsten, etc.) [1]. What we find in the biosphere today are mainly long-lived fission products formed in nuclear explosions (Sr^{90}–Y^{90}, Cs^{137}); they are part of the so-called global radioactive fallout.

As a result of the development of nuclear power, fission products are entering the hydrosphere in increasing quantities; the amount of such fission products in some parts of the oceans and seas in 1967 was several times the amount of Sr^{90} and Cs^{137} resulting from global radioactive fallout [2].

We shall discuss below the biospheric processes in which there is participation by long-lived fission products formed in nuclear explosions. The results obtained in investigations of processes involving Sr^{90}, Cs^{137}, Ce^{144}, and other long-lived fission products formed in nuclear explosions can be used in studying the potential contamination of the biosphere and hydrosphere by installations operating on irradiated nuclear fuel. Other significant processes, which will not be dealt with in this article, are those involving participation by fission products of uranium, protactinium, and thorium (Ra^{226}, Ra^{228}, Ac^{227}, Th^{230}, Po^{210}, etc.), contaminating the biosphere and hydrosphere in the vicinity of installations where uranium and thorium ores are extracted and processed.

The isotopes that have been most thoroughly investigated are the radioisotopes of strontium, cesium, and iodine (the last has been studied chiefly in the thyroid gland). In the radioecology of plants, the most detailed research has been done on Sr^{90} and Cs^{137}, as evidenced by an abundant literature. Less information has been accumulated concerning I^{131}, Ce^{144}, Ru^{106}–Rh^{106}, Zr^{95}–Nb^{95}, and others.

The contamination of plants by radionuclides may take place in two ways: through the leaves and through the roots; in the latter case the contamination depends on the characteristics of the environment – soil system.

The task of radionuclide agrochemistry is to investigate the interrelationships between radionuclides, plants, and soil. In order to carry out such investigations, we must know the principles of sorption and desorption.

The Radioecology of Soils. The radioecology of soils is being developed today on the basis of biophysics, physics, and soil chemistry. It deals with the laws governing the way in which uranium fission products and nuclides resulting from soil activation interact with the soil, their sorption, desorption, and migration in the soil, as well as the migration of these products in the soil–plant system and the deactivation of soils.

Soils are components of the biocenosis which are directly involved in the life of various organisms.

In the investigation of the sorption of elements from aqueous solution by the soil, we must investigate the concentration of the element in question in the aqueous solution (a change in concentration may affect the processes of sorption, desorption, and migration of individual elements in the soil); the chemical form of the element in the solution, which determines the nature of the sorption of the element in each individual case; and the nature of soil absorbing the element (large differences in the properties of soils cause quantitative changes in sorption and desorption).

In investigating the desorption of elements from the soil into an aqueous solution, we must take into consideration the desorbing action of the ions present in the aqueous solution, the complex-forming capacity of organic substances, and the variation in the pH and oxidation–reduction potential of the medium.

The migration of elements in soil, from the physicochemical point of view, is a continuous succession of repeated processes of sorption and desorption of elements. In order to characterize the behavior of an element, we must know how strongly it is sorbed by the soil and know the influence of the external and internal factors determining its migration capability. The internal factors affecting migration include the chemical properties of the individual element, its concentration, and its chemical form, which is determined both by the nature and concentration of the element and by the properties of the medium. The most important external factors affecting migration are the presence of extraneous ions in the aqueous solution, the value of the pH, the oxidation–reduction potential of the medium, the presence of migrating colloids in the solution, and the complex-forming capacity of the organic substances involved.

The data available in the literature are most complete in the case of Sr^{90}. Its coefficient of distribution and percentage of sorption increase with the number of exchange cations contained in soils. The coefficient of distribution depends on the pH of the soil. The migration of Sr^{90} has been investigated in chernozem soils containing moderate amounts and low amounts of podzol. The migration of Sr^{90} is more intensive

in soils with a lighter texture. The larger the amount of exchange calcium in the soil the more Sr^{90} is fixed in it [3].

The coefficient of distribution and the percentage of sorption (up to 92%) are also rather high in burozems (brown soils), although this type of soil contains a lower concentration of exchange cations. In experiments with brown forest soils it was found that as the pH increases to 5, the sorption of Sr^{90} increases because there is less competition from H^+ and Al^{3+}. As the pH varies from 5 to 8, the sorption remains approximately constant. For pH values increasing above 8, the absorption of Sr^{90} depends on the cation contained in the added alkali; the absorption remains constant for sodium, potassium, and NH_4 but decreases for calcium and strontium.

In soils with turf and low podzol the amount of exchange cations is low, and therefore the distribution coefficient and the percentage of sorption of Sr^{90} are low (86%).

Sandy forms of podzol have a lower cation-exchange capacity than loamy and clayey forms, and it may be said that the concentration of Sr^{90} in the upper layers of the soil is inversely proportional to its cation-exchange capacity. As the cation-exchange capacity of podzols decreases, the concentration of Sr^{90} will decrease. Strontium is accumulated in the top 5 cm of podzols. The lowest distribution coefficient and percentage of sorption for Sr^{90} (77%) has been found in sierozem (gray soil).

The desorption of Sr^{90} from turfy meadow soils by univalent cations is low. The highest percentage of sorption is attained in soils with Ca^{2+} (70.3%) and aluminum (90%) [4].

The vertical migration of Sr^{90} depends on the type of soil and the amount of fertilizer used. The effect of fertilizers on migration can be explained by the fact that the rate of vertical migration depends essentially on the concentration of cations in the soil solution.

The transfer of Sr^{90} is also affected by the percentage of organic substances in the soil, the type of clayey minerals present, and the value of the pH. Such processes also include transfer with water and diffusion, but the avilable data on these phenomena are very scanty [5].

The vertical migration of Sr^{90} and Ce^{144} is affected by the texture of the soils. In lighter textured soils the migration of Sr^{90} is more intensive than the migration of Ce^{144} [6]. Essentially, however, the fission products are contained in the top 5-10 cm of the soil, which contains the largest amount of organic substances.

Investigations of horizontal migration have shown that surface runoff removes less than 5% of the Sr^{90} falling on plowed ground. We do not have sufficient information concerning the horizontal migration of Sr^{90} after it has fallen on ground planted in agricultural crops. In observations made 3 years after the introduction of Sr^{90} into pastures, the isotope was found at points 60-65 cm from the point of introduction. It is not yet clear what role is played in horizontal migration by diffusion and by transfer through the root systems of plants.

A fairly large number of reports are available concerning the behavior of Y^{91}, whose sorption by chernozem is 87-97% at acid pH values of 3-5, 84-89% at pH values of 6-7, and 85-94% at pH values of 8-10. This isotope is most strongly absorbed by chernozem. Its sorption by krasnozem (red soil) increases as the pH increases from 3 to 10. In the pH = 6-8 range the percentage of sorption remains unchanged. The highest percentage of sorption (95%) has been observed for pH = 9. The absorption in the A_1 stratum of podzols is 90-95%, and the absorption in the A_2 stratum is 89-94%. The highest percentage of sorption (97%) was observed in the B_1 stratum. In turfy meadow soils the highest percentages of sorption were observed at pH = 3-6. The lowest sorption was observed at pH = 7 (89%).

The desorption of Y^{91} was carried out by means of 0.1 N solutions of NaCl, $Al_2(SO_4)_3$, and $FeCl_3$. In chernozem the lowest desorption was observed when the yttrium was displaced by sodium; aluminum displaced 6% of the Y^{91}, and iron displaced 65%. The desorption by sodium from krasnozem was 1%, while aluminum displaced 42% and iron displaced 78%. The desorption of Y^{91} by aluminum in the three strata of turfy podzols is rather high: in the A_1 stratum aluminum displaced 27% of the yttrium and iron displaced 77%, in the A_2 stratum the corresponding values were 54% and 77%, and in the B_1 stratum the values were 43% and 75%. The lowest desorption of Y^{91} was observed in turfy meadow soil (8% by aluminum and 45% by iron) [7].

Some radionuclides, e.g., Zr^{95}, are so strongly sorbed by the soil that their desorption is very low (less than 10%). The soil may contain Zr^{95} and Nb^{95} chiefly in the form of radiocolloids. The sorption of

these elements reached its maximum value at pH = 4-8; at pH = 8 there was a decrease in the sorptive capacity, followed by an increase at pH values greater than 11 [3].

In contrast to strontium and cesium, Ru^{106} occurs in the soil in anion form, but information on its chemical compounds is very scanty. Different authors give different interpretations of the characteristics of the sorption behavior of Ru^{106}. Some authors assume that sorption is caused by the colloidal state of radioactive ruthenium in solutions [8], while others believe that in the sorption process the ruthenium combines with the organic substances present in the soils [9]. The low sorption of ruthenium may be due to its presence in the solutions in the form of anion complexes.

Relatively little has been published in the literature concerning the soil chemistry of short-lived nuclides, such as I^{131}. It is known that iodine is very rapidly absorbed from soil solutions and transferred to the leaves. The results of investigations of I^{131} sorption by soils from the Iolo and Aiken regions indicate that the isotope is fixed in the organic mass. The amount of I^{131} sorbed by kaolinite and bentonite is very low. Anion exchange plays only a very slight role in the sorption of I^{131}.

Experiments with turf from which the mineral fraction has been removed have shown that the organic fraction strongly sorbs I^{131}: turfy soil sorbed 85.7%, while the extracted organic mass sorbed 80.6%. In the pH range from 4.5 to 8.5, Iolo soils sorbed 60% of the iodine, and Aiken soils sorbed 80-90% [10].

The bond between Cs^{137} and soil is different from the bond between strontium and soil, and this is why Cs^{137} and strontium move in different ways along the soil–plant chain. The Cs^{137} is sorbed onto leached clayey minerals low in potassium. The capacity of cesium to exchange with other cations is low, and it has its specific characteristics if it is present in the soil in microconcentrations. Cesium introduced into mineral soils in low concentrations is sorbed so strongly that it becomes inaccessible to plants. The degree of sorption of Cs^{137} depends on the soil and on physicochemical factors, so that it is impossible to draw any definite conclusions, but it is known that illites and vermiculites sorb cesium very strongly, while montmorillonites and kaolinites sorb it more weakly.

Investigations have determined the ratio between the amount of Cs^{137} sorbed by plants and the organic-substance content of soils caused by Cs^{137} cation exchange [11].

The absorption of Cs^{137} is 98% in chernozem, 95% in krasnozem, and highest of all (99%) in meadow soils.

Very little Ce^{144} in the dissolved state is found in soils; an exception is observed in the case of soils with low pH values. In addition to the pH, the nature of the clayey minerals in the soil also affects the strength of sorption [11]. Molchanova [12] asserts that for neutral and alkaline pH values the sorption of cerium decreases. The absorption value of Ce^{144} in chernozem is 74%. The sorption is strongest in turfy meadow soil and chernozem. Sorbed cerium is easily desorbed from the soil by salts of iron, aluminum, and copper. When iron colloids in solution are present in the soil, the cerium sorption is lower. The sorption of Ce^{144} by soils decreases as the concentration of iron in the solution increases. In the sorption of cerium by chernozem, microquantities of cerium are sorbed onto the most active part of the chernozem: humic acid and substances similar to it.

In [9] it was found that radionuclides may be arranged in the following order with respect to mobility in soils: Ru > Sr > Ce > Y > Co > Cs for sorption, and Sr $\gg$ Ru > Ce > Co > Cs for desorption.

On the basis of the available data, we may conclude that insufficient research has been done on the sorption and desorption of uranium fission products (separately or mixed) by soils, on the effects of pH upon sorption and desorption, and on the effects of the physical and mechanical properties of the organic part of the soils. Very little research has been conducted on individual types of soils from the viewpoint of the above-mentioned requirements.

An analysis of the literature on the radioecology of soils for the planning of further experiments in the Czechoslovak Socialist Republic enables us to draw the following conclusions:

1. In the investigation of soil processes involving Sr^{90}, studies must be conducted on desorption and migration caused by burozem, brown forest soil, podzol, meadow soil, and turfy soil; consideration must be given to the effects of physicochemical properties on migration, sorption, and desorption, due to meadow soil, turf, and sierozem; and account must be taken of the effect of pH on sorption and desorption due to podzol, meadow soil, turfy soil, and sierozem. We have not yet determined the role of the organic part

of the soil in the absorption and migration of strontium in chernozem, burozem, brown forest soil, and sierozem in individual geological strata. Experimental data must be supplemented by information on the deactivation of burozem, brown forest soil, podzol, meadow soil, turfy soil, and sierozem.

2. Extremely little information is available concerning the behavior of Zr^{95} and Nb^{95} in soils. Investigations have been conducted on sorption and desorption by turfy meadow soil and the effect of pH on these processes. For both of these fission products, experimental investigations must be conducted on migration, sorption, and desorption, as well as the effect of pH upon sorption and desorption in the soils mentioned under 1.

The effect of physicochemical and mechanical properties of soils, as well as of their organic part, on migration and adsorption must be determined for all types of soils.

3. It is assumed that Ru^{106} occurs in soils in anion form. Its chemical form must be determined. Attention must be given to the processes of sorption and migration and to the effects of pH, physicochemical properties and mechanical properties of soils on migration and sorption. The deactivation of all types of soils must also be investigated.

4. In the case of yttrium, experimental research must be conducted to determine its migration and the effect of physicochemical and mechanical properties on sorption and migration in the soils mentioned under 1. Additional information must be obtained concerning sorption and the effect of pH on sorption by burozem, brown forest soil, turfy gley, rendzina (humus carbonatic soil), solonets (alkali soil), and sierozem.

5. For Cs^{137} a high percentage of sorption is characteristic. Data about this isotope must be supplemented by information concerning its behavior in burozem, brown forest soil, podzol, turfy gley, solonets, rendzina, and sierozem. Attention must be given to the processes of desorption and migration, the effects of pH on sorption and migration, the effects of physicochemical and mechanical properties of soils on these processes, and the question of deactivation of all types of soils.

6. The soil chemistry of I^{131} requires further research. We must explain the questions of sorption and migration and the effects of pH and of physicochemical and mechanical properties, as well as of the organic part of the soil, on sorption by soils.

7. The authors of this article have found no information whatever in the literature with regard to the behavior of Ba^{140} and La^{140}. The behavior of these products in soils must be determined experimentally.

8. For Ce^{144}, we must determine experimentally its sorption and desorption, as well as the effect of pH on sorption and desorption by burozem, brown forest soils, turfy gley, rendzina, solonets, and sierozem, and we must supplement our information with data on the effect of soil properties upon the behavior of this element.

9. We must clarify the behavior of fission products in all types of soils when different anions are present in them.

10. We must explain the effect of large quantities of mineral fertilizers, as well as the effects of prolonged fertilization with manure and industrial fertilizers, on the behavior of fision products in soils; we must solve the problems of chemical and biological deactivation.

11. We must work out general criteria characterizing the horizontal and vertical migration of fission products and corrosion products, develop appropriate methods for monitoring soils, etc.

Radioecology of Plants. Radioactive contamination results only from those fission products which are deposited in plants during their vegetative period, when their penetration through the root system depends on the total amount of fission products in the soil.

The quantity of radionuclides in the soil may increase if fallout takes place over a long period with relatively constant intensity (for example, during the operation of a nuclear reactor). Radioactive substances settle on the surface of the earth together with particles, vapors, or solutions, they are held by the vegetative cover, and in many cases they are absorbed. Such contamination processes have been fairly thoroughly studied in the literature (see, for example, [11]).

Questions of special interest in the direct contamination of plants by radionuclides are where the radionuclides enter the tissue and what factors influence the rate of absorption. Three ways of direct

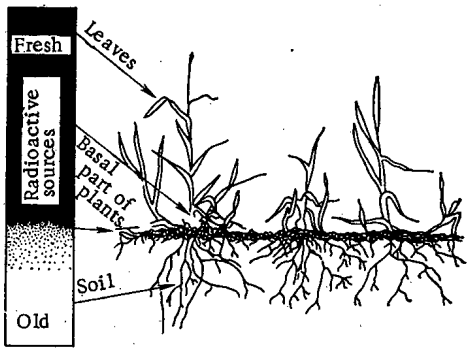

Fig. 1. Mechanism of contamination of perennial forage plants.

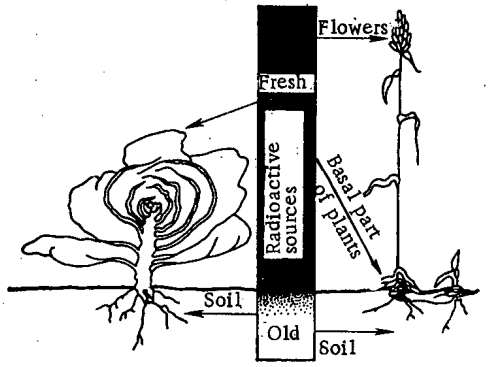

Fig. 2. Mechanism of contamination of annual crops.

absorption are known (see Figs. 1-3): 1) contamination through the leaves; 2) floral contamination (through the flowers); and 3) contamination from the sod (through the basal parts of the plant, or the surface parts in the case of plants which are not in contact with the soil).

When it rains, there is not only absorption of radioactive products but also a washing away of these products from the upper parts of plants and their transfer into the lower parts. Similarly, after radionuclides have been washed out of the basal zone into the soil, the absorption from the sod is replaced by assimilation through the roots. The latter method plays an important role in perennial forage plants. Contamination through leaves and through flowers can result only from those radionuclides which were introduced into the plant during the time of growth of the leaf or flower in question.

While absorption through leaves and flowers depends on the amount of fallout taking place during a relatively short period of time, absorption from the sod continues for a considerably longer time. When enough time has elapsed after the fallout of the fission products, the contribution of direct contamination is reduced, and the contamination of man's food by long-lived isotopes begins to depend increasingly on their absorption through the root systems of plants. The rate of root assimilation of radioactive substances from the soil, which is the principal reservoir of radionuclides, depends not only on the physiological properties of the plants but also on processes taking place in the soil. It must be noted that plants absorb only water-soluble substances. The concentration of electrolytes in the aqueous phase of the soil is so low that the electrolytes are in a dissociated state. Radionuclides are absorbed by plants in the form of ions. The absorption of a nuclide by plants which are in the growing stage is substantially affected by the concentration of the ion in the nutritive medium, its chemical properties, the pH value, the concentration of other ions in the nutritive medium, and the degree to which the ion participates in metabolic processes. It has been found that plants which have grown under identical conditions in the same pasture may exhibit definite differences in the rates of migration of radioisotopes.

Especially important from the agrochemical point of view are investigations on the accumulation of fission products in the harvest of agricultural crops. The absorption of a radioactive isotope in the organs which are above the ground amounts to 90% of the total quantity of the isotope contained in the plant in the case of strontium and to 60% in the case of cesium [13].

Radionuclides such as Y^{91}, Ce^{144}, Ru^{106}, Zr^{95}, and Nb^{95} are concentrated mainly in the root systems of plants (90-99%). In the above-ground part of the plant the bulk of the radionuclides is concentrated in the vegetative organs (90-98% of the total above-ground mass), and the amount in the generative organs is considerably less.

The accumulation of fission products increases with the above-ground mass of the plant, but the nuclide content per unit weight decreases as the organic mass increases, i.e., the laws governing this process are similar to those governing the absorption of nitrogen, potassium, phosphorus, and other elements of biological importance.

The soil constitutes a definite boundary which prevents the fission products from entering the plant, and therefore from entering the food chain. The nuclides interact with the soil, and a smaller amount of nuclides enters the plants from soil than would enter from sand or from aqueous solution. This difference is much greater for Sr^{90} than for Cs^{137}, since radioactive strontium is sorbed by the soil in the metabolic form, while radioactive cesium is sorbed in the nonmetabolic form.

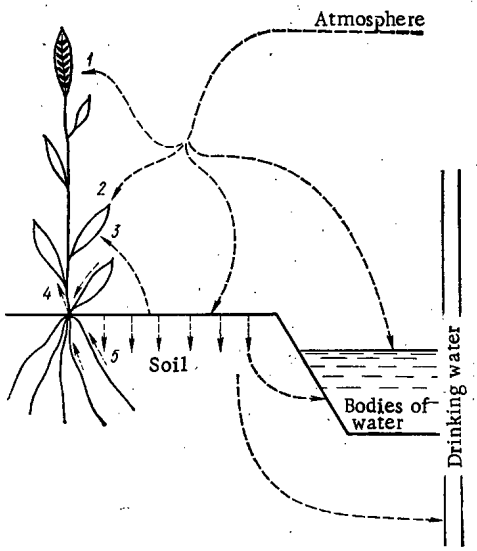

Fig. 3. Direct and indirect contamination of plants. From the atmosphere: 1) floral contamination; 2) contamination through the leaves; from the soil; 3) contamination through the leaves by soil dust; 4) basal contamination; 5) root contamination.

The properties of soil strongly affect the migration of radionuclides. For example, Sr^{90} migrates into plants from turfy podzols to a very large extent, but there is much less migration from krasnozem, sierozem, and chernozem. The strongest radionuclide transfer has been observed to be that from turfy podzol.

The types of soil may be classified according to the Sr^{90} and metabolic-calcium content of the plants. For example, the absorption of Sr^{90} decreases as the amount of metabolic calcium in the soil increases. The Cs^{137} content of plants in turfy podzols and in krasnozems is 10-100 times as much, and sometimes even 200 times as much, as that of plants in sierozems; this is due to the presence of metabolic potassium in the soil. The accumulation of Cs^{137} depends on the presence of metabolic potassium in the soil; as the amount of potassium increases, the cesium content will decrease. In some cases, however, this relation is not observed.

The absorption of Sr^{90} and Cs^{137} is strongly dependent on the texture of the soil.

The presence of silt is thought to be of great importance. Experiments have shown that the accumulation of strontium and cesium decreases if silt particles are added to silica sand. The presence of certain minerals in the soil also affects the absorption and accumulation of radioactive nuclides by plants. Askanite and bentonite (representatives of the montmorillonite group of minerals) are characterized by a high sorptive capacity: they strongly sorb Sr^{90} and reduce its accumulation in plant crops.

In addition, the intensity of absorption of radionuclides depends on the biological properties of plants. We know the relationship governing the accumulation of radionuclides and their chemical analogs. Plants containing large amounts of potassium will accumulate more Sr^{90}. Plants containing little potassium will absorb more Cs^{137}. Plants may be arranged in descending order of the amount of nuclides absorbed in individual organs as follows: Viciaceae > Solanaceae > Asteraceae > Graminae (for the above-ground part) and Viciaceae > Graminae > Asteraceae > Solanaceae (for the root part).

It has been determined that the largest amount of Sr^{90} is found in radishes, which are followed by beets, vetch, potatoes, and peas, with wheat and oats absorbing least of all. This sequence changes if the Se^{90} content is expressed in terms of the amount per gram of calcium.

On the basis of experimental studies concerning the absorption of radionuclides from the soil by plants, the following sequence has been set up: Sr^{89} and $Sr^{90} \gg Cs^{137} > Ru^{106} > Ce^{144} > Zr^{95} > Pu^{239}$. In all soils, the absorption of Sr^{89} was considerably higher than the accumulation of other radionuclides. The absorption of Ru^{106} is higher than the absorption of Cs^{137} in all soils except heavy sandy soil. The accumulation of Ce^{144} is considerably lower than that of the radionuclides preceding it, except in the soil with the most acid reaction (loam). The absorption and distribution of radionuclides are affected to a considerable extent by the properties of the soil, namely: the concentration of other ions in the soil solution, the presence of stable isotopes of the same element, the migration of fission products in the soil profile, etc.

The amount of radionuclides that is assimilated by plants may be expressed in three ways: 1) the ratio of the amount of radionuclide per unit weight of plant biomass to the amount of the same radionuclide per

unit weight of soil; 2) the amount of radionuclide accumulated by the plants growing on a unit area of soil, expressed as a percentage of the total amount of this radionuclide in the soil; 3) the ratio of the amount of a nuclide to the amount of a chemically similar ion in the plant biomass, divided by the ratio of these two ions in the soil.

The concentration of a fission product in plants (particularly in the root system) per unit weight is, as a rule, higher than the analogous concentration for the soil. Some researchers have proposed that this ratio should be called the "coefficient of accumulation," but calculations of this kind have only a limited value from the standpoint of physics. If the coefficient of accumulation is greater than 1, this still does not mean that the ions migrate from the soil into the plants against the concentration gradient. In order to prove this, we must compare the concentration of the ions present in free ionic form in the aqueous phase within the plants with the analogous concentration for the soil. Finding this last value is particularly difficult. The value of the coefficient of accumulation depends on the rate of growth of the plant and on the amount of soil. A calculation of the type mentioned is suitable for a comparison of the amounts of fission products accumulating in plants in cases where the conditions of the external environment are specified; such calculations are, therefore, of relatively little importance. Similar limitations apply to a determination of the quantities excreted by plants.

The results of laboratory experiments in which plants have been grown in small vessels may give a completely different picture of the introduction of radioactive substances into plants than the results of experiments with field plants, since the distribution of plant roots in the soils differs from one case to the other.

There are only scanty data on the accumulation of fission products by plants under field conditions when ordinary methods of cultivation are used. The isotopes most thoroughly studied have been Sr^{89} and Sr^{90}. It has been found that, depending on the type of plants and type of soil involved, 0.2-3% of the Sr^{90} content of the soil is accumulated in the total mass of the harvest in one year. On the basis of these data and of laboratory experiments, it may be expected that under natural conditions the amount of any other radionuclide accumulated in an agricultural crop will be less than 0.1% per year.

We cannot recommend any one method for measuring the accumulation of fission products by plants from the soil; the proper choice of such a method will depend on the observation conditions and on the purpose of the research.

Methods for Predicting the Contamination of the Vegetative Cover by Fission Products. In ecological experiments with radionuclides and in the investigation of the radioactive contamination of the external environment, it is often necessary to determine the total amount of radionuclides contained in various parts of the system, the amounts of radionuclides contained in individual components, and the extraction and accumulation of radionuclides. These processes have been investigated quantitatively by means of analog computers [14]. The migration of fission products in an ecological system was studied at the Oak Ridge National Laboratory in 1961. The investigators successfully overcame the difficulties involved in the calculations and the construction of small models. Interpretation of the data on the rate of migration of radionuclides between the components of ecological systems made it possible to construct mathematical models of the physical processes involved.

The first models described the migration of carbon, energy, and biomass. The migration of carbon includes its separation from organic compounds, its transfer into the atmosphere in the form of CO_2, and its displacement together with atmospheric carbon; this process is repeated after the incorporation of carbon in the biomass as a result of photosynthesis. A large proportion of the biomass of organisms and of organic substances in the soil migrates in the same way as carbon, i.e., from the photosynthesizing organs of plants into the root system, or else it goes into the ground cover and the soil. Nutritive substances migrate from the soil into the root system and are transported into the above-ground organs; after those organs die, the nutritive substances may again migrate into the ground cover and the soil. Radionuclides migrate in the same manner.

Some nuclides, such as cesium, are strongly sorbed by the soil (the form in which they are found in the soil is not very soluble) but become incorporated into the cycle through the action of plants. These models are important because they enable us to investigate and calculate the migration of a nuclide if we have a knowledge of at least some parts of the ecological system (Fig. 4).

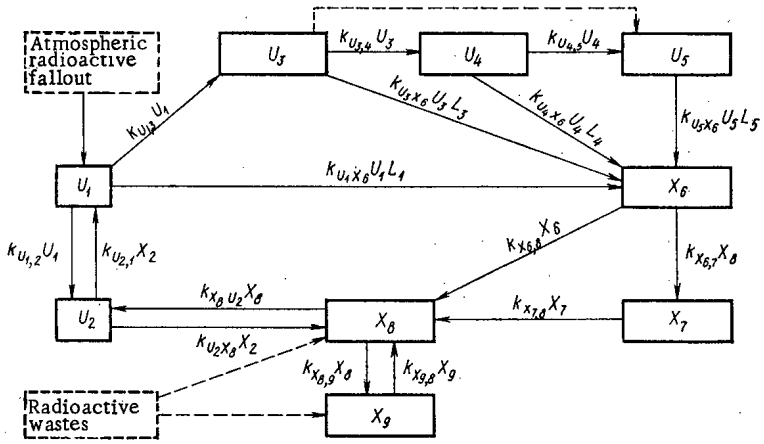

Fig. 4. Migration of inorganic nutritive substances or radionuclides in an ecological system: X, g/m^2) quantity of the element on the surface; L, g/m^2) rate of fallout; U, g) total amount of the element [the subscripts after X and U denote the following: 1) amount of the element present in grass; 2) in roots; 3) in herbivorous organisms; 4, 5) in carnivorous organisms; 6) in organic ground cover; 7) in organisms which decompose the ground cover; 8) metabolic form of the element or isotope in the soil; 9) relatively inaccessible form of the element or isotope in the soil]; k_{UX} and k_{XU}) coefficients of transfer from U to X and vice versa.

General Appraisal of Experiments in the Field of Radioecology; Some Conclusions. In experiments investigating the migration and accumulation of fission products in plants, the nutritive media used were nutritive solutions and sand and soil cultures. On the basis of a comparison of the absorption of fission products from aqueous solutions and from the soil, we can conclude that fission products are absorbed more intensively from aqueous solutions. This can be explained by the fact that the fission products are sorbed in the soil.

The amount of radionuclides accumulated in crops depends on the biological properties of the plants concerned. Plants of the family Viciaceae accumulate a considerably larger amount of fission products than do representatives of the family Graminae. The distribution and accumulation of fission products in plant organs are affected by many ecological factors, e.g., the soil factor. Light-textured soils are of higher quality from the agricultural standpoint, but the amount of fission products transported from them is larger also. In addition to being affected by the texture of the soil, the absorption of nuclides is affected by the amount of organic substances in the soil, the amount of calcium, the pH, and other characteristics. If we compare soils according to the amount of fission products absorbed by plants, we obtain the following sequence: clayey sand > podzol-type sandy loam > podzol-type average loam > podzol-type heavy loam > chernozem.

On the basis of other data, the following sequence has been established for Sr^{90}: sandy loam > loam > sierozem > solonchak (saline soil) > turf > chernozem. The absorption of Sr^{90} and Cs^{137} from the soil by plants depends on time. The concentration of Sr^{90} in plants depends on its concentration in the soil, although it is absorbed differently by different kinds of plants: peas > beans, alfalfa, clover > tubers and root crops > table beets, potatoes > grains and cereal grasses > flax.

Factors in the external environment affect the accumulation more than biological properties do.

The absorption of Sr^{90} by plants from the soil is limited by the amount of calcium present. In experiments in which identical quantities of Sr^{90} were introduced into 1-kg samples of various soils, the amount of Sr^{90} present in the above-ground organs was found to decrease in the following order: clayey sand > average loam > heavy loam > chernozem. A similar relationship was found between Cs^{137} and potassium.

The absorption of Sr^{90} depends on the amount of stable strontium present, the properties of the soil, and the biological properties of the plants concerned. The absorption of nuclides is expressed by the

coefficient of accumulation. Some radionuclides accumulate in plants in large quantities (yttrium, zirconium, niobium, selenium, and prometheum), whereas others (e.g., cesium) have a low coefficient of accumulation. These coefficients vary widely in value. The highest coefficients of accumulation are found in algae (about 10^4), bacteria, and aquatic angiosperms (10^3). Very high coefficients of accumulation are characteristic of the plants and animals in plankton.

Physicochemical properties also affect the absorption of fission products.

Living organisms in bodies of water provide good indicators of the contamination of natural water surfaces. The technology of biological deactivation is being built up on the basis of high accumulation of nuclides by the bottom materials, the mud, and the living organisms in the water.

We must systematize our knowledge of the laws governing the behavior of nuclides in different geochemical regions and different types of biogeocenoses (forest, pasture, and other assemblages), in accordance with the properties of these assemblages. Little research has been done on such radionuclides as selenium, praseodymium, zirconium, yttrium, ruthenium, rhodium, lanthanum, prometheum, and plutonium. The migration and circulation of radionuclides in natural biocenoses constitute a complex process consisting of many cycles of radionuclide transfer, repeated many times, between individual components of the biogeocenosis. One of the practical problems of radioecology is predicting and describing the accumulation and distribution of radionuclides, or mixtures of them, as functions of the time elapsed after single or repeated emission of gaseous radioactive wastes into the environment.

In experiments designed to investigate how the vegetative cover of horizontal and inclined surfaces affects the migration of a mixture of uranium fission products and isotopes of strontium, cesium, ruthenium, and selenium, it was found that the mixture of fission products does not remain at the fallout site but migrates in a horizontal direction whether or not there are any plants present. When there are plants, the migration is twice as rapid as when there are none. It was also found that strontium and cesium are more mobile than ruthenium and selenium.

It was established that the enrichment of soils in calcium and organic substances changes the sorbing capacity of the soils and, at the same time, affects the absorption of nuclides by the plants. Acid soils can be neutralized by other salts, such as carbonates, which considerably reduces the absorption of Sr^{90}. The introduction of potassium into the soil also reduces the absorption of fission products (chiefly Cs^{137}) by the plants. Some agrochemical measures, e.g., deep plowing, combined with the enrichment of the soil in calcium and fertilizers, can reduce the absorption of nuclides.

When the same nuclide Sr^{90} was introduced into the soil in various chemical forms, it was found that the amount absorbed by the plants depended on the anions associated with the Sr^{90} and decreased in the following order: $Cl^- > NO_3^- > SO_4^{2-} > CrO_4^{2-} > F^- > OH^- > CO_3^{2-} > HPO_4^{2-}$. The biological sorption of Ru^{106} and its migration in the soil are also strongly affected by the chemical form of the nuclide; ruthenium in the chloride form is absorbed less than strontium or cesium.

To sum up, we may state the following conclusions.

1. The isotopes most thoroughly studied in the radioecology of plants are those of the following sequence: Sr^{89} and $Sr^{90} > Cs^{137} \gg Ru^{106} > Ce^{144}$.

2. Many studies have been devoted to investigating the behavior of fission products in the biosphere after a nuclear explosion. It is known that the spectra of nuclides emitted by nuclear power stations are different from those of nuclides emitted by a nuclear explosion. Not enough research has been done on the processes in which the radioactive wastes of nuclear-power reactors may participate. The results of studies conducted on processes in which a mixture of fission products resulting from a nuclear explosion may participate are useful only as a rough guide in determining the effect of gaseous radioactive wastes near a nuclear reactor or near a processing plant for irradiated nuclear fuels.

3. The largest amount of research has been conducted on long-lived uranium fission products in the soil–water–plant system. The results of such investigations can be used in predicting the fission-product content of agricultural plants.

4. Uncertainty in the assessment of experiments, lack of sufficient experimental data, differences between experimental conditions, and an insufficiently clear classification system can often lead to contradictory experimental results which cannot be generalized.

5. Relatively little research has been done on I^{131}, which is an important component of the emissions of nuclear-power reactors.

6. There is a growing need for working out radiological methods for the selection and inspection of plants.

7. It is essential to find plants which can be used for deactivating contaminated areas and which are characterized by a high capacity to absorb fission products in their above-ground organs.

8. It is essential to develop methods which can be used for monitoring the effect of a nuclear-power reactor on the environment and which will make possible within a few years of the time the reactor is put into operation a comprehensive estimate of the situation at the points subjected to the greatest contamination. These methods must furnish a sufficient amount of experimental data for making predictions.

9. It is also essential to construct a model of biospheric processes that will make it possible to make predictions for areas with one or more nuclear reactors. The model must include all of the qualitatively important elements that can be characterized quantitatively in the system consisting of fuel element, technological section of nuclear reactor, wastes, air (including fallout and including ground water, natural water, flow-through water, and drinking water), plants, animals, and humans. This must be done not only for nuclear-power reactors but also for installations processing uranium and thorium ore and irradiated fuels. Special attention must be given to the air–water–soil–plant system.

LITERATURE CITED

1. Yu. V. Sivintsev, Radiation Safety at Nuclear Reactors [in Russian], Atomizdat, Moscow (1967).
2. V. M. Vdovenko et al., At. Energ., 31, 4, 409 (1971).
3. R. M. Aleksakhin, Radioactive Contamination of Soil and Plants [in Russian], Izd-vo AN SSSR, Moscow (1963).
4. Radioactivity of Soils and Methods of Determining It [in Russian], Nauka, Moscow (1966).
5. H. M. Squire and L. J. Middleton, Report, ARCRL, 10, 78 (1963).
6. V. M. Bochkarev and Z. G. Antropova, Pochvovedenie, 9, 56 (1964).
7. I. V. Molchanova, Problems of Radiation Biogeocenology [in Russian], Izd. UFAN, Sverdlovsk (1965).
8. D. W. Rodes, Soil Sci. Proc., 21, 389 (1957).
9. N. A. Timofeeva and A. A. Titlyanova, Trudy Ural'skogo Otdelenia MOIP, 2, 195 (1959).
10. M. E. Raja and K. L. Babcock, Soil Sci., 91, 1 (1961).
11. R. Russel, Radioactivity and Human Nutrition [Russian translation], Atomizdat, Moscow (1971).
12. I. V. Molchanova, Behavior of Radioisotopes in Model Systems of Terrestrial and Fresh-Water Biocenoses [in Russian], Izd. UFAN, Sverdlovsk (1968).
13. I. V. Gulyakin and E. V. Yudintseva, Doklady TSKhA, 139, 259 (1968).
14. V. Schultz and A. W. Klement, Radioecology, Proc. of 1st National Symposium on Radioecology, held at Colorado State University, Fort Collins, Colorado, Sept. 10-15, 1961.

MATHEMATICAL MODEL FOR THE OPTIMIZATION OF THE PARAMETERS OF THE POWER SECTION OF AN ATOMIC ELECTRIC POWER PLANT WITH A FAST SODIUM REACTOR

V. M. Chakhovskii and Yu. S. Bereza

UDC 621.039.526

In the study we describe the fundamental systematic position and we give a construction for a calculation-optimization model for choosing the parameters of the power section of an atomic electric power plant with a fast sodium-coolant reactor, having a three-loop thermal circuit and a steam-power cycle with a single superheating of the vapor.

Assumptions are made for constructing the model and determining the accuracy with which the model indicates the physical and economic relations characteristic of actual installations.

An expression is obtained for the integral function, which is the sum of the specific given expenditures over all the elements of the power plant, and depends on the following optimizable parameters of the power section of the power plant: temperature drop in the reactor core, temperature head in the heat exchangers, temperature of the live vapor and the supply water, and pressure of the live vapor. The parameters to be optimized are interrelated by the balance equations. We superimpose some constraints on the parameters: technical and technological, based on the limiting temperature of the covering of the fuel elements, and based on the minimum temperature head in the heat exchangers.

The turbogenerator set is represented in the model in the form of its efficiency as a function of the parameters to be optimized. The dependence was obtained from preliminary calculations of the thermal circuit of the turbogenerator set for various combinations of the initial parameters of the turbine cycle, and then was approximated by power polynomials using a computer.

In the formulation discussed here, the problem of calculating the optimal parameters is an extremal, nonlinear problem, with constraints on the vector of the control parameters.

To solve the formulated problem we develop a calculation-optimization complex of "Kaskad" programs for a "Minsk"-type computer, which uses efficient methods for solving such problems [1, 2].

Based on the model and programs developed, we carried out optimization calculations for the power section of the atomic electric power plant. The initial data were taken for the BN-600 reactor [3].

The calculation results are represented in the form of curves, which show the dependence of the optimal parameters of the power plant on the coolant temperature at the reactor output, and the relative expenditures in the separate elements of the power plant. The model allows us to give answers to questions dealing with the determination of the conditions of the optimal operation of the technological scheme of a power plant and fast reactor.

The calculations showed the efficiency of using the developed algorithm and programs for optimizing the promising scheme of a power plant at various stages of development and design.

The authors are grateful to L. A. Kochetkov, A. A. Rineiskii, and Yu. E. Bagdasarov for useful discussions and comments, which were taken into consideration in this work.

Translated from Atomnaya Énergiya, Vol. 34, No. 5, p. 391, May, 1973. Original article submitted November 19, 1971; revision submitted November 14, 1972.

LITERATURE CITED

1. L. A. Krumm, Elektrichestvo, No. 5, 6 (1963).
2. G. B. Levental' and L. S. Popyrin, Optimization of Thermal-Power Installations [in Russian], Énergiya, Moscow (1970).
3. A. I. Leipunskii et al., At. Énerg., 25, 403 (1968).

DETERMINATION OF OIL IMPURITIES IN CO_2, USED AS A COOLANT IN GAS-COOLED REACTORS, BY THE METHODS OF IR AND UV SPECTROSCOPY

M. I. Ermolaev, L. G. Savenko, K. V. Goryachev, I. B. Strel'nikova, E. F. Kozyreva, P. I. Kondratov, and T. I. Kirienko

UDC 543.42:661.973.4:665.4.062

When carbon dioxide is used as a coolant in nuclear reactors, the need arises to determine impurities of mineral oils in the gas. The IR and UV absorption spectra of solutions of oils used in industrial carbon dioxide apparatuses, both new and after operation and subjection to temperature influences, pressure, and neutron irradiation, as well as samples of oils extracted from gas phases, were studied. It was established by the method of UV spectroscopy that: the first of the two maxima of the spectrum of oils, with greater intensity, corresponds to the wavelength ~230 nm, the second, with intensity $\ln \varepsilon = 3.3$-3.5, corresponds to the wavelength 257-261 nm in pentane, hexane, ethanol, and n-octane, and 265 nm in CCl_4.

A ratio of the hydrocarbons with composition differing from the initial oils is observed in the gas phase; even for the same oil it differs from the time and conditions of its operation. Thus, the ratio of the coefficients of extinction for the two observed absorption maxima for all the oil samples lies within the range 1.9-2.3, while for oil samples extracted from carbon dioxide cylinders, it reaches 5.6. In this case a shift of the absorption maximum into the long-wave region of the spectrum, with a wavelength of 276 nm, is observed. The method of determination of impurities in mineral oils in carbon dioxide according to calibration coefficients of extinction of standard solutions prepared from oils isolated from the products of sample collection, is evidence of the insufficient use of this method. It was established by the method of IR spectroscopy that the nature of the IR spectra of various oil samples is identical. The greatest absorption is observed in the band 2926 cm^{-1}, corresponding to the antisymmetrical valence vibrations of the CH_2 group ($\bar{K}$ = 2.52 liters/g·cm). Bands close to 2962 cm^{-1} ($\bar{K}$ = 1.63 liters/g·cm) and 2860 cm^{-1} ($\bar{K}$ = 1.31 liters/g·cm), corresponding to the antisymmetrical valence vibrations of the CH_3 group and the symmetrical valence vibrations of the CH_2 group [1], have also been demonstrated for all the spectra. For these bands the integral value of $\bar{K}$ = 1.82 liters/g·cm. In this case the relative error is 1.5-3%. A band is noted at 2872 cm^{-1}, corresponding to the symmetrical valence vibrations of the CH_3 group.

For samples of oils extracted from gas phases, an increase in the absorption is observed at the bands 2872 and 2962 cm^{-1}. The differences in the IR spectra are evidence of a different ratio of the hydrocarbons in the gas phase and in the initial mineral oils. Therefore, it is suggested that the oil impurities in carbon dioxide be determined according to the integral intensity of the valence vibrations of the C–H groups. This method is absolute, and does not require preliminary calibration according to artificial mixtures.

Translated from Atomnaya Énergiya, Vol. 34, No. 5, pp. 391-392, May, 1973. Original article submitted May 18, 1972; revision submitted November 23, 1972; abstract submitted September 26, 1972.

LITERATURE CITED

1. L. Bellamy, Infrared Spectra of Complex Molecules [Russian translation], IL, Moscow (1963).

DEACTIVATION OF RADIOACTIVE OFF-GASES FROM A SINGLE-LOOP BOILING-WATER REACTOR POWER PLANT BY EXPOSURE IN A CIRCULATION TUBE

G. Z. Chukhlov, E. K. Yakshin, Yu. V. Chechetkin, and Yu. A. Solov'ev

UDC 621.039.524.4-97.621.039.72

In cases where the pressure seal of fuel elements breaks down, radioactivity carried by off-gases in a nuclear power station based on a boiling-water reactor can attain levels of ~100 Ci/(days · MW). Exposure of those gases in a circulation tube prior to venting them to the atmosphere can result in a 2-fold to 70-fold reduction in the activity. That requires a tube of volume

$$V = t_b G_M / \{\rho(\tau)/[1 + x(\tau)]\}_{av}. \quad (1)$$

where G_M is the mass rate of flow of dry gas through the ejector blower, in kg/h; τ is the gas temperature in the specific cross section through the tube; ρ is the density of the gas, in kg/m^3; x is the steam content of the gas, in kg steam per kg dry gas.

The recommended exposure time t_{exp} for the gas is the root of the equation (2) in t:

$$\sum_{i=1}^{m} c_{i11} \exp(-\lambda_{i1} t) = \sum_{i=m+1}^{l} c_{i11} \exp(-\lambda_{i1} t), \quad (2)$$

where c_{inr} is the concentration of the n-th term in the decay chain of the i-th original gaseous isotope at the r-th end of the exposure tube for the case of the maximum possible probability of fission-fragment gases escaping from the fuel elements, in Ci/m^3; i is the number assigned to the parent gaseous isotope taken in order of increasing decay constants; n is the number assigned to the isotope in the decay chain when the original gaseous isotope is taken as the first in the chain; r is a subscript referable to the entrance (r = 1) or exit (r = 2) of the tube; λ_{in} is the decay constant of the n-th term in the decay chain of the i-th original gaseous isotope, in sec^{-1}; m is the least number assignable to the original isotope with a decay constant greater than that of Xe^{138}; l is the total number of isotopes present in the original gas mixture.

Free gravitational-thermal convection and concentration-related convection through the horizontal tube can shorten the effective exposure time by three or more times. Two free convection streams in the tube must be removed in order to utilize the tube volume to complete advantage. One of these two streams is eliminated when the exit hole is located beneath the tube and the tube end is closed. The other stream can be minimized by precooling the gas to the ambient temperature or by increasing the aerodynamic drag presented to the stream, within limits in which ejector performance will not be impaired. That is achieved by shortening the tube diameter. The fraction A of aerosols in the total radioactivity vented from the tube is

$$A = \left(\sum_{i=1}^{l} \sum_{n=2}^{q} c_{in2}\right) / \left(\sum_{i=1}^{l} \sum_{n=1}^{q} c_{in2}\right), \quad (3)$$

where q is the maximum number of terms in the decay chains of the gaseous isotopes in question, and

Translated from Atomnaya Énergiya, Vol. 34, No. 5, p. 392, May, 1973. Original article submitted February 17, 1972; revision submitted December 26, 1972.

$$c_{in_2} = c_{i11}\left(\prod_{j=2}^{n}\lambda_{ij}\right)\sum_{j=1}^{n}\left[\exp(-\lambda_{ij}t_B)\prod_{\substack{k\neq j\\k=1}}^{n}\frac{1}{\lambda_{ik}-\lambda_{ij}}\right].$$

Calculations performed for the VK-50 fast reactor show that the value of A can attain ~0.6. Installation of an antiaerosol filter at the end of the tube is recommended on that account.

ANGULAR DISTRIBUTIONS OF NEUTRONS BEHIND AN IRON SHIELD

A. I. Kiryushin and Yu. P. Sukharev

UDC 539.125.52:621.039.58

The Monte Carlo method has been used to calculate the angular distribution behind an iron shield of fast and intermediate neutrons from an infinite plane source of fission neutrons. The algorithm of the calculation uses the method of conditional probabilities, which takes account of absorption by and the emergence of neutrons from a layer by introducing the statistical weight. The algorithm of the calculation was described earlier [1].

Angular distributions of fast (E > 1.0 MeV) and intermediate (0.1 MeV ≤ E ≤ 1.0 MeV) neutrons were calculated for shield thicknesses of 0.5, 1, 5, 10, 20, 30, and 40 cm for isotropic, cosine, and monodirectional sources of fission neutrons.

The results show that the angular distribution of the neutron flux behind thin shields (< 5 cm) results from unscattered and singly scattered neutrons. Behind shields more than 20 cm thick the angular distribution is determined by multiply scattered neutrons and is approximated by a function of the form exp (A cos θ), where A is an angular parameter and θ is the angle of emergence of the neutron from the shield.

The dependence of A on the shield thickness and the angular distribution of the source neutrons is shown in Table 1.

Thus the angular distributions of fast and intermediate neutron fluxes behind iron slab shields more than 20 cm thick are weakly dependent on the shield thickness and the angular distribution of the source neutrons, and are approximated by the function exp (A cos θ) with A ~ 1.8 for fast, and A ~ 0.9 for intermediate neutrons.

TABLE 1. Values of A for the Angular Distribution of Intermediate and Fast Neutrons

Shield thickness, cm	Isotropic source		Cosine source		Monodirectional source	
	intermediate neutrons	fast neutrons	intermediate neutrons	fast neutrons	intermediate neutrons	fast neutrons
10	0,1	—	0,2	—	—	—
20	0,65	1,7	0,6	1,6	0,8	—
30	0,75	1,8	0,7	1,7	0,9	1,75
40	0,8	1,8	0,9	1,8	0,9	1,7

LITERATURE CITED

1. A. I. Kiryushin and Yu. P. Sukharev, Atomnaya Énergiya, 26, 455 (1969).

Translated from Atomnaya Énergiya, Vol. 34, No. 5, p. 393, May, 1973. Original article submitted May 6, 1971.

THERMAL FLUX MEASUREMENTS IN NEUTRON CAPTURE THERAPY

V. E. Zaichik, V. N. Ivanov,
V. M. Kalashnikov, Yu. S. Ryabukhin,
and V. F. Stepanenko

UDC 621.387.426

Determination of thermal flux is one of the basic problems in dosimetry, in neutron-capture therapy practice. Neutron detectors must be capable of measuring the space distribution of the flux, with direct determinations of the average flux in a certain volume (say a tumor, an organ, or even the whole organism), as well as obtaining cumulative readings and the capability of storing information for a protracted period.

The article discusses some thermal neutron detectors developed by the authors that meet the specific needs of dosimetric research work in neutron capture theory.

In order to measure the mean thermal flux density within a specified restricted volume of tissue within the organism, we make use of a Li^6-oxygen activation detector, the operating principles of which are based on recording annihilation radiation from F^{18} formed in the reactions $Li^6(n, \alpha) \rightarrow O^{16}(t, n)F^{18}$. The base of the detector is an aqueous solution of the salt Li^6Cl, which is close to tissue in terms of hydrogen concentration. When the average of the cross section of the reaction $O^{16}(t, n)F^{18}$ is taken with respect to triton energy, relying on the Bethe formula for the specific energy loss experienced by charged particles in media of complex chemical composition, the thermal flux density is found from the formula

$$\Phi = 6.5 \cdot 10^2 \frac{n - n_{bg}}{\varepsilon k m_{Li}} \text{ neutrons/cm}^2 \cdot \text{sec},$$

where n is the recorded number of pulses over the measurement time; n_{bg} is the number of background pulses during that same measurement time; ε is the recording effectiveness for the annihilation quanta; $k = (1/\lambda)(1 - e^{-\lambda t_1}) \times [1 - e^{-\lambda(t_3 - t_2)}]e^{\lambda(t_2 - t_1)}$ is a coefficient taking the exposure time t_1, the cooling time t_2, and the measurement time t_3 of the detector into account (in sec); m_{Li} is the mass of the Li^6 atom in the solution, in g.

A Li^6-detector whose operating principles are based on recording α-particles formed in the reaction $Li^6(n, \alpha)t$ in an aqueous solution of Li^6Cl by means of a strip of nitrocellulose film is used as integrating detector in fractionated irradiations. In the case of the materials selected, the design and processing conditions of the nitrocellulose film (nitrocellulose ON-13 base, irradiation in aqueous solution of Li^6Cl, 5-minute etching at $t^0 = 55°$ in 6.25 N NaOH solution), the neutron flux density is given by

$$\Phi = 7.77 \cdot 10^4 \frac{N_{tot} - (N_M + N_{bg})}{qt} \text{ neutrons/cm}^2 \cdot \text{sec},$$

where N_{tot} is the total number of α-tracks per square centimeter of the nitrocellulose film surface, in tracks/cm^2; N_M is the number of tracks due to products of accompanying reactions, in tracks/cm^2; N_{bg} is the intrinsic background of the detector, in tracks/cm^2; q is the Li^6 concentration, in g/cm^3; t is the exposure time, in sec; Li^6-detector retains the stored information for what is practically an indefinitely long period.

Readings of the detectors developed in this work were compared to date obtained with the aid of copper activation detectors calibrated against the Na^{22} photopeak, and also in a known (in terms of gold activation) diffuse thermal neutron flux. The results were found to agree closely.

Translated from Atomnaya Énergiya, Vol. 34, No. 5, pp. 393-394, May, 1973. Original article submitted April 10, 1972.

RATIO OF Cs^{137} – Sr^{90} IN OCEAN AND SEA WATER

A. G. Trusov, L. M. Ivanova,
and L. I. Gedeonov

UDC 621.039.85

Among the artificial radioisotopes that precipitate into the sea medium, the greatest biological hazard is presented by Sr^{90} and Cs^{137}. To correctly determine the pathways of the spread of these radioisotopes in the aqueous medium and to predict their further distribution, it is necessary to know in what state they penetrate into sea water, and in what state they exist in it.

The Sr^{90} and Cs^{137} that have penetrated into the ocean water are in such a degree of dilution that it is difficult to find a direct method of determining their physical state and chemical forms. Valuable information in this respect can be obtained from data on the ratio of the concentrations of Cs^{137} and Sr^{90} in sea water.

In this work we discuss the results of a large number of simultaneous determinations of Cs^{137} and Sr^{90}, performed by the authors since 1963 and according to the same method, as well as the results of later analyses of samples of sea water, collected on the 20th voyage of the scientific research ship "M. Lomonosov" and in the first and second voyages of the scientific research ship "Akademik Vernadskii" for surface waters, waters from intermediate layers (at a depth of 5-700 m), and from great depths (more than 700 m).

Each particular error σ_{x_i} in the radiochemical determination of the concentrations of Sr^{90} and Cs^{137} in sea water is determined by the dispersion of the results, while the total error σ_{y_i} is estimated according to the law

$$\sigma_y^2 = \left(\frac{\partial \varphi}{\partial x_1}\right)\sigma_{x_1}^2 + \left(\frac{\partial \varphi}{\partial x_2}\right)\sigma_{x_2}^2 + \ldots + \left(\frac{\partial \varphi}{\partial x_n}\right)\sigma_{x_n}^2,$$

if

$$y = \varphi(x_1, x_2, \ldots, x_n).$$

A calculation performed according to this method showed that the concentration of Sr^{90} and Cs^{137} in sea water is determined, as a rule, with an error of ±15%, the ratio of Cs^{137} to Sr^{90} with an error of ±22% and with probability of 68%.

In the work some statistical properties of the aggregate of the results obtained are discussed, and if not laws, then at least tendencies in the distribution of the ratio studied are revealed. The entire aggregate of results obtained as a whole and several samples from it were investigated. For each sample the range of values obtained, the arithmetic mean with an indication of the error of the mean, and the standard deviation of a single result were found by calculation.

It is noted that the results for the Black, Mediterranean, North, and Baltic Seas do not deviate from the general set. However, for the Baltic Sea, and especially for the Gulf of Finland, not one value above the mean was obtained; the average value for the Baltic Sea was 1.2 ± 0.05, which differs significantly from the average for the entire Atlantic in 1969-1970 (1.9 ± 0.07). Within the limits of accuracy of the available data, no other deviating regions in the Atlantic Ocean have yet been detected. We cannot consider the difference between the results for the surface and deep waters significant either, nor the difference between the results of observations in 1963-1964 and in 1969-1970. Moreover, no significant differences were noted between the ratio of Cs^{137} to Sr^{90} in the waters of different regions of the Pacific Ocean and at different depths.

Our analysis showed that the difference in the average value of the ratio of Cs^{137} to Sr^{90} in the Pacific and Atlantic Oceans (1.4 and 1.8, respectively) exists at least as a trend, although this conclusion cannot be considered unambiguous as a result of the low accuracy of the experiments. The main thing here is the absence of significant differences in various regions of the same ocean. This can be only in the case of the same behavior of the radioactive isotopes of strontium and cesium that have penetrated into the ocean.

It is believed that radioisotopes that have penetrated into a water medium are rapidly subjected to isotopic exchange with their own stable isotopes and then share the fate of the ocean strontium and cesium, the

Translated from Atomnaya Énergiya, Vol. 34, No. 5, p. 394, May, 1973. Original article submitted January 4, 1973.

ratio of the content of which sea water is uniform. On this basis it can be concluded that in the source of penetration into the ocean, i.e., in the atmosphere, Sr^{90} and Cs^{137} exist in a form accessible for dissolution by water, while the portion that is sparingly soluble constitutes a small fraction, but it cannot be evaluated on account of the large error in the determinations.

LETTERS TO THE EDITOR

ON THE POSSIBILITY THAT CERTAIN ISOTOPIC ANOMALIES ON THE EARTH MAY BE DUE TO AN ANNIHILATION EXPLOSION

N. A. Vlasov

UDC 539.17

Workers at the French CAE have discovered [1] interesting anomalies in the isotopic content of U^{235} and several rare earth elements in the ores of one of the uranium deposits in Gabon. These anomalies are clearly outside the range of variation in the relative isotopic content which has thus far been observed on Earth. Using the rubidium–strontium method, these kinds of deposit were found to be 1740 ± 20 million years old. One can explain [2] the anomalies under the assumption that the species of deposit were exposed to neutron radiation with a total flux amounting to $\sim 10^{21}$ neutrons/cm^2. The neutrons were generated, according to the hypothesis which was proposed, by a fission chain reaction (a "natural" nuclear reactor) which occurred $1.7 \cdot 10^9$ years ago. This hypothesis is very interesting and seems quite likely to be true, since the U^{235} content was higher than, about 3%.

However, this is not the only possible hypothesis. There is another source for the neutrons which would cause such isotopic anomalies. Let us assume that astronomical bodies made of antimatter exist in the universe and that it is possible, although unlikely, that a meteorite composed of antimatter can fall to the Earth. Long ago, such an hypothesis was considered and verified [3] in connection with the Tunguskii meteorite [4]. The annihilation explosion of an antimeteorite is inevitably accompanied by various nuclear transformations, including some which feature the formation of free neutrons. Depending on the conditions, the yield may range from three to five neutrons for each antinucleon annihilated [5].

One can make a rough estimate of the amount of antimatter needed to give rise to the flux of 10^{21} neutrons/cm^2 found by the French authors. If the flux were distributed over the surface of radius 100 m = 10^4 cm, the total neutron yield would be $4\pi R^2 \cdot 10^{21} \approx 10^{30}$; the total neutron mass would be of the order of 10^6 g. The same mass of antimatter (10^6 g) would therefore be enough to obtain the required number of neutrons. This estimate obviously gives a lower limit for the necessary quantity of antimatter, if one takes into account the conditions of a powerful explosion, the entrainment of matter in the cloud and its scattering over a large surface.

Annihilation neutrons are more energetic than are fission neutrons [5]. The mean energy of a considerable fraction of the primary neutrons from nuclear fission is ~60 MeV. In annihilation explosions, not only fast neutrons, but approximately equal fluxes of fast protons and π-mesons must be formed as well; these also cause nuclear transformations. Almost all nuclear transformations which are caused by the products of an annihilation explosion result in the formation of nuclei with 1, 2, 3, or 4 less nucleons than there were in the nuclei exposed to the explosion products. Because of this, the abundances of nuclei of about equal mass are equalized. Such a tendency has already been noted in studies of the neodymium isotopes: the content of the rare odd isotopes Nd^{143} and Nd^{145} increased by a factor of from 1.5 to 2, while the increase for the even isotopes Nd^{144} and Nd^{146} was hardly greater than the average of the normal. However, in this case such fluctuations are explained as a consequence of the fission of uranium. It would be of interest to carry out an analogous investigation for isotopes which are not formed in fission, or for the same isotopes, but without the presence of uranium. The clearest indication which will allow one to discriminate between the annihilation explosion and nuclear reactor hypotheses will be the dependence of the isotopic anomalies on the uranium content and a more probable formation of the neutron-deficient light isotopes. For example, La^{138}, which is normally 0.089% abundant, would have to be found in excessive amounts, since it can be

Translated from Atomnaya Énergiya, Vol. 34, No. 5, pp. 395-396, May, 1973. Original article submitted February 15, 1973.

formed in the reactions La^{139} (n, 2n), Ce^{141} (p, α), Pr^{141}(n, α), and other analogous reactions. One should expect similar excesses in the rare lightest isotopes of other elements as well.

Among the published results of observations there is an interesting comparison [2] of the number of fragments formed with the number of U^{235} nuclei which underwent fission. It seemed that the number of U^{235} nuclei which underwent fission was about half as large as needed for the formation of the observed quantity of fragments. The assumption was therefore made that fission of U^{238} was accompanied by partial regeneration of U^{235}. A large relative probability for the fission of U^{238} is not possible in a reactor using slow neutrons for its operation. A chain fission reaction with fast neutrons is quite unlikely under the natural conditions considered here. The decrease of the U^{235} is offset by formation and subsequent decay of Pu^{239}; this is possible if the average value of the regeneration coefficient is greater than 0.5. In an annihilation explosion, fission can be caused to a large extent by fast neutrons, and the high probability for the fission of U^{238} is much easier to explain. The cross section for the fission of U^{238} by fast neutrons is about half as large as the cross section for the fission of U^{235}; however, its abundance was 30 times as large, so that it would not be surprising even if the fission probability for U^{238} were larger than for U^{235}. A further analysis of the isotopic anomalies of the Oklo deposit in Gabon will make it possible to prove the annihilation explosion hypothesis. The confirmation of either the annihilation explosion or nuclear reactor hypotheses will be of equal interest.

Trances of the annihilation explosion may of course be discovered beyond the uranium deposits, so it will be useful to bear this hypothesis in mind in explaining isotopic anomalies discovered anywhere else.

The possibility of the formation of radioactive spots on the surface of the moon as a result of the fall of antimeteorites was proposed some time ago [4]. It is interesting that the American "Apollo-16" expedition discovered surprisingly radioactive spots on the moon [6].

I wish to thank V. I. Mostov and T. K. Chizhov for a discussion of the hypothesis.

LITERATURE CITED

1. Compt., Rend. Acad. Sci., 275, D-1731 (1972).
2. Compt., Rend. Acad. Sci., 275, D-1847 (1972).
3. Cowan et al., Nature, 206, 861 (1965).
4. N. A. Vlasov, Priroda, No. 2, 85 (1967).
5. N. A. Vlasov, Antimatter [in Russian], Atomizdat, Moscow (1966).
6. Nucl. News, 16, 76 (1972).

NEUTRON FLUX INTEGRATOR

Yu. K. Kulikov, Yu. T. Dergachev,
G. Ya. Voronkov, M. A. Sunchugashev,
and V. V. Fursov

UDC 539.1.074.88

In reactor measurements such as the determination of fuel burnup it is frequently necessary to know the integrated neutron flux in the core over a long period. Ordinarily the integrated neutron flux is determined by activating foils or wires in the reactor. Such measurements require the removal of the irradiated materials from the reactor, and this is inconvenient and frequently technologically undesirable.

A neutron flux integrator was tested in the reactor of the second unit of the Novo-Voronezh atomic power plant. The device consists of a direct-charging detector (DCD) [1] connected through a radiation-resistant cable to a mercury capillary coulometer-integrator [2] extending beyond the core into the service room. The integrated neutron flux is measured without removing the detector from the core and without stopping the radiation. When the total capacity of the coulometer-integrator has been used up a simple change of polarity ensures continuation of measurements "in the other direction." The device is completely automatic and does not require a power supply or auxiliary apparatus to record readings.

The DCD with a rhodium emitter 300 mm long was placed in a dry channel of the reactor of the second unit of the Novo-Voronezh atomic power plant. With the reactor operating at a thermal power of 970 MW the DCD generated a current of 2.2 μA, which corresponds to a neutron flux at the detector location of $3 \cdot 10^{13}$ neutrons/cm^2 · sec.

The mercury coulometer-integrator consists of a glass capillary tube filled with two columns of mercury separated by a gap filled with electrolyte. Metal contacts are inserted into the mercury at the ends of the capillary tube. The operation of the coulometer is based on the dissolution of mercury at the anode and its deposition at the cathode by an electric current. The displacement of the gap of electrolyte along the capillary is a measure of the integrated current through the DCD and is proportional to the charge passed through the integrator:

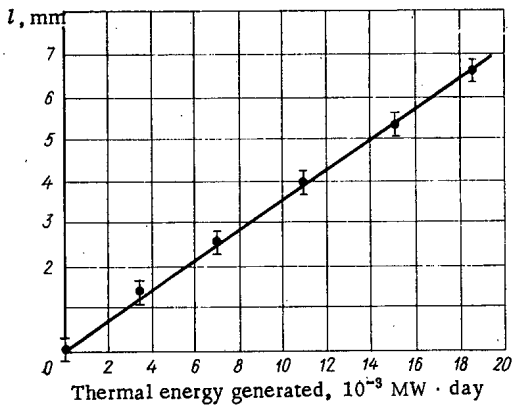

Fig. 1. Displacement of the electrolyte gap of the integrator as a function of the thermal energy generated in the reactor.

$$l = 0.351 \frac{\int_0^{\tau} i(t)\,dt}{d^2} 10^{-3}\,\text{mm}$$

where i(t) = Aφ(t) is the current in μA, φ(t) is the neutron flux at the DCD position in neutrons/cm^2 · sec, A = $0.625 \cdot 10^{-13}$ μA · sec · cm^2/neutron is a proportionality constant, τ is the time of irradiation in hours, d = 0.235 mm is the diameter of the capillary of the integrator, and 0.351 is a coefficient depending on the kind of electrolyte.

The reactor operated 21 days without changes in the neutron distribution; the thermal power of the reactor was directly proportional to the neutron flux at the DCD location. The readings of the device could be compared with the independently measurable integrated reactor heat output. Data on the thermal power and the thermal energy output determined from the flow rate and the temperature drop of the coolant were obtained

Translated from Atomnaya Énergiya, Vol. 34, No. 5, pp. 396-397, May, 1973. Original article submitted September 5, 1972.

from the operation of the Novo-Voronezh atomic power plant. The results of the measurements are shown in Fig. 1.

The total displacement (l = 6.6 mm) calculated by formula is in good agreement with the measured value (6.5 ± 0.25 mm). As shown in Fig. 1 the integrator reading varies linearly with the thermal energy generated over the whole range of measurements to within the error in reading the displacement of the electrolyte gap of the integrator. This error is ±0.25 mm for each measurement, and consequently the relative error decreases proportionally to the integrated current of the DCD.

The measurements were made with an integrator having a capacity of ~20 C which corresponds to an integrated neutron flux of $3 \cdot 10^{20}$ neutrons/cm^2 for the integrator used. An integrated flux of $3 \cdot 10^{13}$ neutrons/cm^2·sec for a year can be measured with an integrator having a capacity of 60 C.

Measurements extending over a long time may require a correction for the burnup of the rhodium emitter; this amount to 0.5% for 100 hours in a flux of 10^{14} neutrons/cm^2 · sec [3]. Under these conditions a vanadium emitter is recommended for the DCD; the burnup of vanadium can be neglected to an accuracy of 1% per year.

LITERATURE CITED

1. E. I. Babulevich et al., Atomnaya Énergiya, 31, 465 (1971).
2. P. S. Lidorenko and G. Ya. Voronkov, Elektrotekhnicheskaya Promyshlennost', 307, 12 (1968).
3. A. Endler, Kernenergie, 13, 45 (1970).

EFFECT OF INTENSE REACTOR IRRADIATION ON THE SHEAR MODULUS AND VISCOSITY OF IRON

E. U. Grinik, A. I. Efimov,
V. S. Karasev, V. S. Landsman,
and M. I. Paliokha

UDC 539.67:546.72

In the present paper we give some results of studying the shear modulus and viscosity of iron during reactor irradiation up to the integral flux $\sim 2.2 \cdot 10^{20}$ neutrons/cm^2 ($E \geq 0.1$ MeV) with intensity $\sim 10^{14}$ neutrons $\cdot$ cm$^{-2} \cdot$ sec^{-1} (reactor power 10 MW).

The apparatus [1] consisted of an ampoule with a reverse torsion pendulum, which was placed in the vertical channel of the VVR-M reactor core and a remote system for recording energy consumption in maintaining constant amplitude of the sample forced vibrations and for measuring the resonance frequency of these vibrations and the temperature of the sample. The errors in determining the shear modulus, the viscosity, and the irradiation temperature were no greater than 2%.

After it was mounted in the pendulum clamps, the polycrystalline iron sample (diameter 0.8 mm, length 70 mm), containing no more than 10^{-2} wt. % impurities, was annealed for 1 h at 750°C at 10^{-4} torr vacuum.

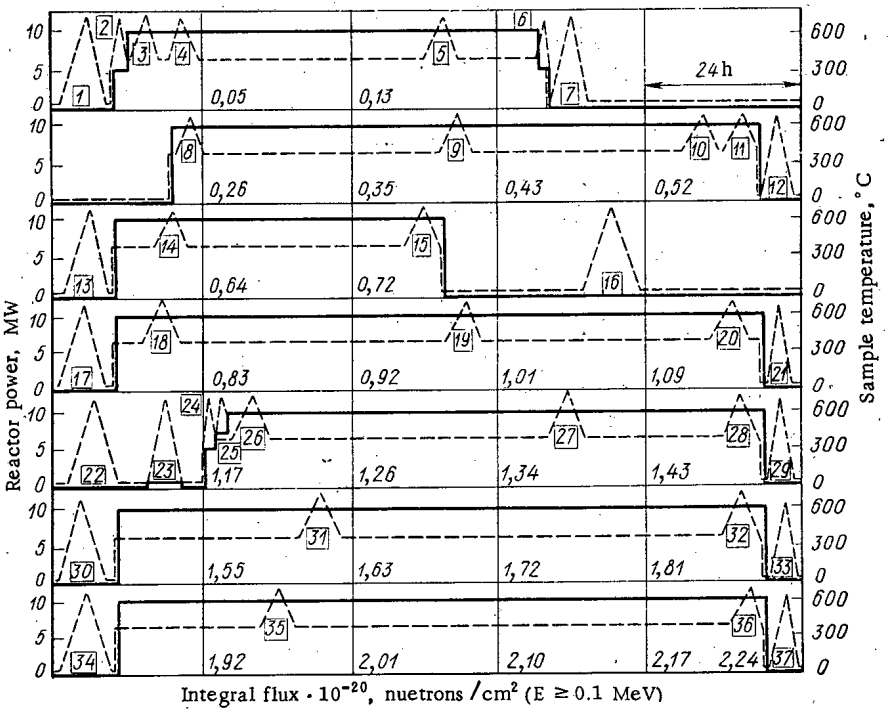

Fig. 1. Irradiation of the iron sample: solid lines show reactor power; dashed lines show sample temperature (the numbers 1-37 are order numbers for the experiments).

Translated from Atomnaya Énergiya, Vol. 34, No. 5, pp. 397-399, May, 1973. Original article submitted August 9, 1972.

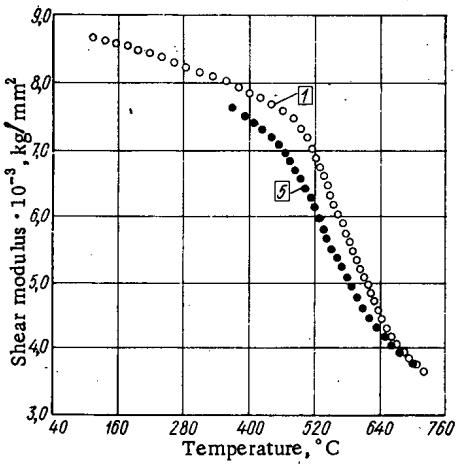

Fig. 2

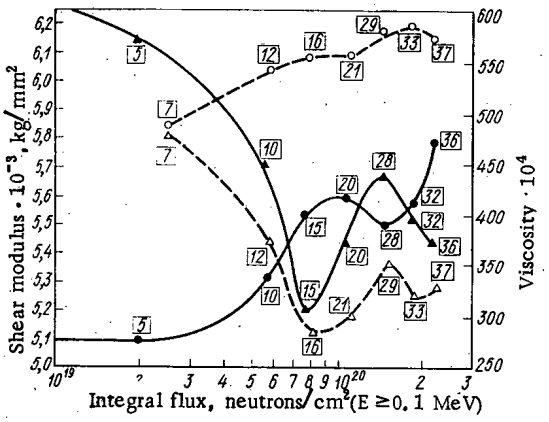

Fig. 3

Fig. 2. Temperature dependence of the iron shear modulus in the initial state (1) and during reactor irradiation (5) of intensity 10^{14} neutrons $\cdot$ cm^{-2} $\cdot$ sec^{-1} (E $\geq$ 0.1 MeV).

Fig. 3. Dependence of the shear modulus (○, ●) and the viscosity (△, ▲) of iron at 580°C on the integral flux during irradiation (●, ▲) and outside the neutron-emission field ((○, △).

With reactor power of 10 MW, the sample temperature was 400°C, and for a short period during the measurements it increased to 700°C. Measurements were made in the temperature interval 60-700°C (see Fig. 1) with the reactor shut down, when the radiant heat evolution in the sample and the ampoule fittings was negligible. Here, the sample resonance vibration frequency varied from 5 to 8 Hz. The relative deformation amplitude on the sample surface was maintained at $3 \cdot 10^{-5}$.

Results of studying the dependence of the shear modulus and viscosity of iron on the temperature, intensity, and integral radiation dose are shown in Figs. 2-4 (the numbers on the curves indicate the experiment order numbers corresponding to those in Fig. 1).

We should note that the value of the iron shear modulus during irradiation is significantly lower than the value without the neutron flux (see Figs. 2 and 3). This change in the shear modulus is related to increased concentration of point defects during irradiation and may be caused by lowering of the linear dislocation energy density, diffuse liberation of dislocations from binding points, climb of some of the dislocations in the slip plane, etc. According to [2] climb of dislocations decreased the shear modulus of metals by 17%, and when the shear deformation is caused only by the glide of dislocations which are distributed randomly over various systems, by only 4%. The decrease of the shear modulus in our experiments at irradiation temperature 580°C was 12%, which agrees with the above-mentioned values. A similar change in the shear modulus (by 16-18%) is observed in metals after low-temperature deformation allowing a significant increase in the concentration of point defects [3]. As the integral neutron flux increases, so does the iron shear modulus, and this is related to the increased concentration and size of accumulations of radiation defects which bind the dislocations. It is characteristic that during irradiation this increase occurs much more quickly (see Fig. 3), since the accumulations which are forming are at the same time efficient sinks which significantly lower the concentration of surplus point defects [4], as a result of which the observed increase in the shear modulus occurs.

In the interval of integral fluxes $(0.9\text{-}1.5) \cdot 10^{20}$ neutrons $\cdot$ cm^{-2} the shear modulus during irradiation decreases somewhat (to approximately $1.2 \cdot 10^{2}$ kg $\cdot$ mm^{-2}). This may be related to the transformation of vacancy accumulations which have achieved corresponding dimensions into dislocation loops, leading to rapid decrease of the modulus.

The variation (see Fig. 3) of iron's viscosity and shear modulus during irradiation correlate well, i.e., decrease in the viscosity is accompanied by increase of the shear modulus, and vice versa. The viscosity outside the neutron-radiation field differs from that during irradiation by 5-20%, depending on the

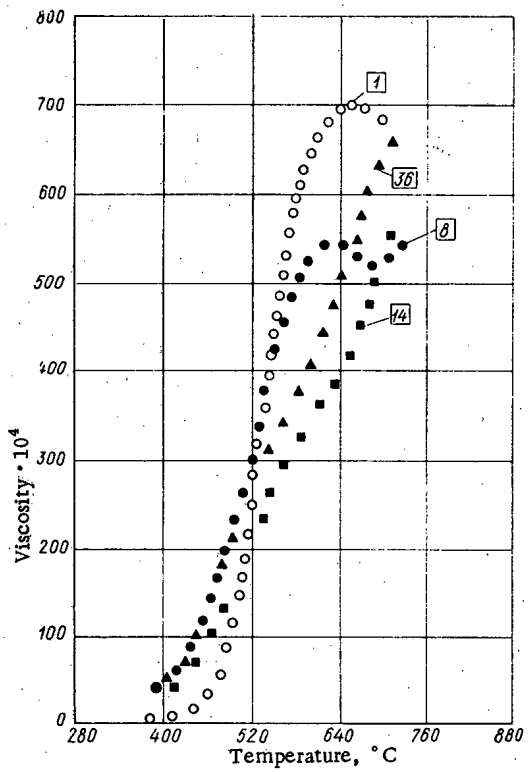

Fig. 4. Temperature dependence of iron's viscosity in the initial state (○) and during irradiation at various integral fluxes (E ≥ 0.1 MeV): ●) $0.26 \cdot 10^{20}$ neutrons/cm^{-2};■) $0.50 \cdot 10^{20}$ neutrons /cm^{-2};△) $2.2 \cdot 10^{20}$ neutrons/cm^{-2}.

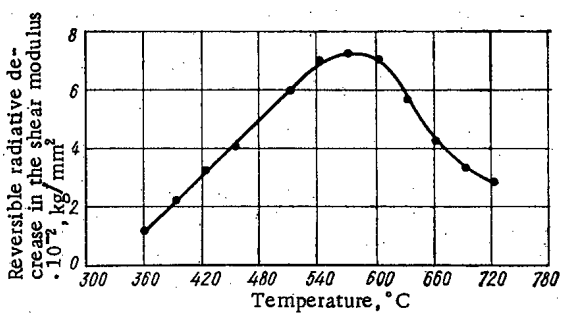

Fig. 5. Temperature dependence of the absolute value of the iron shear-modulus defect reversible component when the integral flux is $1.5 \cdot 10^{20}$ neutrons · cm^{-2} (E ≥ 0.1 MeV).

integral fluxes. Here, the change in the viscosity is minimal with doses corresponding to the minimum decrease in the shear modulus.

Figure 5 shows the temperature dependence of the reversible component of the shear modulus decrease obtained from the data of experiments 28 and 29; this temperature dependence arises when the reactor is turned on and disappears when it is shut down. It is clear from Fig. 5 that at ~0.5 T_{melt} (580°C) the decrease in the shear modulus of iron reaches its maximum. Decrease of the reversible component of the shear-modulus decrease at temperatures greater than 580°C is apparently related to annealing of radiation defects.

The grain-boundary maximum of iron's viscosity decreases when the integral neutron flux increases and already when the flux is $\sim 0.5 \cdot 10^{20}$ neutrons · cm^{-2}, it degenerates into an inflection point (see Fig. 4). This phenomenon, as with the shear-modulus variation, is caused by the increased density of accumulations of radiation defects which decrease the grain-boundary slip. Further change in the viscosity near the grain-boundary relaxation temperatures is related to change of the high-temperature viscosity background (no peak arises for the grain-boundary relaxation).

LITERATURE CITED

1. V. S. Karasev et al., At. Energ., 33, No. 3, 777 (1972).
2. J. Friedel, Dislocations [Russian translation], Mir, Moscow (1967), p. 278.
3. M. Druyvestein et al., Physica, 25, 1271 (1959).
4. S. Harkness et al., Nucl. Appl. and Technol., 9, 24 (1970).

ELECTRON CURRENTS EXCITED BY γ-RADIATION IN A SUBSTANCE

A. V. Zhemerev, Yu. A. Medvedev,
B. M. Stepanov, and G. Ya. Trukhanov

UDC 539.124.17

The process of γ-radiation transfer in a substance is accompanied by various kinds of electromagnetic phenomena [1, 2], which are produced by currents of electrons that are knocked out of the atoms of the substance by γ-quanta. Below we present expressions that relate the electron current and the characteristics of the γ-radiation field in a substance consisting of light elements. Specific fundamental results are obtained for air.

In the formulation of the problem dealing with electron currents generated in a substance by a γ-quanta flux, we assume that the γ-radiation flux varies slowly during the time in which the damping of fast electrons takes place, e.g., for air under normal conditions this time is $\sim 10^{-9}$-10^{-8} sec. Furthermore, we neglect effects of pair production (for light elements with $Z < 25$ a similar approximation is valid for γ-quanta energies less than 3 MeV) and spatial variation of the γ-quanta flux at distances of the order of the mean free path of the fast electron (the mean free path of a γ-quantum is practically always much greater than the electron mean free path). Then the electron current excited in the substance by a γ-quanta flux is

$$\mathbf{j}(\mathbf{r}, t) = \int\int d\varepsilon\, d\Omega' \int d\Omega\Omega f(\mathbf{r}, \Omega, \varepsilon, t) \left[\frac{d\sigma_k(\varepsilon, \Omega, \Omega')}{d\Omega'} l(\varepsilon_e) \rho_e(\mathbf{r}, t) + \frac{d\sigma_p(\varepsilon, \Omega, \Omega')}{d\Omega'} l(\varepsilon_e) \rho_{at}(\mathbf{r}, t) \right], \quad (1)$$

where $f(\mathbf{r}, \Omega, \varepsilon, t)d\Omega d\varepsilon dt dS$ is the number of γ-quanta passing through a small area dS through an element of solid angle $d\Omega$ about the direction Ω (Ω is the normal to the area dS) with energy in the range from ε to $\varepsilon + d\varepsilon$ at the moment of time from t to $t + dt$; $d\sigma_k(\varepsilon, \Omega, \Omega')/d\Omega'$ is the differential scattering cross section of an electron in the direction Ω' by a γ-quantum with energy ε passing in the direction Ω; $d\sigma_p(\varepsilon, \Omega, \Omega')/d\Omega'$ is the differential photoabsorption cross section of a γ-quantum with energy ε passing in the direction

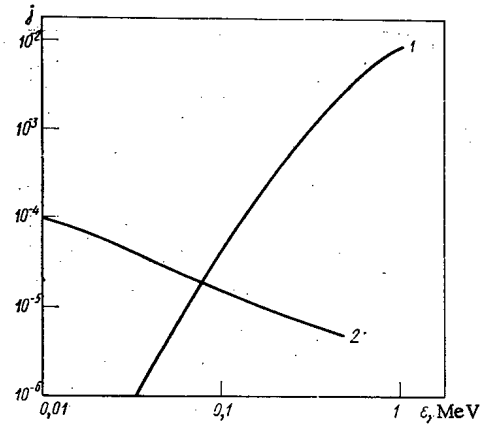

Fig. 1

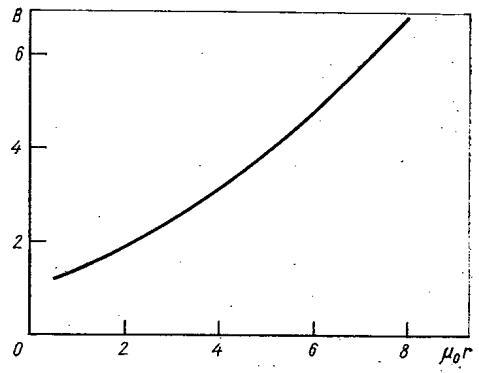

Fig. 2

Fig. 1. Moduli of the currents of Compton electrons 1 and of photoelectrons 2 produced by a single γ-quantum with energy ε.

Fig. 2. Dependence of buildup factor of modulus of electron current B on distance $\mu_0 r$.

Translated from Atomnaya Énergiya, Vol. 34, No. 5, pp. 399-401, May, 1973. Original article submitted September 27, 1972.

TABLE 1. Radial Electron Current Produced by Scattering of γ-Radiation, Electrons /μsec

r, m	Δt, μ sec					
	0–0,125	0,125–0,250	0,250–0,500	0,500–1	1–1,5	1,5–2
100	$1{,}1\cdot10^{-2}$	$1{,}9\cdot10^{-4}$	$2{,}9\cdot10^{-5}$	$3{,}8\cdot10^{-6}$	$4{,}8\cdot10^{-7}$	$2{,}1\cdot10^{-7}$
250	$8{,}7\cdot10^{-3}$	$5{,}2\cdot10^{-4}$	$9{,}0\cdot10^{-5}$	10^{-5}	$2{,}6\cdot10^{-6}$	$9{,}6\cdot10^{-7}$
500	$2{,}3\cdot10^{-3}$	$3{,}6\cdot10^{-4}$	$7{,}2\cdot10^{-5}$	$9{,}2\cdot10^{-6}$	$1{,}5\cdot10^{-6}$	$6{,}3\cdot10^{-7}$
800	$3{,}6\cdot10^{-4}$	$7{,}4\cdot10^{-5}$	$2{,}3\cdot10^{-5}$	$2{,}9\cdot10^{-6}$	$3{,}0\cdot10^{-7}$	$1{,}5\cdot10^{-7}$

Ω (the photoelectron is emitted in the direction Ω) [3]; $\rho_e(\mathbf{r}, t)$ is the density of electrons of the atomic shell of the elements entering into the composition of the medium; $\rho_{at}(\mathbf{r}, t)$ is the density of atoms of the elements of the medium; $l(\varepsilon_e)$ is the resulting displacement of an electron with energy ε_e along the direction of flight of the electron.

Changing the order of integration with respect to Ω and Ω' in Eq. (1) and integrating over Ω', we obtain

$$\mathbf{j}(\mathbf{r}, t)=\int\int d\varepsilon\, d\Omega\Omega f(\mathbf{r}, \Omega, \varepsilon, t)[j_k(\varepsilon, \mathbf{r}, t)+j_p(\varepsilon, \mathbf{r}, t)], \tag{2}$$

where

$$j_k(\varepsilon, \mathbf{r}, t)=\int d\Omega' \cos(\Omega, \Omega')\frac{d\sigma_k(\varepsilon, \Omega, \Omega')}{d\Omega'} l(\varepsilon_e)\rho_e(\mathbf{r}, t);$$

$$j_p(\varepsilon, \mathbf{r}, t)=\int d\Omega' \cos(\Omega, \Omega')\frac{d\sigma_p(\varepsilon, \Omega, \Omega')}{d\Omega'} l(\varepsilon_e)\rho_{at}(\mathbf{r}, t)$$

are the moduli of currents of Compton electrons and photoelectrons generated by a single γ-quantum with energy ε.

Values for $j_k(\varepsilon, \mathbf{r}, t)$ and $j_p(\varepsilon, \mathbf{r}, t)$ for air at normal density are shown in Fig. 1. The displacement $l(\varepsilon_e)$ was chosen according to [4] in the form

$$l=0.917(\sqrt{1+22.4\varepsilon_e^2}-1); \quad [l]=\text{m}, \quad [\varepsilon_e]=\text{MeV}.$$

For γ-quanta energies greater than 70 keV the Compton-electron current predominates. At lower energies the photoelectron current becomes more significant. With increasing atomic number of the element, the role of the photoelectron current will increase because of the increase in the photoeffect cross section in heavy elements.

The functional (2) for radial electron currents excited by a stationary isotropic point source of γ-quanta (ε = 1 MeV) in air was estimated by the Monte-Carlo method. We consider 5000 histories of γ-quanta. The probable error is ~5-10%. The γ-radiation field was calculated according to Berger. The investigation of the history of a γ-quantum was ended when it attained weight 10^{-4}. To increase the accuracy of the calculations we selected singly scattered γ-quanta.

Figure 2 shows the buildup factor of the modulus of electron current B, equal to the ratio of the modulus of the electron current produced by all the γ-quanta to the modulus of the electron current excited by the nonscattered γ-radiation. The values for the calculated buildup factor B are less than the energy buildup factors given in [5].

The buildup factor B in the interval of $\mu_0 r$ values from 0.5 to 8 can be interpolated from the exponential function $B = e^{0.27\mu_0 r}$. The quantity μ_0 is the coefficient of absorption of the γ-quanta current with energy 1 MeV. The interpolation error does not exceed the calculation errors.

The total radial electron current j(r) can be interpolated from the function

$$j(r)=\frac{0{,}01}{4\pi r^2}\exp\left(-\frac{r}{170}\right). \tag{3}$$

On the basis of the obtained equation (2) we could similarly calculate the radial electron current produced by the scattering of γ-radiation from a point isotropic monochromatic (ε = 1 MeV) transient source of γ-quanta in air over the entire surface of a sphere at various distances from the source r at various time intervals Δt, measured from the moment of arrival of the nonscattered radiation. We considered 10,000 histories. The probable error was ~5-20%. The calculation results are represented in Table 1.

We see from Table 1 that the main contribution to the resulting current is produced in the range from 0 to 0.2 μsec. Hence, if the source varies with time no more than 0.2 μsec, for electron currents we can use the interpolation relations (3) for the standard γ-quanta source. The time dependence of the electron current in this case will be determined by the time dependence of the γ-quanta source.

LITERATURE CITED

1. V. Gilinsky, Phys. Rev., 137, 50 (1965).
2. Yu. A. Medvedev, B. M. Stepanov, and G. V. Fedorovich, Zh. Tekh. Fiz., 39, No. 5, 875 (1969).
3. W. Heitler, Quantum Theory of Radiation, Oxford, New York (1954).
4. K. Siegbahn (editor), Beta- and Gamma-Ray Spectroscopy, Interscience, New York (1955).
5. O. I. Leipunskii, B. V. Novozhilov, and V. N. Sakharov, Propagation of γ-Quanta in a Substance [in Russian], Fizmatgiz, Moscow (1960).

TYPE ÉPG-10-1 ELECTROSTATIC ACCELERATOR WITH CHARGE REVERSAL

A. S. Ivanov, G. F. Kirshin,
V. M. Latmanizov, A. V. Lysov,
V. D. Mikhailov, G. Ya. Roshal',
and S. A. Subbotkin

UDC 621.384.65

An ÉGP-10-1 electrostatic accelerator with charge reversal of negative ions at a gas target was developed and tested in the D. V. Efremov Scientific Research Institute of Experimental Atomic Physics. Figure 1 is an overall view of the generator and the beam outlet system. The basic parameters of the accelerator are indicated below.

Energy of the proton beam	3-10 MeV
Stability of the average energy of the accelerated particles	not worse than ±5 keV
Current of the accelerated proton beam	up to 3 ± 0.5 μA
Diameter of the ion beam at the target	less than 10 mm

A vertical electrostatic generator housed in a tank with 3 m diameter and a height of 11.2 m is used as the high-voltage source. The tank is designed for gas pressures of up to 14 atm. The accelerator tubes and columns consist of two identical sections with the columns having a length of 4.25 m. The tank is divided into sections which reduces the height of the building. The equipment comprises an injector of negative particles provided by a "duoplasmatron" source [1], a 90° magnetic analyzer for two directions, and two distributing magnets which can deflect the accelerated particle beam into one of ten selected directions.

The negatively charged particles are introduced into the accelerator tube by means of a 90° injector magnet which analyzes the beam and directs it from the horizontal source into the vertical tube. The injector magnet is two-sided so that two sources can be used and transitions from one species of negatively charged particles to another are possible without interrupting the operation of the accelerator. Collimators, focusing and beam adjusting devices, and instruments for measurements of the beam parameters and the beam position are located between the injector magnet and the accelerator tube. The injector generates at the input to the accelerator tube a negative ion beam with energies of up to 50 keV, currents of up to 40 μA, and a beam diameter of about 2 mm.

Tubes with an inclined field are used in the ÉPG-10-1 accelerator. Porcelain insulators are glued to the 1Kh18N9 stainless steel electrodes with PVA adhesive. The distance between the electrodes of the tube is 25 mm.

The support column of the accelerator consists of four vertical posts of ÉPL-2 epoxy resin with quartz filling. The posts are joined by stainless steel plates and equipotential frames (distance between the frames 50 mm). Four pairs of spark gaps are inserted in each gap of the column and two pairs of spark gaps are inserted in the gaps of each tube. Three tubes are located in the generator column. Two tubes (with the charge-reversing target between them) form the accelerating path. The gas which entered into the target area is pumped off behind the third tube (see Figure 2).

In order to improve the vacuum in the accelerating tubes, the chambers near the target are separated from the tubes by diaphragms. The tube containing the gas target extends beyond the evacuated volume and

Translated from Atomnaya Énergiya, Vol. 34, No. 5, pp. 401-403, May, 1973. Original article submitted July 10, 1972; revision submitted November 30, 1972.

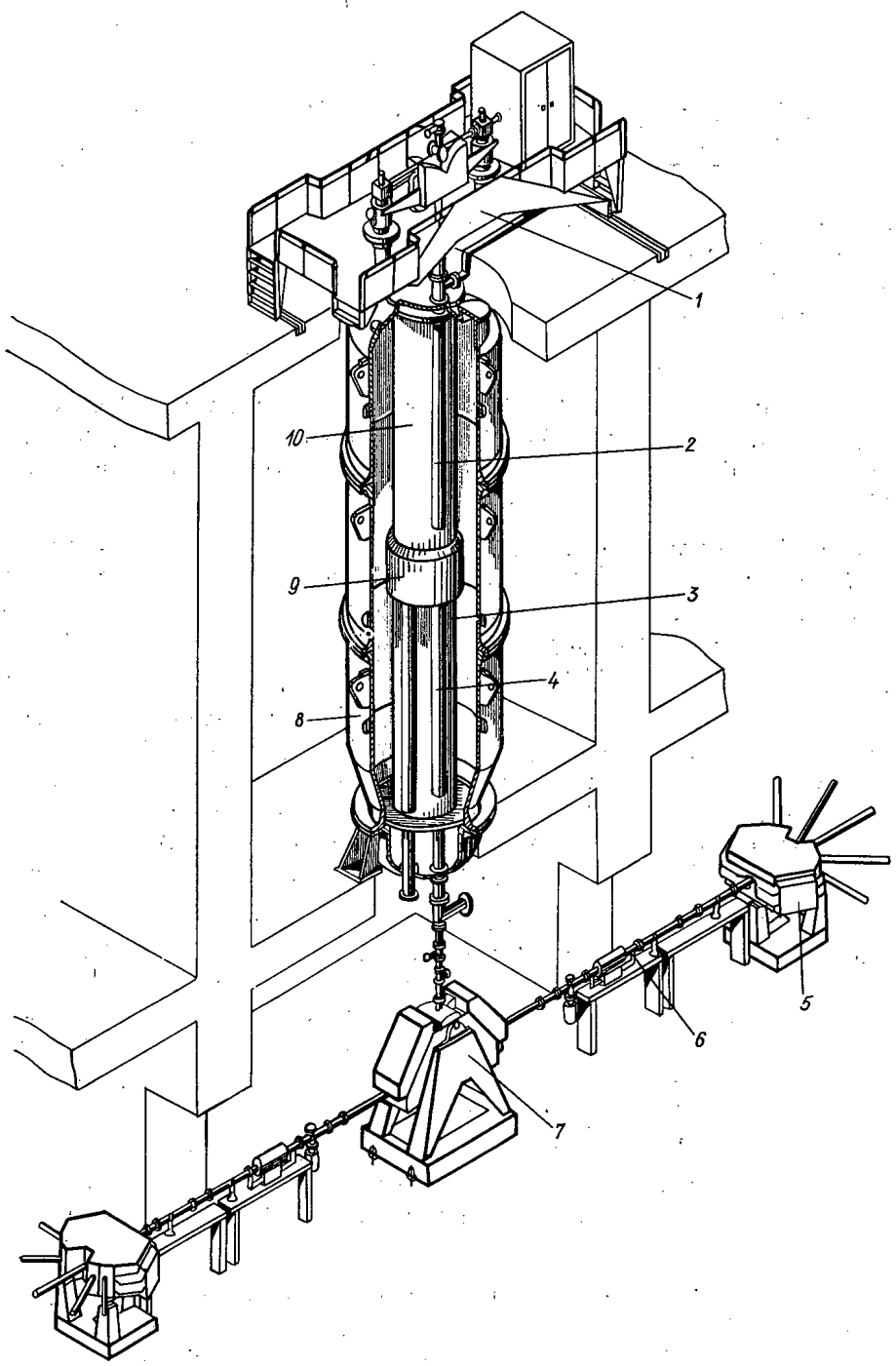

Fig. 1. Cryogenic equipment: 1) sealing gasket; 2) clamping coupling; 3) removable chamber with maintenance of reservoir pressure; 4) valve for pumping off nitrogen vapor; 5) channel for pouring in nitrogen; 6) nitrogen (liquid or solid); 7) outer cylindrical jacket; 8) internal vessel.

is connected to the chambers before the target by means of bellows. This makes it possible to move the gas target tube in any direction by ±3 mm, with the vertical position of the target being preserved. A solenoid actuator can be used to introduce Faraday cylinders into the beam before the target and behind the target. Before the target (around its inlet opening), four insulated sectors were arranged. The currents from these sectors, along with the currents of the Faraday cylinders, make it possible to determine the beam losses in the charge-reversing target and in the accelerating tubes, and to estimate both the focusing and the position of the beam at the inlet area to the target. A single-channel remote measuring system allows successive measurements of 12 beam parameters.

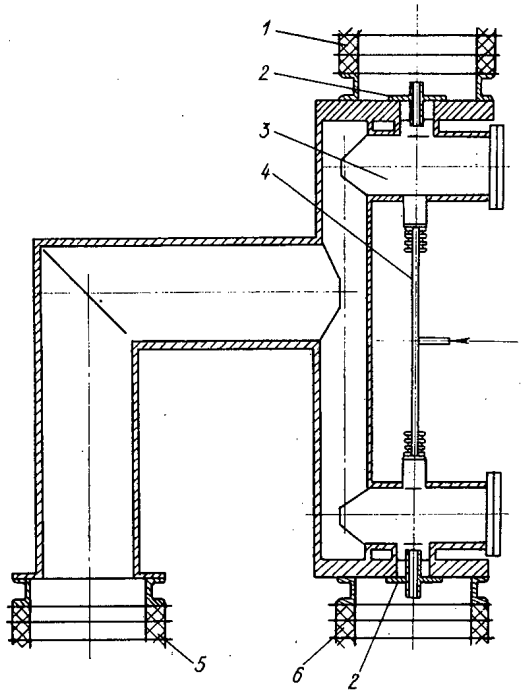

Fig. 2. Charge reversing device: 1) upper accelerating tube; 2) diaphragm; 3) pre-target chamber; 4) charge-reversing target; 5) tube for pumping; 6) lower accelerating tube.

Both the size and the point of beam entry into the magnetic analyzer are given by two slits which are rotated by 90° relative to each other and situated at the focal point of the beam. These devices, combined with the slit sensors of the beam-stabilizing system, which are located behind the magnetic analyzer, determine the constant radius of beam rotation. Both the correction of the particle trajectory and the focusing of the beam at the inlet to the magnetic analyzer are effected with an electrostatic correction lens. Electromagnetic 4K20 × 20-1400 lenses which provide for the required beam size in the ion duct and at the target are located behind the magnetic analyzer. A television system is provided for checking the beam focusing over the entire beam path.

Vacuum in the sources, accelerating tubes, and ion duct was maintained with four VA-2-1R mercury pumps and 12 NÉM-100 magnetic discharge pumps. At a normal influx of gas to the source and to the charge-reversing target during operation, the vacuum in the ion duct and at the exit from the accelerating tubes amounted to $(2\text{-}3)\cdot 10^{-6}$ torr, and to $(6\text{-}8)\cdot 10^{-6}$ torr in the injector.

When a standard mixture of 75% N_2 and 25% CO_2 was used (the moisture of which corresponds to a dew point below −50°C under normal pressure), it was not possible to obtain a voltage in excess of 4.7 MeV in operation "without breakdown" (which means one or two breakdowns in a 24-hour interval). Upon addition of 5-8% freon-12, the voltage at the high-voltage electrode increased to 5.4 MeV during operation "without breakdown."

When no breakdown of the gas insulation in the accelerator occurred, the tubes without "deep" breakdown could be "aged." It was noted that breakdown conditions were reached when the vacuum deteriorated and that x-rays were emitted under these conditions. The voltage was increased in 50-100 keV steps; in this process, the voltage was maintained for time periods required for restoring the vacuum and for the x-ray radiation to disappear. The voltage at the accelerating tubes was increased to 5.1 MeV, i.e., to a value which suffices for obtaining the particular beam energy. When a negative ion beam with a current of 8-10 μA was injected into the accelerating tubes (which corresponds 3 μA at the end of the ion duct), the electric breakdown strength of the tubes was practically not reduced.

The potential distribution over the tube sections was maintained with an accuracy of 1% with the aid of carefully selected KÉV-5 resistors of a voltage divider. The calculated deviation [2] of the beam from the beam axis in the charge-reversing target was less than 0.3 mm. Shifting of the beam at the output of the accelerating tube upon variations of the voltage applied to the device (calculated shifts ±1 mm) were eliminated with a correction lens situated directly underneath the accelerating tube.

The auto-focusing principle of [3] was used in the ÉGP-10-1. Auto-focusing makes it possible to maintain the beam focusing in the region of the charge-reversing target when the generator voltage changes.

The "stripping" of negative ions to protons was studied on hydrogen and oxygen. At a hydrogen influx rate of 100 cm^3/h, the density of the target amounted to $5\cdot 10^{16}$ molecules/cm^3, which guaranteed a 90% stripping of the ions having an energy of 0.7 MeV. An increase in the target density increased the pressure in the tubes, and a glow discharge which greatly reduced the voltage at the generator appeared at the electrodes of the tubes situated close to the target. Ninety per cent of the negative ions with an energy of 5 MeV were stripped when an oxygen target with the same density was used.

Nuclear resonance reactions and threshold reactions [4, 5] were used to investigate whether the beam is monoenergetic, to study the reproducibility and stability of the energy of the charged particles as a function of time, and to determine the constancy of the operation of the magnetic analyzer and the calibration of the rotary voltmeter scale.

It was established in these investigations that the constant of the magnetic analyzer changes monotonically in the interval of 1.4-9.5 MeV, with the variations not exceeding 1%. When the field of the magnetic analyzer was restored to the respective experimental conditions and when the beam focusing at the entry to the magnetic analyzer was disturbed and restored by a correction lens, the reproducibility of the beam energy turned out to be not worse than 250 eV. The variations of the charged particles' energy were less than 850 eV during 6 hours of accelerator operation. The beam was estimated to be monoenergetic to within $(7.5\text{-}7.7)\cdot 10^{-4}$.

LITERATURE CITED

1. M. Abroyan et al., Particle Accelerators, 2, 133 (1971).
2. V. S. Kuznetsov and R. P. Fidel'skaya, Zh. Tekh. Fiz., 35, 11 (1965).
3. A. V. Almazov, Pribory i Tekh. Éksperim., No. 5, 43 (1964).
4. A. L. Bornyanskii and A. I. Graevskii, in: Applied Nuclear Spectroscopy [in Russian], No. 1, Atomizdat, Moscow (1970), p. 314.
5. M. I. Afanas'ev, et al., Atomnaya Énergiya, 31, No. 2, p. 141 (1971).

YIELD OF Ti^{44} WHEN SCANDIUM IS IRRADIATED WITH PROTONS OR DEUTERONS

P. P. Dmitriev, G. A. Molin, and N. N. Krasnov

UDC 621.039.8.002

From the decay scheme (Fig. 1) it follows that the isotope Ti^{44} ($T_{1/2}$ = 48 years) is a long-lived isotope generator of Sc^{44} ($T_{1/2}$ = 3.92 h). The gamma spectrum of the isotope Ti^{44}, which is in equilibrium with the daughter nucleus Sc^{44}, contains the following gamma lines (quantum yields in brackets): 67.8 keV (90%); 78.4 keV (98%); 511 keV (188%, annihilation radiation); 1159 keV (100%). The gamma lines at 2670 (0.14%) and 1514 keV (0.76%) are hardly observed, owing to their low intensity [1]. The scandium fraction emitted by the Ti^{44} does not contain the gamma lines at 67.8 and 78.4 keV.

The isotope Ti^{44} is a typical cyclotron isotope, i.e., it is obtained only in reactions with charged particles. The most effective reactions for the production of Ti^{44} are Sc^{45} (p2n) and Sc^{45} (d3n); the energy thresholds of these reactions are 12.5 and 15.1 MeV respectively.

Data on the cross sections of reactions forming Ti^{44} are given only by McGee et al., [2], who measured the cross sections of the reaction Sc^{45} (p2n) Ti^{44} for ten values of the proton energy between 15 and 85 MeV; the error of measurement of the cross section was ±30%. On the basis of the cross sections

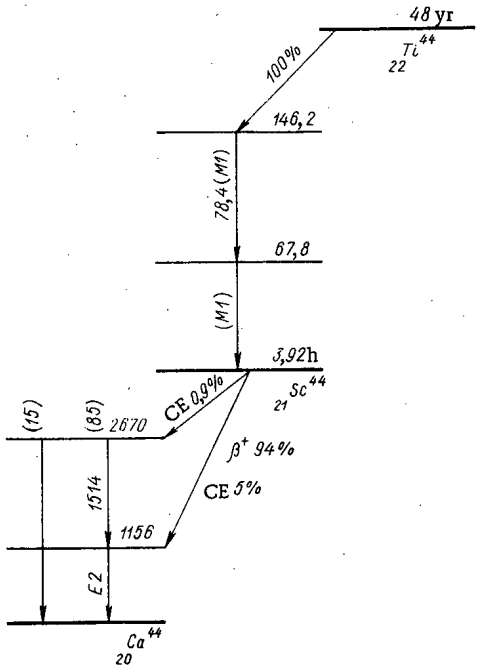

Fig. 1

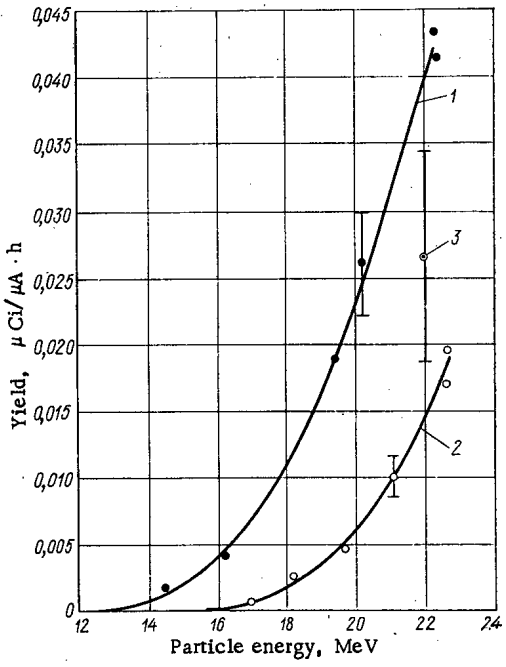

Fig. 2

Fig. 1. Decay scheme $Ti^{44} \rightarrow Sc^{44}$.

Fig. 2. Yield of Ti^{44} vs energy of bombarding particles for thick scandium targets: 1) irradiation by protons; 2) irradiation by deuterons; 3) estimate from data in [2].

Translated from Atomnaya Énergiya, Vol. 34, No. 5, pp. 404-405, May, 1973. Original article submitted October 13, 1972.

obtained in this work, we estimated the yield of Ti^{44} for a thick target for a proton energy of 22 MeV, which qualitatively agrees with our values for the yield of this isotope with $E_p = 22$ MeV.

We have now measured the yields of Ti^{44} as a function of the energy of the bombarding particles when thick targets of metallic scandium are irradiated by protons and deuterons. The maximum particle energies were $E_p = 22.3 \pm 0.3$ MeV, $E_d = 22.6 \pm 0.6$ MeV. The work was performed in the FÉI cyclotron. To measure the activity of Ti^{44} we used the gamma lines at 67.8, 78.4, and 1156 keV. The activity and the Ti^{44} yield curves were measured by a method similar to that described by us in [3].

When scandium is irradiated by deuterons, large yields of Sc^{46} are formed by the reaction Sc^{45} (dp) Sc^{46}. Therefore for specimens irradiated with deuterons we radiochemically separated Ti^{44}. For the proton-irradiated specimens, we did not radiochemically separate the Ti^{44}. The activity of the Ti^{44} was measured 2, 4, and 10 months after irradiation; in all three cases we obtained practically the same value for the activity of Ti^{44}.

Experimental curves of the yield of Ti^{44} are given in Fig. 2. The error of measurement of the Ti^{44} yield is ±15%. The results of the measurements show that, for example, for a particle energy of 22 MeV, the yield of Ti^{44} for bombardment by protons is 0.040 $\mu Ci/\mu A \cdot h$, which is 2.7 times greater than the yield obtained from bombardment by deuterons.

The authors thank G. N. Grinenko and Z. P. Dmitrieva for assistance in their work, and also V. G. Vinogradova for performing the radiochemical separation of the Ti^{44}.

LITERATURE CITED

1. C. Lederer et al., Tables of Isotopes, J. Wiley and Sons, New York (1967).
2. T. McGee et al., Nucl. Phys., A150, 11 (1970).
3. P. P. Dmitriev et al., At. Énerg., 32, 426 (1972).

YIELDS OF Se^{72} AND Se^{75} IN NUCLEAR REACTIONS WITH PROTONS, DEUTERONS, AND α-PARTICLES

P. P. Dmitriev, G. A. Molin,
I. O. Konstantinov, N. N. Krasnov,
and M V. Panarii

UDC 621.039.8.002

The isotopes Se^{72} ($T_{1/2}$ = 8.4 days) and Se^{75} ($T_{1/2}$ = 120 days) are widely used in applied and theoretical research [Se^{75} decays by electron capture forming As^{72} ($T_{1/2}$ = 26 h)].

In this article we describe measurements of the dependence of the yields of Se^{72} and Se^{75} on the energy of the bombarding particles when thick arsenic targets (in the form of powder) are irradiated with protons and deuterons (product Se^{75}) and when germanium (metal) targets are irradiated with α-particles (products Se^{72} and Se^{75}). The activity of the Se^{72} was measured by means of the photopeak of the 835 keV γ-line of the daughter nucleus As^{72} (yield 0.78 quanta per disintegration); the activity of Se^{75} was measured by means of the photopeak of the γ-line at 256 + 280 keV (total yield 0.85 quanta per disintegration). The values of the quantum yields of the γ-lines were taken from [1]. The method of irradiation and measurement of the yields and the activity of the isotopes was similar to that described by us in [2].

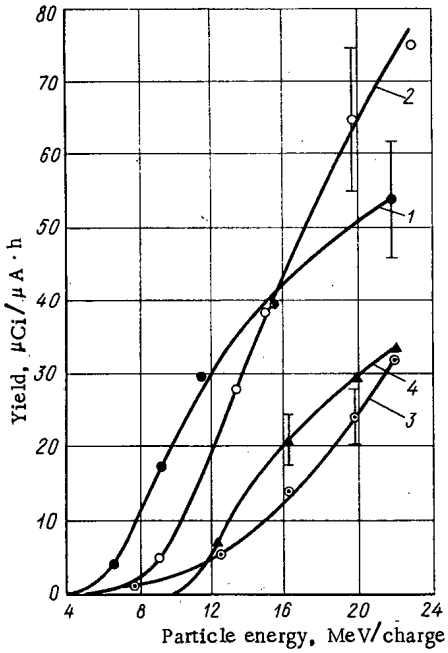

Fig. 1. Yields of Se^{72} and Se^{75} from irradiation of arsenic with protons and deuterons and germanium with α-particles: 1) As + p → Se^{75}; 2) As + d → Se^{75}; 3) Ge + α → Se^{75} (increased fourfold); 4) Ge + α → Se^{72}.

Table 1 lists the reactions in which Se^{72} and Se^{75} are formed, and also the yields, measured at maximum particle energy. The experimental curves of the yields of Se^{72} and Se^{75} vs particle energy are plotted in Fig. 1. The error of the values obtained for the yields are mainly governed by systematic errors in the measurements of the activity of Se^{72} and Se^{75} and the integral current of bombarding particles, and are estimated to be ±15%.

The methods investigated by us for obtainging Se^{72} and Se^{75} are the most effective in utilizing the energy of the particles.

TABLE 1. Yields of Isotopes Se^{72} and Se^{75}

Formation reaction	Energy threshold of reaction, MeV	Content of initial isotope, %	Data on yields: particle energy, MeV	Data on yields: yield, μCi/μA·h
$As^{75}(pn)Se^{75}$	1,67	100	21,8±0,2	52±7,8
$As^{75}(d2n)Se^{75}$	3,97	100	23±0,2	77±12
$Ge^{70}(\alpha 2n)Se^{72}$	17,6	20,6	44±0,5	33±5
			42 *	20 *
$Ge^{72}(\alpha n)Se^{75}$	6,4	27,43		
$Ge^{73}(\alpha 2n)Se^{75}$	13,55	7,84	44±0,5	8±1,2
$Ge^{74}(\alpha 3n)Se^{75}$	24,3	36,40		

*Data from [3], yield obtained by integrating excitation function.

Translated from Atomnaya Énergiya, Vol. 34, No. 5, pp. 405-406, May, 1973. Original article submitted November 9, 1972.

To obtain Se^{75} we also used the reaction $Se^{74}(n\gamma)Se^{75}$; however, in this case the Se^{75} is formed "with a carrier."

In the literature there are no data on the yields of Se^{72} and Se^{75}. We know only of one publication [3] on the reaction cross sections, in which the authors describe measurements of the excitation function of the reaction $Ge^{70}(\alpha 2n)Se^{72}$ up to $E_\alpha = 42$ MeV. Delaunay-Olkowsky et al. [4] measured the cross section of the reaction $As^{75}(pn)Se^{75}$ at $E_p = 11.2$ MeV: their result was 403 ± 60 mbarn. We carried out a numerical integration of the graph of the excitation function of the reaction, taken from [3]; the value obtained for the Se^{72} yield at $E_\alpha = 42$ MeV, also given in Table 1, is in poor agreement with our results. By means of our graph of the yield of the reaction $As^{75}(pn)Se^{75}$ we estimated the cross section of the reaction at $E_p = 11.2$ MeV, which was found to be 420 ± 70 mbarn; this is in good agreement with the cross section obtained in [4].

The authors thank G. N. Grinenko and Z. P. Dmitrieva for assistance in the work.

LITERATURE CITED

1. S. Lederer et al., Tables of Isotopes, J. Wiley and Sons, New York (1967).
2. P. P. Dmitriev et al., At. Energ., 31, 157 (1971); 32, 426 (1972).
3. S. Amiel, Phys. Rev., 116, 415 (1959).
4. J. Delaunay–Olkowsky et al., Nucl. Phys., 47, 266 (1966).

INFORMATION

A NATURALLY OCCURRING URANIUM CHAIN REACTOR ON THE EARTH

N. A. Vlasov

In June 1972, colleagues of the French Commissariat de l'Énergie Atomique made a very interesting discovery. They found [1] a remarkable departure from the normal U^{235} content in a batch of natural uranium mined in Gabon. To date, the mean U^{235} content in all isotope analyses of uranium mined anywhere on the globe has been 0.720% with deviations remaining within 0.1%. But the uranium mined in the Oklo occurrence in Gabon shows departures from the mean content that are decidedly greater: some samples contained as much as 0.44%. Slightly enriched samples with content as high as 0.730% were also encountered. The absolute age of the rocks in the occurrence, as ascertained by the rubidium–strontium method, was 1740 ± 20 million years. The U^{235} content in the highest-grade uranium ores is lower than that. For example, two samples subjected to painstaking analysis were taken from rocks containing 38.5% and 14.9% uranium. The U^{235} content in those rocks was respectively 0.4400 ± 0.0005% and 0.592 ± 0.001% [2].

These samples were analyzed for the isotope content of rare earths: neodymium, europium, and samarium. It was found that the content of seven neodymium isotopes differs radically from the usual natural content. The difference resides in the fact that part of the neodymium apparently forms through fission of uranium. If the normal content of the other isotopes is arrived at on the basis of the content of Nd^{142} of nonfission origin, and the excess is compared to fission, the agreement will become completely apparent.

The marked deviation from the normal content was detected in the ratio of contents of the isotopes Eu^{151}/Eu^{153} and Sm^{149}/Sm^{147}. Isotopes whose neutron capture cross sections are large featured contents well below normal. It is safe to assume that the variation in the content of isotopes is due to neutron capture. An estimate of the neutron flux capable of causing the observed changes in isotope content yields $\sim 10^{21}$ neutrons/cm^2.

One assumption advanced to account for these phenomena holds that $1.7 \cdot 10^9$ years ago, when the normal U^{235} content was ~3%, conditions favorable to a fission chain reaction occurred in this particular deposit. The geological characteristics of the occurrence happened to be favorable for the formation of uranium salt solutions in water. The resulting natural reactor acted slowly, but over a protracted period, leading to burnup of the U^{235} and the formation of fission-fragment rare earth isotopes. The slight excess of U^{235} at some sites can be accounted for in terms of migration of Pu^{239} stemming from the U^{238} present.

The ratio of the number of fission events forming fission-fragment isotopes to the number of deficient (fissioned) U^{235} nuclei was estimated. It was found that there are twice as many fragments, so that above half of them originated not in the U^{235} but in the U^{238} fissioned by fast neutrons, say.

Investigations of the anomalies detected are continuing. But in order to account for the published* results of the observations, it is sufficient to insist on the assumption of local irradiation of the material in the occurrence by a fairly high-intensity neutron flux.

LITERATURE CITED

1. R. Bodu et al., Comptes Rendus Acad. Sci., 275, D-1731 (1972).
2. M. Neuilly et al., Comptes Rendus Acad. Sci., 275, D-1847 (1972).

* The Russian translations of the articles appeared in Atomnaya Tekhnika za Rubezhom, No. 6 (1973).

Translated from Atomnaya Énergiya, Vol. 34, No. 5, p. 407, May, 1973.

THIRD INTERNATIONAL CONGRESS ON PEACEFUL USES OF UNDERGROUND NUCLEAR EXPLOSIONS

I. D. Morokhov, K. V. Myasnikov,
V. N. Rodionov, and A. A. Ter-Saakov

This third international congress was organized by IAEA and held in Vienna, November 27 through December 1, 1972. There were 80 representatives from 30 countries and three international agencies participating (the European Commonwealth Commission, the United Nations Organization, and the World Health Organization). A total of 23 reports* were presented, including 10 from the USA, 6 from the USSR, 4 from France, 2 from Britain, 1 from Sweden, and one joint report by representatives of Venezuela and the USA on construction of a canal connecting the Orinoco and Rio Negro rivers in Venezuela.

As in the two preceding congresses held in 1970 and 1971, the Soviet Union, the USA, and France submitted reports on the results of research on underground nuclear explosions, pilot-scale explosions, and the outlook for developments in the area of peaceful utilization of underground nuclear explosions.

Evidence of the intense interest in this topic is reflected in the broad representation at these congresses on the part of countries lacking nuclear weapons, as well as the efforts they are making to utilize nuclear explosions in accordance with article 5 of the Nuclear Weapons Nonproliferation Treaty in their national industrial development programs.

The exceptional compactness of the charge, the extremely low cost of the energy released, opens up broad possibilities, in principle, for applications of nuclear explosions for industrial purposes and scientific purposes. As experiments staged in the Soviet Union and in the USA have shown, an apparent funnel crater 400 m in diameter and down to 100 m in depth forms when a 100 kiloton charge is set off. A charge releasing that amount of energy can form a storage cavity with a volume of $\sim 300{,}000\ m^3$ in a massive rock salt block. An impressively extensive range of possible practical applications of underground nuclear explosions is related to the preliminary destruction of occurrences of useful minerals and massive rock formations. The problem is how this enormous source of power can be rendered reliably controllable, by eliminating any possible harmful effects on the envinonment and on humans.

Representatives of Venezuela and of Yemen presented reports on the national programs of their countries in the field of peaceful uses of underground nuclear explosions. Venezuela is considering the use of underground nuclear explosions as a tool in building a canal linking the Orinoco river and the Rio Negro, in extracting geothermal heat and petroleum from otherwise nonpaying petroliferous sandstones, and in mining minerals and stimulating the flow of natural gas (D. Rodriguez Diaz, Venezuela). Of the trends covered in the national programs on peaceful uses of underground nuclear explosions, estimates of a preliminary nature were forthcoming only on the canal construction project (F. Paz-Castillo, Venezuela, and P. Kruger, USA). The use of chemical explosives and nuclear explosives in combination is being proposed for the job of excavating a canal 62 km in length, including the task of building canal sections through hard rock extending to 15.5 km, using 157 10-kiloton nuclear charges. The width of the canal is 77 m, the depth 16 m, and the proposed construction schedule calls for completion within four years.

The Yemeni national developmental program calls for setting off underground nuclear explosions in order to intensify exploitation of oil and gas deposits, to build buried storage reservoirs in rock salt blocks, and to extract geothermal heat (M. El-Qebeili, E. El-Shazli).

* These reports will be published by the IAEA at the end of 1973.

Translated from Atomnaya Énergiya, Vol. 34, No. 5, pp. 407-409, May, 1973.

The Plowshare program (utilizing underground nuclear explosions in the USA) centers its attention, as earlier, on applications of nuclear explosions to intensify exploitation of gas deposits, following the example of the experiment staged at Gas Buggy and Rulison, where research work is being continued (R. Taylor, USA).

Laboratory work on extraction of petroleum from bituminal schists is being conducted on a large scale, with nuclear explosions viewed as a tool for the formation of underground retorts (G. Zonz, USA).

The Plowshare geothermal program has seen some far-reaching changes. USA specialists have now given up the idea of using high-power explosions (in the range of hundreds of kilotons) to fragment rocks to a great depth in order to facilitate extraction of geothermal heat. Current work on extraction of geothermal heat is being carried on in two following directions:

1) hydraulic disruption of the stratum at depths of 2000 m, with rock temperatures at 300-380°C, so that additional breakdown of the host rock will occur as a result of sudden cooling by water (two experimental boreholes were sunk near Los Alamos to test out this concept);

2) the use of chemical high explosives to diminish the hydraulic resistance to escape of geothermal waters to the earth's surface;

3) the use of nuclear explosions of comparatively modest power to handle problems covered in the two preceding points.

Research on applications of nuclear explosions to fragment copper ores with the expectation of subsequently leaching out the copper present is being continued in the USA. Attention is being centered on winning copper from primary sulfide minerals such as chalcopyrite (A. Lewis et al., USA).

The reports made by French specialists (A. Bartou et al.) on that country's national programs, and the papers they delivered, centered attention on the use of underground nuclear explosions to carve out storage reservoirs. A report prepared by Soviet specialists describing pilot plant work to discern the scientific-technical fundamentals of building underground storage reservoirs by means of nuclear explosions set off in a massive block of rock salt (K. V. Myasnikov, E. A. Leonov, and N. M. Romadin, USSR) was heard with great interest in this context. A report was made on advanced experience in the Soviet Union in building rock-fill dams by means of exploding chemical charges, on the Vakhsh river (Baipazan dam) and on the Malaya Alma-Atinka (dam protecting a nearby village) (V. N. Rodionov and A. N. Romashov, USSR). These examples demonstrate successful applications of new technological solutions through the use of powerful explosions.

Most of the reports presented by American specialists dealt with more profound investigations of phenomena accompanying the explosions; these studies relied on simulation, studying results of full-scale experiments, and theoretical investigations utilizing electronic computers.

The investigations are being pursued in such disparate directions as development of the theory of motion and destruction of the medium through an underground nuclear explosion, improvements in techniques for experimental study of the development of explosions, building adequate simulation facilities, detailed development of specific projects for utilizing nuclear explosions in building canals, or in intensifying extraction of natural gas from occurrences, and the study of the propagation of seismic waves determining safety conditions for nuclear explosions.

In the area of excavation work, the USA presented reports on the stability and filtration characteristics of the rims of explosion craters. Analog computer simulation was relied on in this work.

A method involving estimating the extent of fragmentation of rock in an underground nuclear explosion, which was presented in a report on investigations of explosions of several charges in a single borehole, by computer simulation, is of a certain interest in terms of techniques developed. A count was made of how many times each of the cells, into which the entire space was broken up in calculating the flow of the medium, attained the critical stressed state. Zones with multiply "disrupted" cells are taken to be fragmented. This approach made it possible to discern conditions under which a group explosion could exert a greater effect than the sum of sequential explosions delivering the same amount of energy.

A USSR report on the seismic effects of underground explosions outlined methods useful in forecasting seismic vibrations and the consequent damage to buildings (V. N. Kostyuchenko, V. N. Rodionov, D. D. Sultanov, and V. M. Shamin, USSR). It is interesting to note that a somewhat different method is being developed in the USA as an approach to describing seismic vibrations (a report on this topic was submitted

at the previous conference). What is termed the action spectrum, which lays bare the nature of distinct groups of waves, is being used as a characteristic of the vibrations, and that seems convenient for statistical treatment of damage, but unfortunately adds exorbitant difficulties to prognosis of the "spectrum" in an area of surroundings where no explosions have been staged previously. Empirical data fail to indicate any explicit advantages inherent in any of these approaches.

A considerable portion of the reports was devoted to radiation safety in underground nuclear explosions for peaceful purposes. Either methods for forecasting the radiation situation, or estimates of the degree of radiation hazard, were considered in the reports submitted on this topic.

Some of the reports contained useful information on the initial data needed for forecasting models, new ideas and approaches on forecasting. For example, a paper presented by R. Siddons (Britain) based on analysis of published data cited characteristics of basic sources of radioactivity appearing in underground explosions, and estimated the contribution made by those sources to the total quantity of radioactive products formed, while taking note of the decline in the total amount. The opinion was voiced that the information available on this topic constitutes a basis for forecasting radiation hazard when any project involving the use of nuclear explosions for peaceful purposes comes up for discussion.

A USSR paper presented by Yu. A. Izraél' reviewed published data on radioactive contamination of basic zones (clouds, epicentral region, close and distant traces) in underground explosions hurling debris into the air, and on that basis formed a concept of the phenomenology of radioactive contamination of the environment.

A certain amount of interest was shown in a paper by M. Dupuis (France) in which approaches to estimates of the distribution of various isotopes in the vapor phase, liquid phase, and solid phase, under conditions typical of a closed cauldron type cavity at different times after an explosion, were discussed. The principal approach in this paper is based on the thermodynamic equilibrium principle. In line with the model developed here, we find a gradual accumulation of the particular radioisotope in a layer of fused soil. For example, estimates indicate that the maximum amount of Kr^{85} ending up in the melt of soil caused by the explosion is 10 to 20% of the amount formed and accumulated within ~150 sec. At the same time, according to our data, the same amount of gaseous radioisotope (e.g., Xe^{137}) becomes accumulated in the melt within seconds or fractions of a second, in the case of excavation explosions. This suggests that reliance on the laws of thermodynamical equilibrium for all radioisotopes may prove illusory. Another Soviet paper on this topic (Yu. A. Izraél', A. Ter-Saakov, V. A. Petrov, G. A. Krasilov) was devoted to an investigation of the radiation characteristics of the principal carriers of radioactive products, and to developing models of the formation of radioactive products in underground nuclear explosions.

As for estimates of the degree of radiation hazard, we first have to consider the report by M. Kelly (USA) which provides estimates of the comparative hazard due to radioisotopes present in natural gas extracted from occurrences by means of underground nuclear explosions.

Three aspects of this topic came under consideration in that paper:

1) possible concentrations of different radioisotopes in gas (on the basis of data relevant to the "Gas Buggy" and "Rulison" explosions);

2) comparison of proposed doses which can be experienced by different persons and by the population as a whole when radiation-contaminated gas is used, and the theoretically calculated exposure doses due to other sources;

3) comparison of the hazard prognosis for calculated mean exposure doses and other forms of non-radiation hazard encountered in daily human life, a procedure which is in our opinion of unquestionable interest for the development of research pertaining to utilization of nuclear energy.

This exchange of information revealed a unanimity of opinion among specialists on all the basic questions in principle concerned with the peaceful uses of underground nuclear explosions, and mutually enriches all of the seminar participants with the experiences of their colleagues. The next conference is scheduled for 1974.

PRESENT RESEARCH ON THE PHYSICOCHEMICAL STATE OF RADIOISOTOPES IN SEA WATER

A. G. Trusov

The widespread industrial application of nuclear power and radioactive isotopes, as well as the nuclear weapons testing in the atmosphere that is being continued by some countries, is stimulating the study of the properties and behavior of artificial radioisotopes in sea water, since the seas and oceans act as the final and eventual reservoirs where radioactive substances become concentrated. The extent to which radioactive isotopes partake in processes of sedimentation and biological concentration and assimilation depends to an appreciable degree on the chemical form and on the physicochemical state of those isotopes. Topics pertaining to the physicochemical state of isotopes also come to the fore when practical problems involving deactivation of water are to be solved, and when waters are to be analyzed for their content of radioisotopes.

Taking into cognizance the interest shown in this set of problems by specialists in different fields, the Oceanographic Commission of the USSR Academy of Sciences (Marine radioactivity subsection) and the Institute of the Biology of the Southern Seas under the jurisdiction of the Academy of Sciences of the Ukrainian SSR (Radiobiology division) convened on All-Union symposium on the physicochemical state of radioisotopes in sea water which was held at Sevastopol', November 21-23, 1972.

The following topics came under discussion:

1) theoretical aspects of the behavior of chemical elements in solution at ultrasmall concentrations;
2) techniques for studying the physicochemical state of ultrasmall amounts of elements present in sea water;
3) results of observations of the state and chemical form of artificial radioisotopes and stable elements in sea water;
4) the effect of the forms and state of radioisotopes on their interaction with living organisms in the marine environment.

The fundamental topics pertaining to techniques for displaying the various physicochemical forms of matter in solution at very high levels of dilution occupied a central place in the program agenda.

A report by I. A. Skul'skii (Institute of Evolutionary Physiology and Biochemistry of the USSR Academy of Sciences) developed a new concept of the familiar adsorption method, proposed earlier by I. E. Starik, for use in studying the state of matter in solution. The change in sorbability of hydrolyzable elements in response to the pH of the solution can be due not only to the transition of an element from the ionic state to the uncharged (colloidal) state, but also to some difference in the properties of the simple ions and hydrolyzate ions, or hydrolyzate ions of different degrees of hydrolysis, or monomeric and polymeric forms of hydrolyzates. This interpretation of the pH vs adsorption of the element curve resolves many contradictions plaguing the adsorption method when the classical prerequesites of that method are retained.

Theoretical analysis of the reasons for the appearance of the peak on the pH-adsorption (of the element) curve was attempted in a report by N. D. Betenkov et al. (Urals Polytechnic Institute). The authors showed that this peak corresponds, as a rule, to the isoelectric state of the system of hydroxo complexes.

A report by Yu. P. Davydov (Nuclear Power Institute of the Academy of Sciences of the Belorussian SSR) dealt with the relationship between adsorption, colloidal formation, and polymerization phenomena in hydroxo complexes. The familiar physicochemical concept known as the "solubility product" of sparingly

Translated from Atomnaya Énergiya, Vol. 34, No. 5, pp. 409-411, May, 1973.

soluble hydroxides was placed under criticism. In the author's view, this product ceases to be a constant for any elements whose hydrolysis takes place by a polymerization mechanism.

N. I. Popov (Institute of Oceanology of the USSR Academy of Sciences) discussed thermodynamical equilibrium forms of hydrolyzable elements as parameters typical of sea water. It was found that the typical form in which such elements are presented in the dissolved fraction of sea water are uncharged hydroxide molecules. The concentrations of any of the hydrolyzable elements in the ocean are such that these molecules are incapable of forming an independent solid phase or of forming polymer chains. The view was also put forth that, despite the generally accepted concept, artificial radioisotopes gaining access to ocean waters cannot be entirely bound to the solid phase of sea water, apparently, because of the exceptionally low content of that phase in the waters of the high seas, and because of the limited adsorptivities involved.

Practical methods in the study of the state of radioisotopes present in the ocean waters received a good deal of attention at the symposium. Methodological difficulties in these lines of research are due to two sets of circumstances. On the one hand, all known familiar methods have been designed for laboratory work. Isolation of a restricted volume of water and transport of the sample under investigation within the confines of a laboratory can alter considerably the natural conditions under which the radioisotope persists in a marine environment. And on the other hand, when the water is seeded with the radioisotopes under investigation in a laboratory setting, there is no assurance that the initial forms by which the isotopes are introduced into the sea water in the laboratory and in nature are identical.

The special approaches maximizing identification of laboratory forms of access to sea water on the part of some naturally occurring radioactive isotopes and the natural forms were dealt with in a report by Yu. V. Kuznetsov and colleagues (V. G. Khlopin Radium Institute). These authors also addressed themselves to a set of techniques for discerning regularities in the behavior of naturally occurring radioactive isotopes in situ in ocean waters.

A new method of laboratory investigation of the state of aggregation of radioisotopes in solution, the "daughter atoms" method, was described by I. A. Skul'skii and V. V. Glazunov.

Electrofiltration of sea water for the purpose of isolating the finest solids fraction was reported on by Yu. B. Kholin and L. M. Khitrov (Institute of Geochemistry and Analytical Chemistry of the USSR Academy of Sciences).

The interactions between the chemical forms of elements in a solution of natural waters and adsorption of those elements on ion exchange resins were the subject of reports by P. D. Novikov and co-workers (Institute of Oceanology of the USSR Academy of Sciences) and A. P. Sorochan and G. M. Vartol (Institute of Geochemistry and Analytical Chemistry of the USSR Academy of Sciences).

In a section reflecting the results of observations and experiments, new data were presented on the physicochemical state of artificial radioisotopes of manganese, cobalt, cerium, copper, zinc, ruthenium, and iron (L. M. Khitrov and Yu. B. Kholin; V. K. Legin, Yu. V. Kuznetsov, and Yu. N. Lobanov; Yu. M. Petrov, the Polar Science Research and Planning Institute of Sea Fisheries and Oceanography; A. A. Lyubimov and L. I. Rozhanskaya, Institute of Biology of the Southern Seas of the Academy of Sciences of the Ukrainian SSR).

A comparative juxtaposition of the behavior of Sr^{90} and Cs^{137} in the ocean environment was presented in a paper submitted by A. G. Trusov, L. M. Ivanova, L. I. Gedeonov (GKAE SSSR), of the V. G. Khlopin Radium Institute.

Recalling that the state of radioisotopes in the ocean, as products of nuclear explosions, can depend on the specific initial state, forms of fission-fragment isotopes in atmospheric fallout were discussed (M. I. Zhilkina, L. I. Gedeonov, A. G. Trusov).

Realistic possibilities of interactions between artificial radioisotopes gaining access to sea water and organic material dissolved in sea were discussed. V. P. Parchevskii and Yu. M. Serdyukov (Institute of Biology of the Southern Seas, Academy of Sciences of the Ukrainian SSR) found that some radioisotopes are bound by surfactants released from sea water, under laboratory conditions. However, N. I. Popov, in a survey of literature data, showed that no reliable critera for organic complexing of artificial radioisotopes in situ in ocean waters has been forthcoming to date.

A separate session of the symposium was devoted to the influence exerted by the state of radioactive isotopes on absorption of those radioisotopes by marine hydrobionts. Using ample original material in the literature, A. Ya. Zesenko (Institute of Biology of the Southern Seas, Academy of Sciences of the Ukrainian SSR) demonstrated the exceptionally high receptivity of living organisms to the forms and state of chemical elements and their isotopes when concentrated from water. G. G. Polikarpov, V. G. Tsytsugina, and A. V. Tokareva (Institute of Biology of the Southern Seas, Academy of Sciences of the Ukrainian SSR) showed that localization of, say, Y^{91} in different components of the cell is a function of the "aging" of the radioisotope in solution.

A relationship was established between the state of radioisotopes and absorption of those radioisotopes by zooplankton (V. N. Ivanov, Institute of Biology of the Southern Seas of the Academy of Sciences of the Ukrainian SSR), and by higher-order algae (N. I. Buyanov, Polar Science Research and Planning Institute of Sea Fisheries and Oceanography).

Lively discussions were stimulated by all of the presentations.

The symposium materials are to be published in a separate edition.

SYMPOSIUM ON NEUTRON DOSIMETRY FOR RADIOLOGICAL PROTECTION

M. M. Komochkov

A symposium organized by IAEA was held December 11-15, 1972, in Vienna, on neutron dosimetry in radiological protection work. There were 145 specialists in attendance, from 30 countries and 9 international agencies. A total of 63 reports were presented, as well as several brief communications.

Neutron spectra and depth dose distributions were in the spotlight as key information in establishing radiation hazard, calibration of instrumentation, interpretation of results of measurements of radiation fields, and in critical comparison of rival techniques and instruments in dosimetry. New results on neutron energy spectra in the 90 keV-11 MeV range, from Ra–Be-sources, Am–Be-sources, and Pu–Be-sources were reported (H. Kluge et al., West Germany). With the aid of a spectrometer designed by R. Madey and F. Waterman (USA), the energy distributions of neutrons forming when a beryllium target is bombarded by 447 MeV deuterons or by 724 MeV protons were measured. Experimental results were specifically useful in finding the degree of reliability of Monte Carlo data. Some interesting reports were forthcoming on the energy distributions of neutrons beyond the shielding of nuclear physics research installations. The spectra were studied in relation to the composition of the shielding, the composition of the material, and the radiation source. For example, a paper presented by V. E. Aleinikov et al. (JINR) dealt with neutron energy distributions in the 10^{-2} to 10^{9} eV range beyond the shielding of a synchrocyclotron and in the vicinity of the JINR synchrophasotron (proton synchrotron). The measurement results showed that the neutron spectra are dependent not so much on the energy of the accelerated protons as on the configuration and design of the shielding. As a consequence, the contribution made by relativistic neutrons beyond the solid concrete shielding around the synchrocyclotron which accelerates protons to 660 MeV is about 80% of the total equivalent dose, whereas this contribution amounts to ~20% of the total equivalent dose near the synchrophasotron machine accelerating protons to 10 GeV, in the region of the "penumbra" created by the iron core of the accelerator and its ancillary equipment.

Of the reports on depth dose distribution in tissue-equivalent phantoms, we should note one contribution by G. M. Obaturov, which was presented at the symposium by I. V. Filyushkin (USSR). These data constitute an excellent supplement to similar results published by W. Snyder in 1970.

A proposal put forth by G. Stevenson in the name of a group of authors, on standardization of the conversion ratio from flux to equivalent dose, in total body irradiation by neutrons, provoked keen interest and a lively floor discussion. They recommended that the equivalent dose transferred to the surface of the phantom irradiated on both sides by a unit flux of monoenergetic neutrons be taken as the standard. The basis for this proposal was the recent set of ICRU and ICRP recommendations which serve as guidelines under which different equivalent doses can be arrived at for the same radiation field, and also the exacting difficulties encountered in trying to determine radiation hazard in terms of the maximum equivalent dose in a phantom over a protracted period, when the radiation exhibits a space-energy distribution of complicated configuration. On analyzing known data from calculations of the distribution of equivalent dose throughout the bulk of the phantom at a unit flux of monoenergetic neutrons in the energy range from 10^{-2} to 10^{12} eV, the authors recommend numerical values of the conversion ratio from neutron flux to equivalent dose useful for the range of energies from thermal to 100 GeV.

The most popular method in dosimetry of neutrons over a broad energy range for operational purposes remains, as earlier, the method based on slowing down of neutrons with subsequent recording of slow neutrons and thermal neutrons. Several types of instruments operating on the basis of that principle were presented in the reports.

Translated from Atomnaya Énergiya, Vol. 34, No. 5, pp. 411-412, May, 1973.

Up-to-date techniques and instruments in dosimetric monitoring of mixed γ-neutron radiation were reported on in a review paper by M. Zelczynski (Poland). Specifically, this paper went into detail on methods of measuring equivalent dose with the aid of an LET-sensitive detector; the advantages and disadvantages of that approach, and the range of suitable applications, are discussed.

Individual or personnel neutron dosimetry was the subject of about one third of the reports presented. It is clear from the reports that considerable efforts are being expended at the present time towards implementing techniques based on counts of radiation damage events in films, or utilization of LiF^6 and LiF^7 detector pairs, in personnel dosimetric monitoring practice. But the high cost and some remaining shortcomings of this type of dosimeter still stand in the way of general acceptance and use. Counts of recoil proton tracks in nuclear emulsion (P. Krishnamurti, India) retain their place in personnel neutron dosimetry in most cases, for that reason. The unsatisfactory state of personnel dosimetry has lead to the formation of a permanent panel in the USA staffed by representatives of ten different laboratories interested in solutions to the problem. In the case of nuclear accidents, the most reliable results in establishing neutron dosage are arrived at through a combination of two methods: restitution of the neutron spectrum on the basis of readings of activation detectors, and measurement of sodium radioactivity in the blood. The symposium participants arrived at that concensus in the course of discussing reports devoted to that problem.

Several reports contained results of comparisons of different methods and dosimetric monitoring equipment. H. Segouin (Luxemburg) obtained the mean deviation of readings from standard values for several different fast neutron energies, as a result of comparing readings of fast-neutron personnel monitoring dosimeters originating in different laboratories. At 0.7 MeV neutron energy, the average registered neutron dose is one order of magnitude below the true dose and differs from the dose expected on the basis of data in the literature by a factor of six. With increasing neutron energy, this discrepancy narrows down. As a result of a comparison of readings of different instruments in the radiation field of high-energy proton accelerators, reported on in a paper by M. M. Komochkov et al. (JINR), the deviation of readings of most of the instrument from the most reliable values was found to be characterized by a coefficient of 2. Readings of personnel dosimeters were more than double the true values, which is a response typical of those fields of radiation in which the contribution made to the total radiation dose by relativistic neutrons is greater than 10%.

Some of the reports reflected the ways in which instruments were calibrated, and the design of the standard sources. For example, a report by H. Liederman (West Germany) showed that commercially available rem-meters for neutrons show an equivalent dose ~2 times too high in the energy range from 140 keV to 5 MeV, and ~4 times too high in the 24 keV energy range.

In a concluding report which served as a sort of summary of the symposium's deliberations, Axier (USA) noted further progress achieved in the field of neutron dosimetry for radiological protection.

UNSCHEDULED MEETING OF THE ICRP LEADING BODY

Yu. I. Moskalev

This meeting was held November 11-13, 1972, in Egam (Britain).

A draft report by the working term of the fourth committee, which was drawn upon as part of the job of reworking paragraph 52 of the ICRP publication No. 9, and a draft report of the working team of the ICRP Leading Commission on exposure dose limits, were discussed.

Members of the ICRP Leading Commission and of working groups engaged in preparing drafts of the reports mentioned took part in the special meeting.

At the 1969 meeting, the Commission reiterated its earlier decision to verify the correctness of the system of dose limits. For that purpose, it commenced a careful study of available information on estimates of hazard due to ionizing radiation, and on the actual consequences of exposure at existing dose limits and at the safety levels attained in industry at the present time. In addition, other areas of human activity not connected with radiation effects were also discussed. As a result of this survey, the Commission reached the conclusion that there is no basis for lowering the exposure dose limits for the whole body or for discrete organs either in the case of professionals or individual representatives of the population at large. The Commission is of the opinion that the exposure limits for red bone marrow and the gonads can be increased moderately and thereby brought into line with the levels accepted for the whole body and for other tissues. The Commission does not see any need, in that context, for recommendations to immediately increase the existing system of dose limits.

One important feature of the Commission's recommendations is the requirement that all doses be kept at such a low level that economic and social factors be met. This requirement played a significant role in keeping radiation exposures at a low level, and particularly in limiting exposure doses of individuals or of the population as a whole. However, the Commission acknowledges the difficulties in fulfilling this requirement consistently, and in working out a report which would throw more detailed light on ways of achieving that goal; guidelines are given on how to deal with that requirement in practice. Analysis of each operation is provided, so that the plan and the operating methods of radiation-hazardous systems could be taken into account to lowering exposure levels to such an extent that further lowering of possible exposure would be unfeasible, since it would lead to economic and social costs which would defeat the economic and social gain resulting.

The Commission's recommendations remain the same as laid down in the ICRP Publication No. 9 [1], with certain corrections [2, 3] taken into account. During 1973, the Commission is examining the need to bring forth a new ICRP publication on this topic. That publication will be published sometime in 1976 or thereabouts.

LITERATURE CITED

1. Recommendations of the International Commission on Radiological Protection (adopted September 1965). Publication 9, Oxford, Pergamon Press (1966).
2. Health Phys., 17, 389 (1969).
3. Health Phys., 21, 615 (1971).

Translated from Atomnaya Énergiya, Vol. 34, No. 5, p. 412, May, 1973.

DECEMBER SESSION OF THE CERN – IFVE SCIENTIFIC COMMISSION

A. V. Zhakovskii

The eighth session of the CERN (Switzerland) Scientific Commission acting on the basis of an agreement on scientific and technical collaboration between CERN and GKAE SSSR was held at CERN's Switzerland headquarters December 4-8, 1972.

J. Goldschmidt-Clermont, P. Bernard, A. Kelberg, B. Kuiper, B. Langezet, V. Lokk, Z. Werkerk, and D. Wiskot took part in the work of the Commission as CERN representatives; representing the IFVE [Institute of High-Energy Physics, JINR] were R. M. Sulyaev, Yu. D. Prokoshkin, V. I. Kotov, K. P. Myznikov, and V. A. Yarba. Also present was the CERN general director W. Entschke, as well as H. Schopper, H. Müller, and others.

Basic topics in the area of collaboration, involving preparation and staging of joint work using the Serpukhovo accelerator, and also on the status of fast extraction systems, beam transport systems, and RF particle separation systems, were discussed at the meeting. It was pointed out that, starting June 1972, all of these systems have been operated successfully by IFVE personnel. Specific topics pertaining to the performance of equipment used in fast extraction systems, proton beam transport systems, and RF particle separation systems were discussed, and several recommendations were advanced on ways to improve reliability in service, and other improvements as well.

Information on the performance of the Mirabel bubble chamber was heard, as well as preliminary results of an analysis of plates taken with the chamber, and on the next scheduled exposure sessions of the chamber.

Results of a joint experiment using the boson spectrometer installed at the Serpukhovo accelerator, the second experiment staged within the framework of the agreement signed by CERN and GKAE SSSR on scientific and technical collaboration, were discussed. The set of experimental statistics was completed in April 1972. Elastic scattering of negatively charged π-mesons and K-mesons and antiprotons on protons was studied. Analysis of the experimental results showed that the slopes of the π^-p- and K^-p-scattering cones did not vary over the range of momenta studied. In the case of $\bar{p}p$-scattering, slight variation of the slope is possible over the momentum range from 25 to 40 GeV/c. Investigation of processes involved in the formation of boson resonances showed that there are three anomalies present in the mass spectrum of the system of three π-mesons: A_1, A_2, A_3, of which only A_2 is a pure resonance in the energy range beyond 25 GeV/c.

These experimental findings were presented at the international conference on hadron collisions at Oxford, and at the XVI international conference on high-energy physics at Chicago.

The Commission discussed the preparation of new joint experiments involving electronics. Installation of equipment for the n–p-charge transfer experiment (the third joint experiment under CERN and ITEF auspices) was completed in September 1972. The beam channel was adjusted, prior to November, and the entire set of experimental equipment was tested and calibrated. The experiment is planned for some time in 1973.

The fourth joint experiment, the NICE experiment under combined CERN and IFVE auspices, investigates interactions between π-mesons and protons in which only neutrals are formed. The installation of equipment at IFVE began in August 1972. The beam channel, momentum 25 GeV/c, focus 8×14 mm^2,

Translated from Atomnaya Énergiya, Vol. 34, No. 5, pp. 412-413, May, 1973.

beam pulse intensity 10^6 π^--mesons, was adjusted in September. All of the equipment, except for the γ-ray detector, was adjusted in November during subsequent sessions. The experimental as a whole is scheduled for operations in early 1973.

In concluding the meeting, the Scientific Commission discussed topics involving processing of experimental data from bubble chambers.

The next session of the Commission is scheduled for the first half of 1973, at IFVE.

The Soviet delegation was invited to be present at the session of the European Commission on Fast Accelerators (ECFA), the regularly scheduled session of which was held at CERN on November 30 and December 1, 1972. Preparations for a scientific research project using the new 300 GeV CERN accelerator, a machine which is to be completed in 1975, were discussed.

V/O "IZOTOP" SEMINARS AND CONFERENCES

A combined exhibit and seminar on the theme "Isotope techniques, radioisotope equipment, and engineering cost aspects of applications of isotopes in nonferrous metallurgy" was held in October 1972 in Orsk. The exhibit and seminar was inaugurated by the second secretary of the Orsk CPSU State Commissariat, A. S. Kostenyuk. Representatives of GNIItsvetmet (Moscow), Yuzhuralgazstroi (Orenburg), and other organizations took the floor with reports.

The seminar participants received consultations on applications of radioisotope equipment and techniques in metallurgy.

* * *

A conference on techniques and equipment for nondestructive testing in machinery and instrument manufacture was held in the Leningrad interrepublic division of V/O "Izotop" agency in November 1972, with representatives of various industrial plants in the Leningrad area in attendance.

Representatives of the Admiralty plant were on hand to deliver reports on their experience in this field.

* * *

A scientific and technical conference on radiation safety was held in November 1972 at the Leningrad interrepublic division of V/O "Izotop" agency, with workers of γ-ray nondestructive testing laboratories in TsZL and KIP works in the Kalinin district of Leningrad.

Reports on γ-ray nondestructive testing equipment being manufactured in large lots, and on new developments in that area, were heard.

* * *

A technical conference with workers engaged in research and development work on process monitoring and control instrumentation for the paper and pulp industry was held at the Leningrad interrepublic division of V/O "Izotop" in November 1972.

Applications of radioisotope equipment at enterprises in the paper and pulp industry were discussed.

* * *

The mobile exhibit "The Atom–The Toiler" sponsored by the Leningrad interrepublic division of V/O "Izotop" agency was open to the public in Minsk in November and December 1972, at the "Science" hall in that city.

While the exhibit was open, meetings were organized for those interested with representatives of industrial enterprises, and reports were presented on applications of radioisotope equipment and techniques in the various branches of the nation's national economy.

* * *

The topical mobile exhibit "Radioisotope instruments used in the country's national economy" sponsored by the Sverdlovsk interdistrict division of V/O "Izotop" agency was open to the public in Perm' during December 1972, at the House of Industry of the NTO [Scientific and Technical Society] district council premises.

Three seminars were organized for the benefit of engineers and technicians employed at enterprises in Perm', Bereznikov, Solikamsk, Lys'va, and other cities of the region, and for colleagues on the staff

Translated from Atomnaya Énergiya, Vol. 34, No. 5, p. 413, May, 1973.

of scientific research institutes of Sverdlovsk. The common themes of these seminars were: exchanges of experience, developmental outlook, applications of radioisotope equipment in the national economy, and organization of health physics and safety monitoring work.

NUCLEAR POWER SEMINAR AT ZITTAU*

K. Meier

On the eve of the second scientific conference of the Advanced Engineering School at Zittau, on November 7, 1972, the third seminar on the nuclear power industry was held. The seminar, under the chairmanship of the director of the panel on electric power generating stations and power conversion stations, Prof. Dr. Ackermann, was attended by famous instructors of the Zittau Advanced Engineering School and other engineering schools in the German Democratic Republic, by representatives of the power industry, and also by guests from the Moscow Power Institute and the Budapest Advanced Engineering School.

This seminar was devoted to a set of problems pertaining to getting a nuclear power station on the line. The following basic topics came under discussion:

1. Time required to build a nuclear power station and get it started feeding power into the national grid, from the standpoint of optimizing the lead time.
2. Measures to be taken to minimize malfunctions during the starting period.
3. Shaping mutual relations between the customer and the subcontractor in order to attract operating personnel to carry out the startup operations in good time.
4. Selection and training of operating personnel.

The seminar participants noted that the basic preparations for putting the nuclear power station on the line must involve selection of the most correct sequence of separate operations that would aid in finding the operationally optimum solutions and in improving those solutions in the course of the startup process, with existing jurisprudential norms taken into account. It is also necessary to take into account the experience in the construction and startup of the Rheinsberg nuclear power station.

In addition to technical and organizational preparations, an important role is also played by ideological problems, since the correct solution of those problems would smooth the way for clarifying problems facing all of the specialists taking part in the startup operations. That would then pave the way for important conclusions to be drawn in aiding the training of young specialists in the field.

* Based on article in Kernenergie, 16, 116 (1973).

Translated from Atomnaya Énergiya, Vol. 34, No. 5, pp. 413-414, May, 1973.

EXHIBITS

THIRD INTERNATION ATOMIC INDUSTRY AND ATOMIC ENGINEERING EXHIBIT (BASEL, OCTOBER 1972)

V. I. Mikhan

The third international exhibit and fair for atomic industry Nuclex-72, was held in Basel, October 16-21, 1972. There were 322 firms from 22 countries participating in the exhibit. The largest exhibits were those demonstrated by Britain, Canada, the USA, France, West Germany, and Switzerland. Some countries featured one or two displays. A technical conference devoted mostly to the nuclear power industry was held at the same time as the exhibit.

The basic purpose of the Basel fairs, which have been held once every three years, is to afford firms a chance to display their wares and accept orders from prospective clients. The principal content of the exhibit, and of the conference as well, was therefore a matter of demonstrations of improvements in atomic equipment and facilities as entire entities or separate pieces of equipment, sophisticated manufacturing and assembling technology, automation of control processes, simple and safe operation, low operating and production costs, etc. The slogan of Nuclex-72 was "Experimental experience and improved products." Analysis of the materials on display at the exhibit and of the papers submitted at the technical conference constituted yet another demonstration of the fact that reactor design and construction has come to occupy a firm place in power industry on a worldwide basis.

Operating models and design projects of high-temperature gas-cooled reactors of different design concepts, with electric power ratings in ranges on the order of 1000-1100 MW, were demonstrated in the exhibits set up by West Germany, France, Britain, and Switzerland. Work on liquid-metal fast breeders currently underway in Britain, France, and in a consortium of countries including Belgium, Netherlands, West Germany, and Luxemburg, was also featured. At the present time, these countries are building or designing reactor prototypes with electric power ratings on the order of 250-300 MW.

Close attention has been given to demonstrating achievements in the field of the design and production of various lines of equipment for nuclear power stations. Operating models, prospectuses and pamphlets, full-size models of pumps, heat exchangers, piping runs, etc., are among the displays. Products by the Swiss firm Sulzer (e.g., a working model of a 33,000 m^3/h circulating pump developing a head of 140 m, for a 1300 MW(e) pressurized-water reactor) attracted a good deal of attention. This firm is now running a 45,000 m^3/h capacity pump through tests.

A large portion of the exhibit was taken up with electronic instruments, including instruments designed as components of nuclear power process control and monitoring systems, systems for monitoring the leak-tightness of fuel element jackets and cladding, dosimetric monitoring instrumentation, and so on. Work now underway geared to incorporating digital monitoring of nuclear power station performance variables and digital computer output monitoring and feedback in reactor control was also displayed and publicized. The instruments manufactured by different firms were distinguished by their contrasting design formats.

Much space was reserved at the exhibit for materials devoted to maintaining set point for many nuclear power station performance parameters, in particular maintaining the required coolant quality. Equipment for cleanup of coolants, and equipment for automatic monitoring of the state of reactor loop coolant, was on display. Cermet filtering elements ("Poral" of French manufacture) fabricated from powders of different metals (bronze, molybdenum with additions of carbon, monol, inconel, titanium, platinum) were of special interest to water treatment specialists. These components are being fabricated in the shape of disks, tubes, plates, etc., and feature adequate mechanical strength, chemical inertness, and stability to

Translated from Atomnaya Énergiya, Vol. 34, No. 5, p. 414, May, 1973.

heat (to 600°C). Their filtering capacity covers the range from 0.1 to 100 μ. "Poral" elements are being employed in the filtration of liquids, gases, and organic materials. These or other materials are used depending on the medium and on the temperature.

A large number of specialized firms joined the front-rank leading firms in exhibits on reactor design and manufacture of products useful to the nuclear power industry.

One typical feature shared by all of the firms exhibiting their wares and capabilities as stringent observance in production of all pertinent design and manufacturing specifications, so as to achieve products of superior quality. Precision casting is widely used, high-temperature soldering is being worked into the production process, and special welding equipment is being developed for high-quality welding of tubes to tubesheets through holes in the tubesheets, and so forth.

The Nuclex-72 exhibit and the concurrent technical conference were unquestionably of unusual interest, and aided in more widely publicizing the present state of the art in reactor design and prevailing trends in the field, while also demonstrating the role, and the degree of participation, of industry in this area, and the possibilities and opportunities open to organizations and firms.

VINT-20 SINGLE-HELIX TORSATRON MACHINE WITH THREE-DIMENSIONAL MAGNETIC AXIS

A. V. Georgievskii, V. A. Suprunenko, and E. A. Sukhomlin

A new thermonuclear machine, a single-helix toroidal torsatron facility with the Vint-20 three-dimensional magnetic axis (see Fig. 1), has been put into service at the Khar'kov Physics and Engineering Institute [KhFTI] in 1972. This machine is designed for research on confinement of hot high-density plasma in a closed stellerator type magnetic system. In contrast to the classical stellarator design, the Vint-20 system established both a longitudinal magnetic field and a helical magnetic field solely by means of a single-helix winding with a modulated helix angle. Figure 2 shows the magnetic system of the facility.

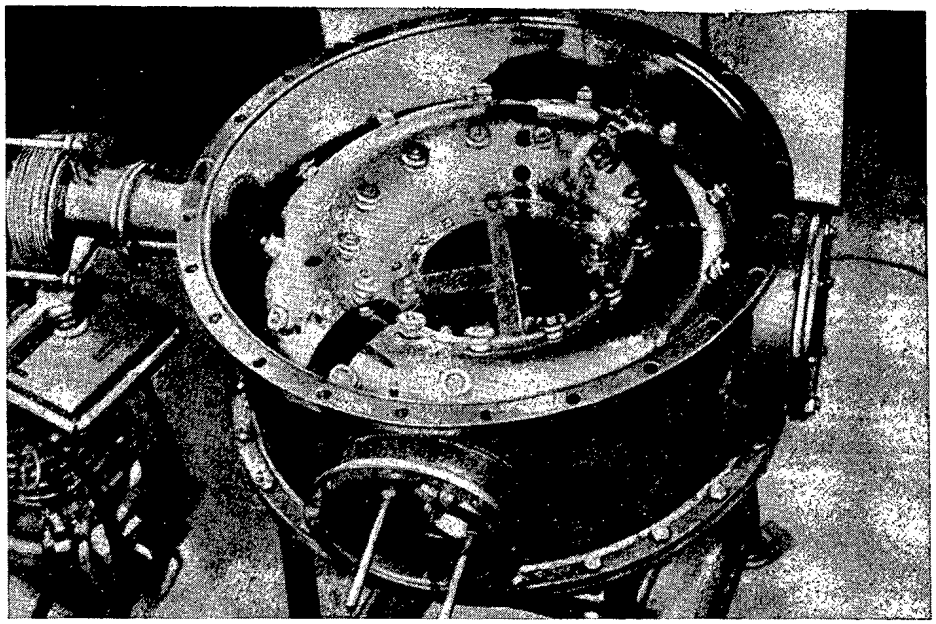

Fig. 1. General view of facility with top cover of vacuum chamber removed.

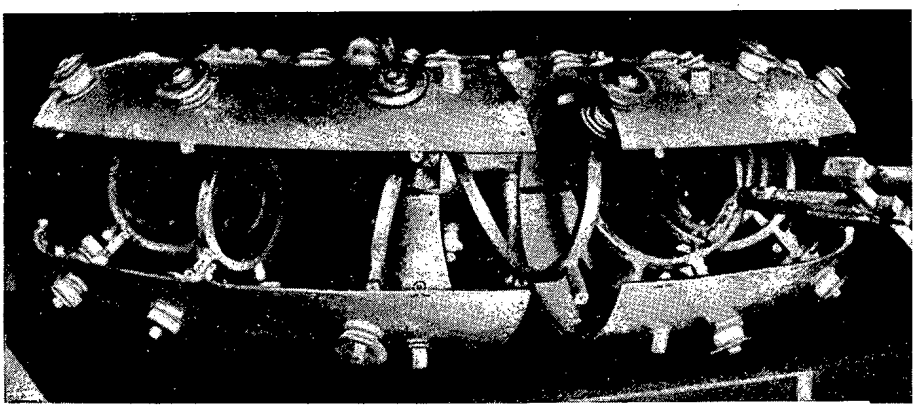

Fig. 2. Magnetic system of Vint-20 thermonuclear machine.

Translated from Atomnaya Énergiya, Vol. 34, No. 5, pp. 415-416, May, 1973.

The positioning of the winding in the vacuum chamber, in the immediate vicinity of the plasma, makes for highly efficacious utilization of the magnetic field, and moderate power drain on the power supplies. The new arrangement of the winding and the modulation of the helix angle make it possible to reduce the level of ponderomotoric forces and to do without a special winding to compensate the vertical component of the magnetic field in the effective volume. Those simplifications in turn greatly cut down cost of installing the Vint-20 machine, as compared to the building and installation costs of a comparable classical stellarator with the same parameters.

The basic parameters of the Vint-20 machine are: longitudinal pulsed-mode field strength 20 kOe; large radius of helical winding ~ 32 cm; small radius ~ 7 cm. The structure of the magnetic field was studied experimentally with the aid of an electron-beam procedure. The measurements showed that the effective volume is bounded by a helicoid corrugated (cusped) magnetic surface (mean radius 7 cm) with a three-dimensional magnetic axis. The rotation transform angle $\geq 2\pi$ on that surface; the shear is 0.5; the relative variation in field strength is 1.5. It was also shown that the parameters of the magnetic surfaces can be varied over a broad range by superposing a relatively small transverse magnetic field (on the order of a percent of the longitudinal field).

A high-density plasma with temperatures of 1 keV is to be generated with this machine, by using the high-frequency method of heating plasma and the turbulent method.

GU-200 VERSATILE MODULAR γ-IRRADIATION FACILITY

S. A. Kel'tsev, V. P. Smirnov,
G. I. Lukishov, and M. S. Kuptsov

The γ-ray irradiation facility GU-200 has been developed at the State Union Design Institute. This facility is intended for a broad range of radiation research problems, and uses an irradiator of 200,000 γ-equivalents radium activity, producing a dose rate as high as 2200 r/sec at the center of the irradiator.

The arrangement of the facility is shown in Fig. 1. The storage tank is encased in concrete between two floors of the building. Sixteen vertical channels of round cross section run through the biological shield of the storage tank; this shield is made of iron and lead slugs. The channels are uniformly spaced on the periphery of a 260 mm diameter circle. Cartridges with radiation sources are moved through the channels by means of the push rods.

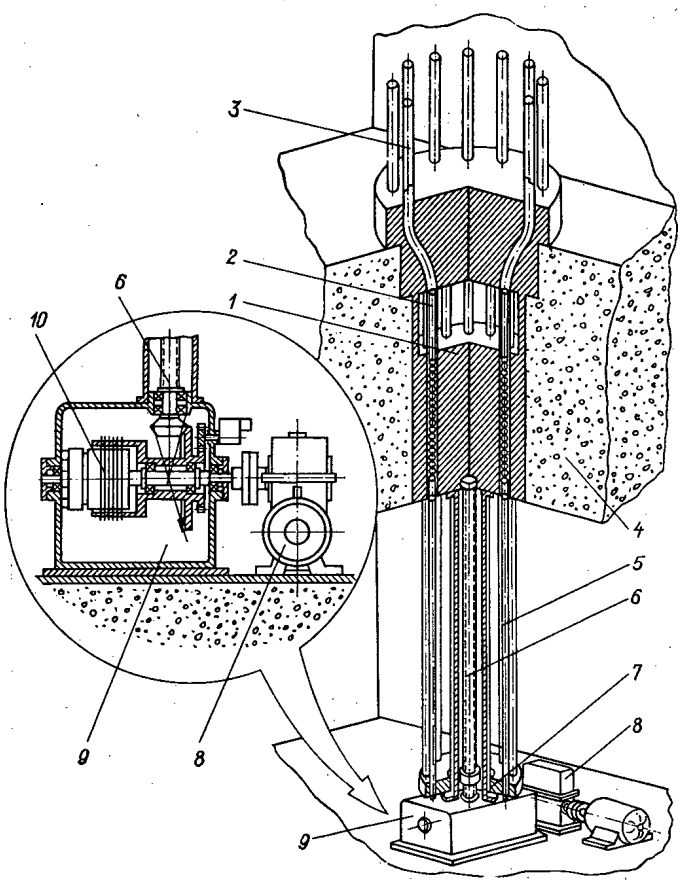

Fig. 1. GU-200 arrangement: 1) storage tank; 2) cartridge with sources; 3) guard assembly; 4) shielding cover; 5) push rod; 6) source hoist; 7) carriage; 8) power drive; 9) reducing gearbox for source hoist; 10) electromagnetic clutch.

Translated from Atomnaya Énergiya, Vol. 34, No. 5, pp. 416-417, May, 1973.

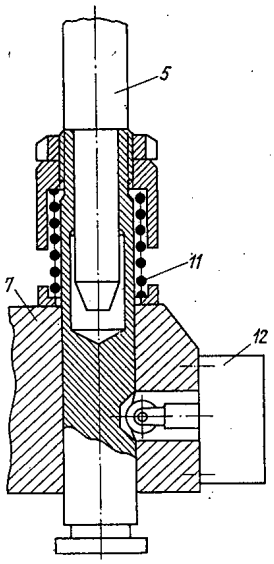

Fig. 2. Diagram showing how push rods are coupled to carriage: 5, 7) see Fig. 1; 11) spring; 12) limit switch.

The channels are bent in the top part of the storage tank in order to facilitate biological shielding against radiation from the sources when these are located in the storage position. The ends of the channels, which protrude into the irradiation chamber, connect to the guard assembly.

The flexible tops of the push rods, made in the form of beads, are firmly coupled to the source-carrying cartridges and to the rigid parts of the push rods, in order to facilitate moving the sources through the bent channels.

The push rods are driven by a spiral hoist mechanism mounted underneath the storage tank on the lower floor of the building. The screw in this mechanism does not exert braking action on its own, and when electric power is shut off (in a scram situation) the carriage drops together with the push rods and the sources, by its own weight to the bottom position, the source storage position.

Braking by means of an electromagnetic clutch situated in the housing of the source hoist reducing gearbox is provided in order to prevent a sudden impact when the carriage falls to the bottom position.

The push rods (Fig. 2) are coupled to the carriage by means of springs connected to the limit switches. In case one of the push rods gets jammed in the storage channel, the spring will become strained beyond admissible limits, the limit switch is activated, and that stops the source hoist power drive. The source-carrying cartridges and the push rods are protected from damage in that manner.

The facility has a system for cooling the sources in storage position. Air or water can be used as the cooling medium. The sources are loaded in from the irradiation chamber end. The carriage and the push rods are dropped to the bottom position, and the guard assembly is removed from the storage tank, in the loading operation. A special reloading cradle to accommodate the container is moved into position over the channel to be loaded, by means of a jib crane, and the container itself with the sources is brought into position, after which the sources are moved from the container into the storage channel. This setup has been designed for loading radiation sources from a KTB-26-12 shipping container (bottom-unloading type).

Radiation sources are also unloaded from the facility back into a KTB-26-12 container. In that case they have to be in the storage position; they are transferred to the shipping container by means of a special remote-control instrument mounted on the shipping container.

Experience in the design and operation of most existing research radiation facilities was taken into account in developing the GU-200 system, which offers the following advantages over its percursors:

1) all mechanisms and electrical components are kept outside the confines of the irradiation chamber per se, and are entirely accessible for inspection and maintenance, no matter what position the sources are in;

2) only the guard assembly, to which the sources are raised during an irradiation session, and the hand-operated jib crane for moving heavy objects about within the radiation exposure zone, and for assembling and disassembling the facility completely for repairs and maintenance, are located within the irradiation chamber; no other mechanisms are needed to assemble and dissassemble the facility;

3) the space within the guard assembly (irradiator) is open from above, and is readily accessible for inspection and maintenance;

4) when the facility is operating normally, or during a scram, and even during reloading and unloading, the radiation sources are exposed to minimum hazard of mechanical damage.

5) the position of the source-carrying cartridges is precisely known in all cases.

PILOT RADIATION FACILITY FOR PRODUCTION OF TETRACHLOROALKANES

G. M. Karpov and G. I. Lukishov

Experimental verification of the radiation method of tetrachloroalkane production [A. A. Beer et al., At. Energ., 29, 461 (1970)] has been achieved on a pilot radiation-chemical facility utilizing a Co^{60} source, and developed by the State Union Design Institute.

Two radiation-chemoreactors with irradiators loaded with Co^{60} radiation sources each of 18,000 gram-equivalents radium activity were placed in special equipped hot caves lined with reinforced-concrete walls forming biological shielding.

The equipment installed in each of the hot caves (Fig. 1) includes the telomerization chemonuclear reactor; a storage tank for the three channels, two of which are standby or reserve channels; a pool filled with water to a height of 4000 cm (used to test radiation sources for leaktightness), also to encapsulate the sources and load them into the working channels; a reloading cradle by which the sources are transferred from the shipping container to the pool; a maintenance access hole 1600 mm in diameter for assembling and disassembling the chemonuclear reactor; a protective ion shielding door dimensioned 2000 × 900 × 100 mm; a leaktight door dimensioned 200 × 900 × 100 mm, with an interlock.

The equipment in the facility also includes a test stand used in checking sources for leaktightness. The facility is controlled from a desk installed on the second floor in the operations room. The control desk is combined with the operator's worktable, on which the startup, alarm annunciation, and interlock equipment is mounted.

The standard sources are enclosed in a third shell and encapsulated in a shielded capsule with a threaded cover, in order to enhance their viability. This reinforced shielding of the sources is dictated by the fact that a pneumatic method is used in the facility to move the sources, and impacts resulting in possible damage to the outer protective shell around the source are a problem.

The sources, when in nonworking position, are positioned in the dry metal-shielded storage tank; this shielding consists of iron shot 1.5 mm in diameter; the shot is filled to a height of 2100 mm.

Figure 2 shows how radiation sources are moved about within the facility. The sources are moved out of the storage tank and into the reactor by a stream of compressed nitrogen. The nitrogen enters the plenum chamber from a compressor station, under 5 kg/cm^2 pressure. Before the nitrogen enters the working channel, its pressure is reduced to 0.8 kg/cm^2. The nitrogen is fed in by electromagnetically actuated globe valves. The electromagnetic valve controls are located on a special panel outside of the hot caves. There are four globe valves serving each working channel; two of them open when the sources are raised, while the other two open only when the facility is scrammed.

The globe valves are controlled from the control desk. When the electromagnetically actuated globe valves are open, the compressed nitrogen is admitted into the working channel, and upon encountering the piston in its path, it raises the piston together with the radiation sources into the irradiation zone until the top piston is driven home against the rod of the source height control device. The radiation sources when in the working channel are positioned between two pistons. Nitrogen proceeds from the working channel through the electromagnetically actuated valve and through a filter into the hot cave. When the nitrogen stream is shut off, the sources and the pistons drop back to the storage tank under their own weight. Forced lowering of the sources can be brought about automatically by switching the other pair of electromagnetically actuated globe valves on to feed in compressed nitrogen from above.

Translated from Atomnaya Énergiya, Vol. 34, No. 5, pp. 417-419, May, 1973.

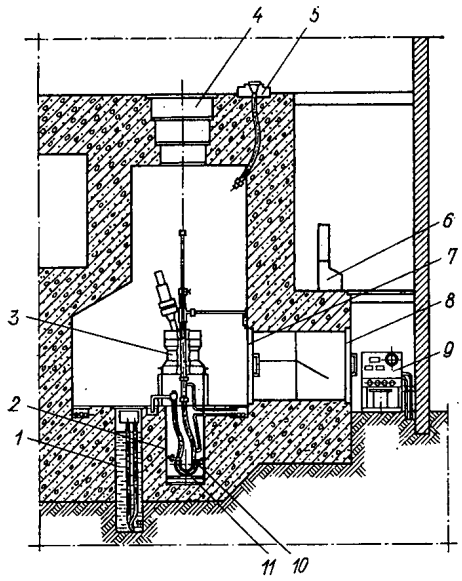

Fig. 1. General view of radiation-chemical facility for telomerization of tetrachloroalkanes: 1) pool; 2) storage tank; 3) chemonuclear reactor; 4) maintenance access hole; 5) reloading cradle; 6) control desk; 7) shielding door; 8) leaktight door; 9) test stand for checking leaktightness of radiation sources; 10) piston; 11) sources.

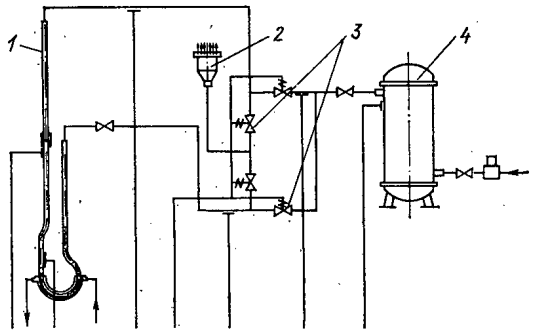

Fig. 2. Basic layout of pneumatic transport of sources within facility: 1) working channel; 2) filter; 3) electromagnetically activated globe valve; 4) plenum chamber.

The position occupied by the sources is monitored by RPED-0.2-56 type pneumatic differential relays mounted on monitor tubes, and signal lamps connected to the relay indicate the position of the sources on a control desk panel. Each of the working channels has three monitor tubes 10 × 1.6 mm in diameter, one of them being connected to the bottom of the channel, the second to the top of the channel, and the third mounted at the point where the channel exits from the chemonuclear reactor. These monitor tubes lead out into the corridor, terminating on the pneumatic differential relays panel. When the sources are raised, a pressure of 1.2 to 1.3 kg/cm^2 is maintained within the plenum chamber, a pressure of 0.75 to 0.8 kg/cm^2 is maintained at the channel exit, and a pressure of 0.25 kg/cm^2 is maintained at the exit from the working channel.

The sources arrive at the facility in shipping containers, and are loaded into the working channels by two methods: they are first unloaded from the container into the reloading pool, then they are checked for leaks, are encapsulated, and are transferred from the pool to the working channels.

The facility is provided with an irradiator lift interlock system to ensure the safety of the operating crew. The electromagnetically actuated globe valves controlling the feed of compressed nitrogen can be opened only when the following conditions are met: the shield door is closed; the leaktight door is locked shut; the maintenance access plug is closed; the decision switch is in the "entry prohibited" position; the reactor is in working order.

Access to the hot cave is possible only with the decision of the operator, when there is no γ-radiation present there. The leaktight door is held closed by two locks, one electromagnetic and the other mechanical. The former acts as a latch. The rod of the electromagnetic lock must be in recessed position for the door to be either opened or closed. The mechanical lock is opened or closed by means of a key. The interlock on the electromagnetic lock allows the leaktight door to open only when two conditions are satisfied simultaneously: the decision switch must be in the "entry permitted" position and there must be no γ-radiation present in the hot cave or in the access labyrinth.

The following dosimetric monitoring measures are provided for:

1. Continuous remote monitoring of the γ-radiation level by means of USIT-2 type monitoring and alarm systems. USIT-1-2A sensors are placed in the hot caves, and USIT-1-2B sensors are placed in the access labyrinths. Secondary instruments are located on the control desk in the operations room. The instruments' contacts are used to interlock the doors and to annunciate alarms as soon as the background in the hot caves deviates from acceptable levels. USIT-1-4 signal alarm units are located ahead of the entry to the hot caves.

2. Stationary continuous monitoring of the γ-radiation level in the operations room, by means of USIT-2 type systems using USIT-1-2A sensors mounted on the control desk.

3. Periodic monitoring of γ-radiation throughout the building, with the aid of type RUP-1 portable instruments.

4. Personnel dosimetric monitoring, using DK-0.2 dosimeters.

Four years of experience in operating the facility has demonstrated the reliability with which all of the basic parts of the system perform. No radioactive contamination has been detected on the filters in all that time, and that is taken as evidence of the complete leaktightness of the radiation sources, and of how reliably the sources are protected from mechanical damage.

BIBLIOGRAPHY

NEW BOOKS

Nad Chem Dumayut Fiziki. Vyp. 9. Fizika Elementarnykh Chastits [What physicists are thinking about. No. 9. Physics of elementary particles], a collection of articles in popular science format, translated from the English, A. D. Sukhanov translation editor, Moscow, Nauka, 1973.

This collection of articles translated from foreign popular science periodicals was written by leading scientists directly engaged in this branch of physics. This ninth edition in the series contains articles devoted to the most important theoretical and experimental topics in the physics of elementary particles. They include articles predicting new particles with unusual properties (magnetic monopoles, tachyons), and also describe new experimental facilities. The live language and the simplicity of the presentation render the collection of articles readable and interesting to a broad audience (ranging from senior high-school students, college undergraduates, and graduate students to specialist-physicists).

* * *

B. M. Troyanovskii, Turbiny dlya Atomnykh Elektrostantsii [Turbines for nuclear electric power generating stations], Moscow, Energiya, 1973.

The design of turbines for nuclear electric power generating stations is discussed, with coverage of such topics as: selection of performance parameters, thermal layouts, sizes and models, rotation frequencies. Special features of the design and operation of such turbines are analyzed, topics involving flow of live steam are examined, reliability and dynamics in control processes are covered. A procedure is presented for thermal calculations of saturated-steam turbines. Materials on turbines manufactured by foreign concerns are furnished.

The book is intended for engineers and technicians engaged in the design, manufacture, operation, and investigation of steam turbines.

* * *

T. Kh. Margulova, Primenenie Kompleksonov v Teploenertetike [Applications of sequestering agents in the power industry], Moscow, Energiya, 1973.

Soviet and foreign experience in applications of sequestering agents and compositions based on sequestering agents in prestartup deactivation and in-performance deactivation of heat power equipment, and especially in deactivation of high-pressure high-temperature boilers operating at above critical parameters, is presented, along with recommendations on the best ways to carry out cleanup operations. The present outlook and recommendations on water treatment in the interior of boilers, using sequestering agents, are given. Methods for enhancing the corrosion resistance of structural materials when sequestering agents are employed are also presented. The outlook for applications of sequestering agents in nuclear power facilities is also covered.

The book is written for research scientists, heat power engineers, and chemists.

* * *

Vozbuzhdennye Chastitsy v Khimicheskoi Kinetike [Excited particles in chemical kinetics]. Edited by C. Bamford and C. Tipper (Comprehensive Chemical Kinetics. The Formation and Decay of Excited Species 1969). Translated from the English, Moscow, Mir, 1973.

This book is devoted to chemical processes involving excited particles, a topic which has acquired exceptional importance in the recent period with the development of chemically pumped lasers. Problems

Translated from Atomnaya Énergiya, Vol. 34, No. 5, pp. 421-422, May, 1973.

concerning excited molecules, excited atoms, excited radicals and ions, forming in photolysis, radiolysis, and in electrical discharges, are discussed.

The book is intended for research scientists, including physical-chemists and chemical-physicists, working in the fields of chemical kinetics, combustion, radiation chemistry, or molecular physics.

* * *

J. Schwinger, Chastitsy, Istochniki, Polya [Particles, sources, fields, London, 1970]. Translated from the English, Moscow, Mir, 1973.

Nobel prize winner J. Schwinger tackled the problem of writing a book accessible to student readers which would go into high-energy physics with concepts of physical sources as a prerequesite for the reader, with no references of any kind to the standard operator formalisms of field theory. This approach, in J. Schwinger's opinion, is dictated by the unsatisfactory position now prevailing in the physics of high-energy particles, by the frustration of hopes for an operator (quantum) field theory, which has lost any real contact with physics, and by the lack of confidence in current algebra containing within itself anything more fundamental than a simply low-energy phenomenology.

Reading the book requires a prerequisite acquaintance only with nonrelativistic quantum mechanics, on the basis of which the author brings the reader to an understanding of the most recent achievements in high-energy physics. The presentation contains many elements of interest not only to students, but generally to anyone concerned with high-energy physics.

* * *

A. Abraham and B. Bleany, Elektronnyi Paramagnitnyi Rezonans Perekhodnykh Ionov, T. 2 [Electron paramagnetic resonance of transition ions, Vol. 2, Oxford, 1970]. Translated from the English, Moscow, Mir, 1973.

This monograph was written by leading specialists in the field of magnetic resonance: A. Abraham (France) and B. Bleany (Britain), and is the first thorough introduction to this field of physics in the world-wide literature. Volume 1, published in Russian by Mir publishing house in 1972, comprised the first two parts of the original monograph. The present volume includes the third part, which encompasses the fundamentals of the theory of paramagnetic resonance. Elements of group theory needed for a deeper grasp of paramagnetic resonance, the method of equivalent operators, the theory of the hyperfine structure of EPR spectra, and various effects responsible for the hyperfine structure, are considered. The monograph is distinguished by the rigor of the presentation and the way it constitutes an integral unit.

The book is intended for physicists, chemists, biologists, specialists in quantum electronics, and also graduate and senior undergraduates majoring in physics and engineering physics at the college level.

* * *

Radiation-Chemistry-III. Proceedings of the Third Tihany Symposium on Radiation Chemistry, Vols. I, II [in English], Budapest, Akademiai Kiado, 1972.*

This publication is a compendium of reports in two volumes, edited by J. Dobe and P. Hedvig. The introduction, written by the president of the symposium Organizing Committee D. Hardy, notes the keen interest manifested by scientists of various countries in the symposium held. A total of 136 papers are published along with the discussions from the floor. Some of the reports appear as abstracts at the close of the second volume. The first volume, devoted to the memory of the renowned Soviet scientist V. V. Voevodskii, is in two parts. The first part ("Organic materials") includes texts of 38 reports on reactions of free radicals, ion-molecular reactions, the effect of physical structure on chemical reactions in solution, radiolysis of some specific systems, and radiation-chemical synthesis.

The second part of the first volume acquaints the reader with 58 reports on the radiation chemistry of polymers, dealing mainly with solid-phase and liquid-phase polymerization, copolymerization, and modification of polymers. The third part is reserved for the second volume ("Aqueous solutions"). Here we find 31 reports on such topics as radiolysis of aqueous solutions in steady state, pulsed radiolysis, radiolysis of solutions of biologically important substances, and so forth.

The symposium proceedings are appended with an authors index and topical index, and a list of the participants in the conference.

* An informational report on this symposium was published in Atomnaya Énergiya, 31, 545 (1971).

R. D. Vasil'ev
FUNDAMENTALS OF THE METROLOGY OF NEUTRON RADIATION*

Reviewed by V. S. Yuzgin

This book by R. D. Vasil'ev surveys and systematizes the experience accumulated to date in the field of neutron radiation metrology. A special place is reserved in the text for methods of metrological treatment of what are termed direct, indirect, and combined measurements of neutron radiation. The author starts out with a review of the basic concepts in modern metrology, and formulates the most important metrological problems, placing special attention on measurements of specific physical variables, and also on simultaneous measurements of several distinct physical variables with the object of unearthing relationships between those variables. At the conclusion of the first chapter, the author dwells briefly on the development and improvement of the jurisprudential bases for measuring work and practice, emphasizing the primary goal of bringing about conditions favoring reliable measurement results with the least expenditures in material resources and time.

The second chapter provides a detailed discussion of the characteristics of neutron fields and neutron sources. Examples are given of differential and integral equations and dependences, and of variables describing fields, of neutron sources, and the process by which neutrons and nuclei interact. Such concepts as neutron yield, anisotropy factor, and asymmetry of the radiation emitted by a source are discussed. The relationship between the neutron yield of a point source and the flux density near the source is used as an example illustrating the interrelation between those factors, in this chapter.

The short third chapter discusses the principles underlying metrological planning, and the basic features of metrological classification of methods typical of different types and modes of measurements; recommendations are given on how to best go about analyzing neutron measurements.

The literature on general metrology and special trends in metrology deals primarily with direct measurements, while metrological servicing of indirect and combined measurements, particularly those commonly encountered in neutron physics, have not gotten their due share of attention. These topics are covered and surveyed in the book under review, in the fourth to the ninth chapters of the text.

Indirect and combined measurements are discussed on the basis of neutron cross sections in fields with an arbitrary angular distribution of neutrons, relying on almost transparent, gray, and black specimens of material. Techniques of measurements in which cross sections of different types of interactions between neutrons and matter, including activation techniques, are discussed. The material in this chapter, which is the largest in extent in the text, can serve as a sort of reference manual on its own, where the experimentalist will find not only a systematized rundown of the principal procedures to be followed in measuring neutron characteristics, but also useful hints on the practical applications of those methods. The chapter concludes with a discussion of ways to restore the true shape of the neutron energy spectrum from the results of measurements.

The fifth chapter deals with methods of determining the characteristics of neutron sources exhibiting slight geometrical dimensions. These methods, based on utilization of ratios of neutron cross sections, are virtually insensitive to the energy distribution and angular distribution of neutrons and of the accompanying γ-radiation.

*Atomizdat, Moscow, 1972.

Translated from Atomanay Énergiya, Vol. 34, No. 5, pp. 422-423, May, 1973

Indirect measurements based on cross sections of reactions involving neutron production, and the accompanying reactions, are discussed. It is shown that the neutron yield from target specimens irradiated in accelerators can be estimated approximately.

The eighth chapter analyzes indirect measurements which do not require data on cross sections. Here we find five groups of techniques under discussion: measurements with the aid of specimens placed in moderators (spatial and optical integration); techniques involving "negative" sources; methods of accompanying particles; coincidence techniques.

The concept of a "standard," primary and secondary techniques of indirect and combined measurements, the approach to selection of constants and their standard values, certification of standard specimens, and metrological design and coordination of instruments, form the subject matter of the ninth chapter.

Techniques based on direct measurements of arbitrary physical variables characterizing fields and sources of neutrons, are analyzed in the tenth chapter. Measurements taken with the aid of comparing instruments are considered with particularly close attention. The author, demonstrates, on the basis of a comparison of the initial formulas for direct and indirect measurements, that direct measurements are not at all less complicated than indirect measurements in the general case, since a number of additional partial coefficients, many of which are occasionally recalcitrant to valid estimates under real conditions under which measurements are taken in actual work, have to be taken into consideration. Conditions under which the instrument can be considered spherical and responsive equally to all wavelengths are discussed. The use of instruments with the calibration dependence built into them is discussed.

The eleventh chapter deals with the conditions for metrological handling of direct measurements, in a brief treatment of the topic. The next chapter is used by the author to present a detailed discussion of mutual intercomparisons of measurement equipment, and classification of measurement equipment. The illustrations in this chapter contain interesting data on international direct and indirect comparisons of standard instruments and isotope sources at different metrological laboratories, carried out within the past decade.

In conclusion, we may note that the regularities discussed in the monograph have been verified by a host of measurements taken of arbitrary physical variables and dependences typical of neutron physics. The approach to the solution of the problem of proper meterological handling of different types of neutron measurements can also be used in other fields of measurements. The bibliography appended to the text includes 315 reference titles.

The book will prove useful to specialists working in the field of neutron physics, and also to graduate students and senior undergraduates in technical colleges.

M. L. Fel'dman and A. K. Chernovets

SPECIAL FEATURES OF THE ELECTRICAL EQUIPMENT IN NUCLEAR ELECTRIC POWER STATIONS*

The book's authors confronted the task of shedding light on a fairly narrow and insufficiently covered problem, as far as the present literature goes: describing in as great detail as is feasible the special features and construction of electric power supplies and circuitry for mechanisms used in the functioning of nuclear power stations, as well as the basic electric circuit layouts and connections. These are important questions in the design of nuclear power stations, since efficient design of electrical circuitry and electrical equipment in nuclear power plant installations has an important effect on engineering costs and on efficiency and performance.

Clearly, the most important feature of the electrical equipment layout in the thermal power part of a nuclear power station is in reliable power supplies to the mechanisms, and also in the use of equipment providing reliable and rapid removal of residual heat from the reactor in planned shutdowns and in scram situations. These topics are the subject matter of chapters one through five, and seven. The role played by electrical layouts and electrical equipment in the cycle of conversion of heat energy into electrical energy, electrical connections and circuitry serving the needs of the plant, how to determine the reliability of electrical equipment for nuclear power plant mechanisms, reliable uninterrupted supply of electrical power in scram situations, and other features of the principal electrical components and circuitry, are discussed in the text.

The presentation of the material in these chapters is typified by attention to practical needs, which is even more clearly emphasized by some of the appendices (in tabular form), which in essence constitute a helpful reference aid on the book's main topic.

Unfortunately, we cannot voice a positive estimate of the sixth chapter, which is devoted to operating conditions of nuclear power stations as part of the national power grid.

If the authors had limited their scope to a presentation of operating condition specifications, in the requirements imposed by the power grid on the nuclear power station feeding power into it, and descriptions of the ways and means of satisfying those requirements and the effect of those factors on the electrical circuitry and equipment of the nuclear power station, this would have corresponded to the style, character, and basic concept of the book. But the authors decided on a rush job utilizing fairly obsolete material, to present a rather complicated picture of the operating conditions of nuclear power stations as part of the power grid, an undertaking which would better have formed the topic of a separate book. Hence the chapter did not turn out well, it was poorly conceived, is most unconvincing, and abounds in arguments that are too general.

That part of the chapter in which the part played by the nuclear power stations in covering the power grid is discussed is based on the familiar procedure of distributing loads between blocks of fossil-fuel-burning electric power stations. Arbitrary reclassification of nuclear power stations as fossil-fuel power stations by converting nuclear fuel to units of conventional fossil fuel is possible, generally speaking, but such an approach fails to reflect the actual state of affairs prevailing, since it leaves out of account many of the factors which are determined by the operating conditions of nuclear power stations as part of the nationwide power system. A comprehensive integrated systems approach is what is needed here. The participation of nuclear power stations in meeting the load schedules for the overall power grid must be estimated on the basis of a minimum expenditures criterion.

* Énergiya, Moscow, 1972.

Translated from Atomnaya Énergiya, Vol. 34, No. 5, p. 423, May, 1973.

It is of the utmost importance to take into cognizance not only existing structures of power generating equipment in the national power system, but also their developmental dynamics, i.e., optimization and study of nuclear power station operating conditions must take into consideration those economic consequences which can be reflected in the entire subsequent development of the nuclear power industry. And any discussion of the operating conditions of nuclear power stations cannot afford to ignore such a major feature of the nuclear power picture as the breeding of secondary nuclear fuel, namely plutonium.

On the whole, and with the exception of the sixth chapter, the book makes a useful contribution to the list of literature on nuclear power engineering.

breaking the language barrier

WITH COVER-TO-COVER ENGLISH TRANSLATIONS OF SOVIET JOURNALS

in mathematics and information science

Title	# of Issues	Subscription Price
Algebra and Logic *Algebra i logika*	6	$120.00
Automation and Remote Control *Avtomatika i telemekhanika*	24	$195.00
Cybernetics *Kibernetika*	6	$125.00
Differential Equations *Differentsial'nye uravneniya*	12	$150.00
Functional Analysis and Its Applications *Funktsional'nyi analiz i ego prilozheniya*	4	$110.00
Journal of Soviet Mathematics	6	$135.00
Mathematical Notes *Matematicheskie zametki*	12 (2 vols./yr. 6 issues ea.)	$185.00
Mathematical Transactions of the Academy of Sciences of the Lithuanian SSR *Litovskii Matematicheskii Sbornik*	4	$150.00
Problems of Information Transmission *Problemy peredachi informatsii*	4	$100.00
Siberian Mathematical Journal of the Academy of Sciences of the USSR Novosibirski *Sibirskii matematicheskii zhurnal*	6	$195.00
Theoretical and Mathematical Physics *Teoreticheskaya i matematicheskaya fizika*	12 (4 vols./yr. 3 issues ea.)	$145.00
Ukrainian Mathematical Journal *Ukrainskii matematicheskii zhurnal*	6	$155.00

Back volumes are available.
For further information, please contact the Publishers.

SEND FOR YOUR FREE EXAMINATION COPIES

PLENUM PUBLISHING CORPORATION
Plenum Press • Consultants Bureau
• IFI/Plenum Data Corporation
227 WEST 17th STREET
NEW YORK, N. Y. 10011

In United Kingdom
Plenur Publishing Co. Ltd., Davis House (4th Floor)
8 Scruba Lane, Harlesden, NW10 6SE, England

breaking the language barrier

WITH COVER-TO-COVER ENGLISH TRANSLATIONS OF SOVIET JOURNALS

in physics

Title	# of Issues	Subscription Price
Astrophysics *Astrofizika*	4	$100.00
Fluid Dynamics *Izvestiya Akademii Nauk SSSR mekhanika zhidkosti i gaza*	6	$160.00
High-Energy Chemistry *Khimiya vysokikh énergii*	6	$155.00
High Temperature *Teplofizika vysokikh temperatur*	6	$125.00
Journal of Applied Mechanics and Technical Physics *Zhurnal prikladnoi mekhaniki i tekhnicheskoi fiziki*	6	$150.00
Journal of Engineering Physics *Inzhenerno-fizicheskii zhurnal*	12 (2 vols./yr. 6 issues ea.)	$150.00
Magnetohydrodynamics *Magnitnaya gidrodinamika*	4	$100.00
Mathematical Notes *Matematicheskie zametki*	12 (2 vols./yr. 6 issues ea.)	$185.00
Polymer Mechanics *Mekhanika polimerov*	6	$120.00
Radiophysics and Quantum Electronics (Formerly Soviet Radiophysics) *Izvestiya VUZ. radiofizika*	12	$160.00
Solar System Research *Astronomicheskii vestnik*	4	$ 95.00
Soviet Applied Mechanics *Prikladnaya mekhanika*	12	$160.00
Soviet Atomic Energy *Atomnaya énergiya*	12 (2 vols./yr. 6 issues ea.)	$160.00
Soviet Physics Journal *Izvestiya VUZ. fizika*	12	$160.00
Soviet Radiochemistry *Radiokhimiya*	6	$155.00
Theoretical and Mathematical Physics *Teoreticheskaya i matematicheskaya fizika*	12 (4 vols./yr. 3 issues ea.)	$145.00

Back volumes are available. For further information, please contact the Publishers.

SEND FOR YOUR FREE EXAMINATION COPIES

PLENUM PUBLISHING CORPORATION
227 WEST 17th STREET
NEW YORK, N. Y. 10011
Plenum Press • Consultants Bureau
• IFI/Plenum Data Corporation

In United Kingdom
Plenum Publishing Co. Ltd., Davis House (4th Floor)
8 Scrubs Lane, Harlesden, NW10 6SE, England